

Temporal Berry Phase and the emergence of Bose-Glass-Analog Phase in a Clean U(1) Superfluid

Ryuichi Shindou,^{1,*} Pengwei Zhao,¹ and Xiaonuo Fang²

¹*International Center for Quantum Materials, Peking University, Beijing 100871, China*

²*School of Physics, Peking University, Beijing 100871, China*

(Dated: March 11, 2026)

A U(1) nonlinear sigma model (NLSM) with a one-dimensional temporal Berry phase term describes the critical theory of phase-fluctuation-driven superfluid (SF) transitions. We clarify that the temporal Berry phase leads to space-time anisotropic interference in vortex proliferation, resulting in a quasi-disordered phase characterized by short-range spatial order but persistent temporal phase coherence. This phase shares the essential SF phase correlation properties of the Bose Glass phase known from disordered boson systems, suggesting a unified topological origin for the emergence of the glassy phase in phase-fluctuation-driven superfluid transitions.

Introduction— Topology serves as a fundamental element in the formation of emergent phases and phase transitions, manifesting itself as topological terms in partition functions for quantum many-body systems [1–7]. Prominent examples are the θ -term in Grassmannian nonlinear sigma models (NLSMs), which characterize quantum Hall phases and transitions [8–10] and the Wess-Zumino-Witten term in O(3) NLSMs, describing unconventional phases and transitions in low-dimensional quantum magnets [11–16]. Phase transitions in the sigma models are driven by the spatial (space-time) proliferation of topological defects [17–23], alongside conventional spin-wave fluctuations [24–30]. The topological terms interfere with the defect proliferation by conferring phase factors upon the defect configurations [8, 9, 11, 12, 14–16, 31, 32]. Among them, the U(1) NLSM provides an ideal platform for studying the topological-term-induced interference effect, as its transitions are entirely driven by the defect proliferation [33–35].

The U(1) NLSM with a temporal Berry phase term, $\mathcal{S} \equiv \frac{1}{2g} \int d^D \mathbf{x} |\nabla \theta|^2 + i\chi \int d^D \mathbf{x} \partial_\tau \theta$, is the $T = 0$ effective theory for phase-fluctuation-driven superfluid transitions. Here, the superfluid (SF) phase θ fluctuates in space \mathbf{r} and (imaginary) time τ with $\mathbf{x} \equiv (\tau, \mathbf{r})$, while SF amplitude is constrained by mechanisms such as quenched disorder and/or electron correlation [36, 37]. The Berry phase term χ along the temporal direction originates from the quantum-mechanical commutation relation between superfluid density and phase [38–40]. Its role in the quantum phase transitions has been discussed in clean Bose-Hubbard (BH) models on lattices [41, 42]. However, its precise impact on the space-time anisotropy of SF phase correlations – the hallmark of glassy dynamics – remains an open question [36, 41, 43]. This is particularly relevant for understanding the Bose glass phase [36, 44–47], which is characterized by short-range spatial order but persistent temporal phase coherence. The stability of the glassy phase in the disordered BH

models is tied to the dynamical exponent z of its underlying Φ^4 theory [36], suggesting that the temporal Berry phase term in the corresponding U(1) NLSM is the key ingredient stabilizing the Bose glass.

By a duality transformation, the (2+1)-dimensional U(1) NLSM with the temporal Berry phase maps onto a three-dimensional (3D) type-II superconductor model in an external magnetic field [40, 41, 48–53]. The latter has been studied in the context of magnetic vortex physics in layered high- T_c cuprates [54–56]. The materials undergo a first-order melting transition from magnetic vortex line lattice (VLL) state [57, 58] to normal (or vortex liquid [59, 60]) phase, [61–65] where the VLL phase is characterized by anisotropic magnetic-monopole-field (MMF) correlation: the correlation remains long-ranged along the field direction, while short-ranged in the perpendicular directions [41, 56]. Such anisotropic MMF correlation in the superconductor corresponds, in the dual picture, to the space-time anisotropic U(1) phase correlation in the NLSM. Yet, the mechanism of the correlation anisotropy and associated phase transition have not been fully investigated in the NLSM framework.

In this Letter, applying renormalization group (RG) theory to the (2+1) dimensional U(1) NLSM with tem-

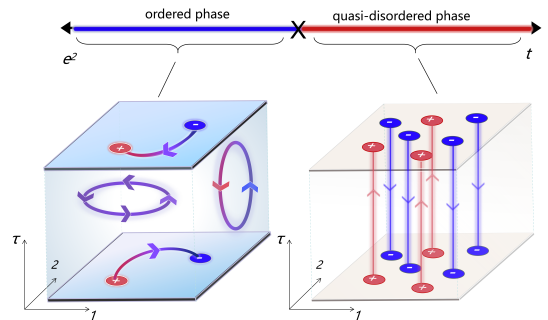


FIG. 1. A schematic picture of quasi-disordered phases in (2+1) dimensional U(1) NLSM with temporal Berry phase.

* rshindou@pku.edu.cn

poral Berry phase, we clarify that the Berry phase interferes with the space-time proliferation process of vortex loops, such that the ordered phase in the sigma model undergoes a generic instability to a quasi-disordered phase with short-ranged spatial order but persistent temporal phase coherence: the same correlation anisotropy as the Bose glass, and (after the duality mapping) the same magnetic-monopole-field correlation anisotropy as the magnetic VLL state. The transition between ordered and quasi-disordered phases is driven by a spatial proliferation of vortex lines polarized along the (imaginary)

time direction [Fig. 1]. The RG analysis suggests that the transition is first order, being consistent with numerics [66–71] and experiments on the melting transition of the magnetic FLL [61–65].

vortex membrane model— The D -dimensional $U(1)$ NLM with the Berry phase can be studied by a vortex membrane model [33–35, 72–82], which comprises a D -dimensional generalization of the Maxwell action and a coupling between the gauge field and $(D-2)$ -dimensional closed vortex hypersurfaces. The partition function is given by the integral over the gauge field, and a configuration sum over possible vortex surfaces,

$$Z_{D,v} = \int \mathcal{D}\mathbf{u} \exp \left[-\frac{1}{2} \int_{|\partial u| < \Lambda|u|} d^D \mathbf{x} \left\{ \gamma_\tau (\partial_\mu u_{\mu\tau}) (\partial_\lambda u_{\lambda\tau}) + \sum_{\nu=1}^{D-1} (\partial_\mu u_{\mu\nu}) (\partial_\lambda u_{\lambda\nu}) \right\} \right] \left\{ 1 + \sum_{N=1}^{\infty} \frac{1}{N!} \prod_{j=1}^N \left(\int \mathcal{D}^D \mathbf{X}_j \int_{|\mathbf{Y}_j| > a_0} \mathcal{D}^D \mathbf{Y}_j \int \mathcal{D}\mathbf{g}_j(\mathbf{s}) y_j \right) \exp \left[-\frac{i}{2} e \int_{|\partial u| < \Lambda|u|} d^D \mathbf{x} u_{\mu\nu}(\mathbf{x}) v_{\mu\nu}(\mathbf{x}) - i2\pi\chi \sum_j \mathcal{A}_{\tau,j} \right] \right\}. \quad (1)$$

Here $\mathbf{x} \equiv (\tau, \mathbf{r})$, and an antisymmetric tensor $u_{\mu\nu}(\mathbf{x})$ ($\mu, \nu = \tau, 1, \dots, D-1$) is the gauge field. In the presence of the temporal Berry phase, the electromagnetic constitutive constant in the Maxwell action acquires a space-time anisotropy, parameterized by γ_τ [see below]. The gauge field couples with vortex excitations via electromagnetic coupling constant $e \equiv 1/\sqrt{g}$. The vortex excitations are described by an antisymmetric tensor field, $v_{\mu\nu}(\mathbf{x}) \equiv \frac{2\pi\epsilon_{\mu\nu\lambda\rho\cdots\sigma}}{(D-2)!} \sum_{j=1}^N \int_{\partial\Gamma_j} d^{D-2} \mathbf{s} \mathbf{g}_{j,\lambda\rho\cdots\sigma}(\mathbf{s}) \delta^D(\mathbf{x} - \mathbf{R}_j(\mathbf{s}))$, whose intensity is concentrated on the j th vortex surface $\partial\Gamma_j$ ($j = 1, \dots, N$: N is the total number of vortex surfaces), and whose direction is dictated by the tangential vectors along the surface. $\mathbf{R}_j(\mathbf{s})$ is the space-time coordinate of the vortex surface element parameterized by a $(D-2)$ -dimensional vector \mathbf{s} . An oriented volume $\mathbf{g}_j(\mathbf{s})$ of a parallelepiped at $\mathbf{R}_j(\mathbf{s})$ is formed by $(D-2)$ linearly independent tangential vectors, $\mathbf{g}_{j,\lambda\rho\cdots\sigma}(\mathbf{s}) \equiv \epsilon_{ab\cdots c} (\partial_{s_a} R_{j,\lambda}) (\partial_{s_b} R_{j,\rho}) \cdots (\partial_{s_c} R_{j,\sigma})$ ($a, b, \dots, c = 1, \dots, D-2$). \mathbf{X}_j is the center of mass of the j th vortex surface, and $\mathbf{Y}_j/2$ is a relative coordinate between \mathbf{X}_j and $\mathbf{R}_j(\mathbf{s} = \mathbf{0})$. $|\mathbf{Y}_j|$ parameterizes a linear size of the j th vortex surface. $y_j \equiv \exp[E_j]$ is the fugacity for the j th vortex surface with $E_j \equiv w + \int_{\partial\Gamma_j} d^{D-2} \mathbf{s} t(\hat{\mathbf{g}}_{j,\tau}(\mathbf{s}), \hat{\mathbf{g}}_{j,\mathbf{r}}(\mathbf{s}))$. $t(\hat{\mathbf{g}}_\tau, \hat{\mathbf{g}}_\mathbf{r})$ is a vortex core energy density per surface element, which is a function of the temporal component $[\hat{\mathbf{g}}_{j,\tau}]_{a,b} \equiv (\partial_{s_a} R_{j,\tau}) (\partial_{s_b} R_{j,\tau})$, and spatial component $[\hat{\mathbf{g}}_{j,\mathbf{r}}]_{a,b} \equiv \sum_{\lambda=1, \dots, D-1} (\partial_{s_a} R_{j,\lambda}) (\partial_{s_b} R_{j,\lambda})$ of metric tensors on the surface [81, 82]. $\mathcal{A}_{\tau,j}$ is a $(D-1)$ dimensional volume inside the j th vortex hypersurface projected onto a $\tau = \text{const.}$ plane: $\mathcal{A}_{\tau,j} \equiv \int_{(\tau,\mathbf{r}) \in \Gamma_j} d^{D-1} \mathbf{r}$ [23, 32, 42, 83]. A Gaussian integration over the gauge field leads to the $1/|\mathbf{x} - \mathbf{x}'|^{D-2}$ Coulomb interaction between two surface

elements at \mathbf{x} and \mathbf{x}' . When \mathbf{x}' is integrated over the same surface as \mathbf{x} , the interaction leads to a logarithmic divergence from $\mathbf{x}' \simeq \mathbf{x}$. To regularize this ultraviolet (UV) divergence, we introduce a UV cutoff in the momentum-energy integral for the Maxwell action, $|\partial u| < \Lambda|u|$, and a UV cutoff for the linear size of vortex surfaces, $|\mathbf{Y}_j| > a_0$. When the vortex surface size is at the lattice constant scale a_0 [$|\mathbf{Y}_j| \simeq a_0$], we assume that the surface takes the form of a symmetric sphere [72, 74, 75, 82, 83].

The vortex membrane model can be studied using a renormalization group analysis [5, 40, 84], where short-distance degrees of freedom (DOF) are recursively integrated out. Firstly, the integral over the vortex surface size can be decomposed into the smallest surface case and a larger surface case, $\int_{|\mathbf{Y}_j| > a_0} \mathcal{D}^D \mathbf{Y}_j = \int_{ba_0 > |\mathbf{Y}_j| > a_0} \mathcal{D}^D \mathbf{Y}_j + \int_{|\mathbf{Y}_j| > ba_0} \mathcal{D}^D \mathbf{Y}_j$, with an infinitesimally small positive $\ln b$. By regarding the smallest vortex surface as the symmetric sphere with its diameter a_0 , we employ a gradient expansion for the electromagnetic coupling between $u_{\mu\nu}(\mathbf{x})$ and $v_{\mu\nu}(\mathbf{x})$ created by the small vortex sphere. We can further integrate out the small-surface DOF entirely by expanding its integrand in powers of a dimensionless coupling constant $e^2 a_0^{D-2}$. The perturbative treatment of e^2 recursively renormalizes the constitutive constant in the Maxwell action and the Berry phase term [82]. The renormalizations can be regarded as screening effects due to the small vortex excitation.

The renormalization to the vortex fugacity parameter comes from a short-range part of the Coulomb interaction [82, 85]. To this end, we decompose the Maxwell action into short-ranged and long-ranged parts,

$\int_{|\partial u| < \Lambda|u|} = \int_{\Lambda b^{-1}|u| < |\partial u| < \Lambda|u|} + \int_{|\partial u| < \Lambda b^{-1}|u|}$, and integrate out the fast component of the gauge fields. The integration gives rise to the Coulomb interaction between neighboring vortex surface elements on the same vortex surface, which can be included into the vortex core energy density $t(\hat{\mathbf{g}}_\tau, \hat{\mathbf{g}}_r)$ [82]. For the sake of convenience, we normalize the gauge field amplitude such that the spatial component of the constitutive constant is invariant after the length rescaling. This completes a derivation of renormalization group equation for e^2 , γ_τ , χ and fugacity parameters [82]. In the following, we study this general- D RG equation in two simpler limits, (i) general- D dimension around the isotropic plane [$\chi = 0$], and (ii) $D = 3$ case with $\chi \neq 0$.

ϵ -expansion — The perturbative treatment of e^2 can be justified by the use of small $\epsilon = D - 2$ expansion around a saddle fixed point on the isotropic plane [$\chi = 0$ and $\gamma_\tau = 1$]. On the isotropic plane, the fugacity density becomes a function only of the first fundamental form $\hat{\mathbf{g}} \equiv \hat{\mathbf{g}}_\tau + \hat{\mathbf{g}}_r$, $E_j = w + t \int_{\partial \Gamma_j} d^{D-2} \mathbf{s} \{ \det \hat{\mathbf{g}}_j(\mathbf{s}) \}^{1/2} \equiv w + t S_j$, [81, 82] where the fugacity is characterized by a $(D - 2)$ -dimensional surface area S_j of the vortex surface $\partial \Gamma_j$ with a scalar quantity t . As $\gamma_\tau = 1$ and $\chi = 0$ are invariant under renormalization [82], the RG equation reduces to two equations for e^2 and t , respectively. By normalizing e^2 and t by the surface area S_0 of the small vortex sphere [$S_0 \equiv (a_0/2)^{D-2} 2\pi^{(D-1)/2} / \Gamma((D-1)/2)$], the two equations are given by [82],

$$\frac{dt}{d \ln b} = (D - 2)t - e^2, \quad (2)$$

$$\frac{de^2}{d \ln b} = (D - 2)e^2 - \frac{4\sqrt{\pi}}{D - 1} \left(\frac{\pi}{2}\right)^D e^4 \exp[t]. \quad (3)$$

With the small $\epsilon = D - 2$, the differential equation has a saddle fixed point at $(t, e^2) = (t_*, \epsilon t_*)$ and $t_* = t_{(0),*} + \epsilon t_{(1),*} + \mathcal{O}(\epsilon^2)$ [$t_{(0),*} = 0.048\dots$, $t_{(1),*} = 0.036\dots$]. For $D \gtrsim 2$, the small e^2 value at the fixed point justifies the perturbative treatment. The saddle fixed point corresponds to the Wilson-Fisher (WF) fixed point for XY universality class. The critical exponent is evaluated perturbatively in small ϵ as $\nu = 0.977/\epsilon - 0.0167 + \dots$ [$\nu \simeq 0.960\dots$ for $\epsilon = 1$]. Note also that the scaling dimension y_χ of the Berry phase parameter χ is always 1 around the WF fixed point, being independent of the dimension D . $y_\chi = 1$, after the duality map, is consistent with the power of the gauge-field correlation at the critical point in the 3D Anderson-Higgs (AH) model [71, 86, 87]. $y_\chi = 1$ stems from the absence of the renormalization factor to the electric charge, reminiscent of an argument on the anomalous dimension for the gauge field in the AH model. [40, 86]

$D = 3$ RG analysis— In $D = 3$, the two metric tensors, $\hat{\mathbf{g}}_\tau$ and $\hat{\mathbf{g}}_r$, reduce scalar quantities, g_τ and g_r , respectively, with an identity $g_\tau + g_r = 1$, where the RG

equation becomes simplified [82],

$$\frac{de^2}{d \ln b} = e^2 - \frac{\pi^5}{2} e^4 Z_{2,r}(t_\tau, t_r, \nu), \quad (4)$$

$$\frac{d\nu}{d \ln b} = 2\nu - \frac{\pi^5}{2} e^2 \gamma_\tau^{-1} Z_1(t_\tau, t_r, \nu), \quad (5)$$

$$\frac{d\gamma_\tau}{d \ln b} = \frac{\pi^5}{2} e^2 \left(Z_{2,\tau}(t_\tau, t_r, \nu) - \gamma_\tau Z_{2,r}(t_\tau, t_r, \nu) \right), \quad (6)$$

$$\frac{dt_\tau}{d \ln b} = t_\tau - \pi e^2, \quad \frac{dt_r}{d \ln b} = t_r - \pi \frac{e^2}{\sqrt{\gamma_\tau}}, \quad (7)$$

with $\nu \equiv \frac{\pi^2 a_0^2}{2} \chi$. Here, the vortex core energy density $t(g_\tau, g_r)$ is parameterized only by two scalar coupling constants, t_τ and t_r [82],

$$t(g_{j,\tau}, g_{j,r}) = t_\tau \left(\frac{d\mathbf{R}_{j,\tau}}{ds} \right)^2 + t_r \sum_{\sigma=1,2} \left(\frac{d\mathbf{R}_{j,\sigma}}{ds} \right)^2. \quad (8)$$

They are the core energy densities per length along time and space directions, respectively. In the RG equation, e^2 , t_τ and t_r are normalized by $1/a_0$. $Z_{2,\tau}$, $Z_{2,r}$, and Z_1 in Eqs. (4,5,6) are the recursive screenings by the smallest vortex ring to the temporal and spatial components of the constitutive constants, and the Berry phase term, respectively,

$$\left(\begin{array}{c} Z_{2,\tau} \\ Z_{2,r} \end{array} \right) = \frac{35}{4} e^{\frac{\pi}{2} t_\pm} \int_{-1}^1 du \left(\frac{u^2}{\frac{1-u^2}{2}} \right) \frac{e^{-\frac{\pi}{2} t_\pm u^2}}{(1 + i\nu u)^{\frac{9}{2}}}, \quad (9)$$

$$Z_1 = \frac{5}{2} e^{\frac{\pi}{2} t_\pm} \int_{-1}^1 du \frac{iue^{-\frac{\pi}{2} t_\pm u^2}}{(1 + i\nu u)^{\frac{7}{2}}}, \quad (10)$$

with $t_\pm \equiv t_\tau \pm t_r$. u on the right hand side is a sine of the angle between the temporal axis and a plane coplanar with the vortex ring. That says, vortex rings near the 1-2 (spatial) plane [$u \simeq \pm 1$] mostly contribute to the temporal component $Z_{2,\tau}$ of the screening, while vortex rings parallel to the temporal axis [$u = 0$] goes to the spatial component $Z_{2,r}$ of the screening. When the Berry phase χ and its screening are considered as the magnetizing field and magnetization, respectively, $\partial_\nu Z_1 = Z_{2,\tau}$ can be regarded as an analogous relation between magnetic susceptibility and permeability. In the isotropic plane with $\nu = 0$, the RG equation shows the same second-order phase transition as in the previous section.

By adding a finite Berry phase ν to the isotropic limit, the partition function with the vortex ring acquires a complex phase factor $e^{-i\nu u}$, which effectively suppresses the temporal screening $Z_{2,\tau}$ from $u \simeq \pm 1$. Conversely, the spatial screening $Z_{2,r}$ from $u \simeq 0$ remains relatively intact, realizing $Z_{2,\tau} < Z_{2,r}$ [Fig. 2]. Such an anisotropic screening dramatically reduces the space-time anisotropy parameter γ_τ from its isotropic value [Eq. (6)].

The smaller $\gamma_\tau < 1$ tends to polarize vortex loop elements locally along the temporal direction [Eqs. (7)]. Namely, the anisotropic Coulomb interaction energy within a vortex loop favors its loop elements along τ

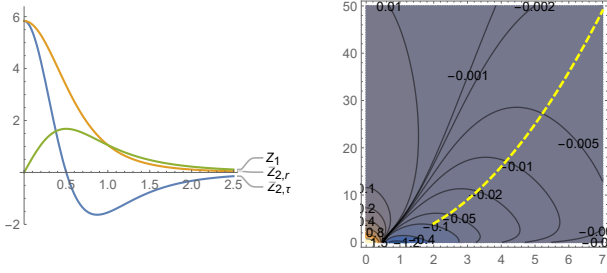


FIG. 2. (left) $Z_{2,\tau}$, $Z_{2,r}$, and Z_1 as a function of ν (horizontal axis) with $t_\tau = t_r = 0$. (Right) Contour plot of $Z_{2,\tau}$ as a function of ν (horizontal axis) and $t_- \equiv t_\tau - t_r$ (vertical axis) with $t_+ = 0$. A Dashed yellow line ($t_- = \nu^2$) depicts a ‘gorge’ of negative value of $Z_{2,\tau}$ (see the text).

over loop elements otherwise. The Coulomb interaction energy $E(C, \gamma_\tau)$ of a vortex loop C is given by

$$\exp[-E_{\text{Coul}}(C, \gamma_\tau)] \equiv \int D\mathbf{a}(\mathbf{x}) \exp\left[-\frac{1}{2} \int d^3\mathbf{x} (\nabla \times \mathbf{a})^T \begin{pmatrix} \gamma_\tau & 0 \\ 0 & \mathbf{1}_{2 \times 2} \end{pmatrix} (\nabla \times \mathbf{a}) - 2\pi i e \oint_C d\mathbf{l} \cdot \mathbf{a}(\mathbf{l})\right], \quad (11)$$

with $\mathbf{x} \equiv (\tau, \mathbf{r})$, $\nabla \equiv (\nabla_\tau, \nabla_{\mathbf{r}})$, $\mathbf{l} \equiv (l_\tau, \mathbf{l}_r)$, and $\mathbf{a} \equiv (\mathbf{a}_\tau, \mathbf{a}_r) \equiv (u_{12}, u_{2\tau}, u_{\tau 1})$. A scale transformation, $\tau' = \tau$, $\mathbf{r}' = \mathbf{r} \frac{1}{\sqrt{\gamma_\tau}}$, $\mathbf{a}'_\tau = \mathbf{a}_\tau$, $\mathbf{a}'_r = \sqrt{\gamma_\tau} \mathbf{a}_r$, relates the anisotropic Coulomb energy of C to the isotropic Coulomb energy of C' , $E_{\text{Coul}}(C, \gamma_\tau) = E_{\text{Coul}}(C', \gamma_\tau = 1) + \dots$, where C' is a transform of C by the stretching in the spatial direction by a factor $1/\sqrt{\gamma_\tau}$ [Here “ \dots ” is independent of the loop]. The Coulomb interaction energy is generally dominated by the UV logarithmically divergent contribution, which comes from the interaction between neighboring loop elements, and is proportional to a vortex loop length $L(C')$ in the isotropic limit [81]:

$$E_{\text{Coul}}(C', \gamma_\tau = 1) = \frac{\pi e^2}{2} L(C') |\ln a_0| + \dots \quad (12)$$

with the UV cutoff a_0 . Thus, when $\gamma_\tau < 1$, the dominant part of the anisotropic Coulomb energy $E_{\text{Coul}}(C, \gamma_\tau)$ prefers vortex loop elements polarized along τ , as any loop segments along the spatial direction will be elongated by a factor $1/\sqrt{\gamma_\tau}$, having larger Coulomb energies with the UV divergence in $E_{\text{Coul}}(C', 1)$, i.e. $e^2 |\ln a_0| / \sqrt{\gamma_\tau}$. Being consistent with this argument, Eq. (7) with $\gamma_\tau < 1$ generally indicates that the renormalization leads to $t_\tau > t_r$. Given $t_- = t_\tau - t_r > 0$, the dominance (absence) of the screening of Eqs. (9,10) is determined by positively (negatively) divergent $t_+ \equiv t_\tau + t_r$.

The RG equation in the large RG scale b drives the coupling constants into a weak coupling region for the ordered phase, an intermediate region for the quasi-disordered phase, or a strong coupling region for the disordered phase [Fig. 3]. The weak-coupling region is

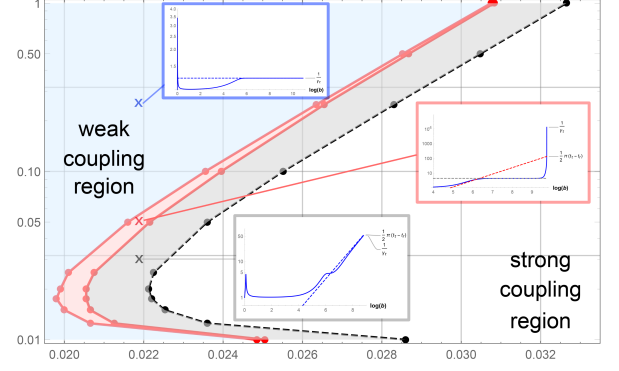


FIG. 3. Phase diagrams obtained from numerical solutions of the $D = 3$ RG equations with initial values of e^2 (vertical axis), $t_\tau = t_r \equiv t$ (horizontal axis), $\gamma_\tau = 1$ and $\nu = 1.2$. Initial parameters in the light blue (gray or white) region go to the weak-coupling (strong-coupling) region with divergent (vanishing) e^2 and ν , and negatively (positively) divergent $t_+ \equiv t_\tau + t_r$. Initial parameters in the light red region are in the intermediate coupling region, where γ_τ goes to zero at a finite RG scale b with positive t_τ and finite e^2 . Three inset figures show how the inverse space-time anisotropy parameter γ_τ^{-1} is renormalized in these three regions.

characterized by the vanishing screening effect, where t_+ diverges negatively as $t_+ \sim A_+ b \ln b$ ($A_+ < 0$), e^2 and ν diverge as $e^2 \sim b$ and $\nu \sim b^2$, and the space-time anisotropy γ_τ converges to a finite positive value less than 1 [Fig. 3]. The strong coupling region is characterized by the divergent screening effect, where t_+ diverges positively as $t_+ \sim A_+ b$ ($A_+ > 0$), e^2 and ν vanish as $e^2 \sim b^{\frac{3}{2}} \exp[-\frac{\pi}{2} A_+ b]$ and $\nu \sim b^2 \exp[-\frac{\pi}{2} A_+ b]$, and γ_τ converges to zero as $\gamma_\tau^{-1} \sim A_- b \sim t_-$ ($A_- > 0$) [Fig. 3]. Importantly, a transformation of initial parameters between these two regions necessitates passage through the intermediate region, where γ_τ goes to zero at a finite RG scale b with positive t_τ and finite e^2 [Fig. 3]. The intermediate region arises universally because of a negative value of $Z_{2,t}$ at $\nu \neq 0$ region [Fig. 2]. Upon any transition from the weak-coupling to the strong-coupling regions, the Berry phase parameter ν in Eq. (5) begins to decrease from the large value, only after t_+ goes to large positive values. Thus, by the time ν enters a gorge of the negative value $Z_{2,t}$ [Fig. 2], t_+ has already grown significantly large and positive. Then, from the first term on the right hand side of Eq. (6), the large negative $Z_{2,t}$ always reduces γ_τ to zero at a finite RG scale b , where $t_\tau > t_+/2 > 0$ and e^2 is finite.

The onset of $\gamma_\tau = 0+$ with positive t_τ and finite e^2 indicates that the system in the intermediate region undergoes an instability to the quasi-disordered phase with persistent temporal correlation and short-ranged spatial correlation. Namely, the anisotropic Coulomb energy with $\gamma_\tau \rightarrow 0+$ and finite e^2 polarizes all the vortex loop elements along τ , where only the temporal component

$\mathbf{a}_\tau(\tau, \mathbf{r})$ of the gauge field couples with the vortex lines. Thus, the (2+1) dim. partition function reduces to the classical partition function for the 2D isotropic Coulomb gas;

$$\lim_{\gamma_\tau \rightarrow 0} Z_{3,v} = \int \mathcal{D}\mathbf{a}(0, \mathbf{q}) \exp \left[-\frac{1}{2} \frac{1}{L_\tau} \int \frac{d^2 \mathbf{q}}{(2\pi)^2} q^2 |\mathbf{a}_\tau(0, \mathbf{q})|^2 \right] \left\{ 1 + \sum_{N=1}^{\infty} \frac{1}{N!} \prod_{j=1}^N \left(\int \mathcal{D}^2 \mathbf{r}_{2j-1} e^{w+L_\tau t_\tau} \int \mathcal{D}^2 \mathbf{r}_{2j} e^{w+L_\tau t_\tau} \right) \exp \left[-i2\pi e \sum_{j=1}^{2N} (-1)^j \int \frac{d^2 \mathbf{q}}{(2\pi)^2} e^{i\mathbf{q} \cdot \mathbf{r}_j} \mathbf{a}_\tau(0, \mathbf{q}) \right] \right\}. \quad (13)$$

Here L_τ is the inverse temperature of the (2 + 1)-dim. partition function $Z_{3,v}$, \mathbf{r}_j ($j = 1, \dots, 2N$) denotes the 2D spatial coordinate of the j th vortex line within the 1-2 plane, $e^{w+L_\tau t_\tau}$ is the fugacity of each vortex line, and $(-1)^j$ denotes the vorticity of the j th vortex line. As the vortex line is fully polarized along τ , only the temporally-uniform component $\mathbf{a}_\tau(\omega = 0, \mathbf{q})$ couples with the vortex line DOF with $\mathbf{a}_\tau(\tau, \mathbf{r}) = \frac{1}{L_\tau} \sum_\omega \int \frac{d^2 \mathbf{q}}{(2\pi)^2} e^{i\mathbf{q} \cdot \mathbf{r} - i\omega \tau} \mathbf{a}_\tau(\omega, \mathbf{q})$, playing the role of the electrostatic potential of the 2D Coulomb gas. The zero-temperature limit [$L_\tau \rightarrow \infty$] with positive t_τ brings relevant parameters of $\lim_{\gamma_\tau \rightarrow 0} Z_{3,v}$ into a 2D disordered re-

gion *far above* a separatrix of the KT transition line [82]. Thus, the onset of $\gamma_\tau \rightarrow +0$ with positive t_τ and finite e^2 results in a spatial proliferation of vortex lines polarized along τ . The vortex-line proliferation destroys the spatial correlation of the U(1) phase, but not the temporal correlation: the system undergoes a transition into a quasi-disordered phase with persistent temporal correlation and short-ranged spatial correlation. The ordered-to-quasi-disordered transition must be the first order: when $\gamma_\tau \rightarrow 0+$ from the weak-coupling side, the spatial correlation length ξ_r jumps from infinity to a finite value, not showing any critical divergence [82].

Summary—This Letter proposes a topological mechanism for the emergence of the quasi-disordered phase in (2+1) dimensions. U(1) NLsM, that shares key signatures (spatial short-range order, temporal long-range order, compressible) with the Bose Glass phase. After the duality transformation, the quasi-disordered phase also shares the same correlation anisotropy as the magnetic vortex line lattice phase in type-II superconductors in an external magnetic field.

Acknowledgements—RS thank Gary A. Williams for communications. The work was supported by the National Basic Research Programs of China (No. 2024YFA1409000) and the National Natural Science Foundation of China (No. 12074008 and No. 12474150).

-
- [1] S. C. Zhang, T. H. Hansson, and S. Kivelson. Effective-field-theory model for the fractional quantum hall effect. *Phys. Rev. Lett.*, 62:82–85, Jan 1989.
- [2] A. O. Gogolin, A. A. Nersisyan, and A. M. Tsvelik. *bosonization and strongly correlated systems*. Cambridge University Press, 1998.
- [3] Andreas P. Schnyder, Shinsei Ryu, Akira Furusaki, and Andreas W. W. Ludwig. Classification of topological insulators and superconductors in three spatial dimensions. *Phys. Rev. B*, 78:195125, Nov 2008.
- [4] Alexei Kitaev. Periodic table for topological insulators and superconductors. *AIP Conference Proceedings*, 1134(1):22–30, 05 2009.
- [5] Alexander Altland and Ben D. Simons. *Condensed Matter Field Theory*. Cambridge University Press, 2010.
- [6] Xiao-Liang Qi and Shou-Cheng Zhang. Topological insulators and superconductors. *Rev. Mod. Phys.*, 83:1057–1110, Oct 2011.
- [7] Ching-Kai Chiu, Jeffrey C. Y. Teo, Andreas P. Schnyder, and Shinsei Ryu. Classification of topological quantum matter with symmetries. *Rev. Mod. Phys.*, 88:035005, Aug 2016.
- [8] D. E. Khmel'nitskii. Quantization of hall conductivity. *Soviet Journal of Experimental and Theoretical Physics Letters*, 38(10):552–556, 1983.
- [9] A.M.M. Pruisken. On localization in the theory of the quantized hall effect: A two-dimensional realization of the θ -vacuum. *Nuclear Physics B*, 235(2):277–298, 1984.
- [10] The quantum hall effect. *Graduate Texts in Contemporary Physics*, pages 117–173. Springer, 1990.
- [11] F. D. M. Haldane. Nonlinear Field Theory of Large-Spin Heisenberg Antiferromagnets: Semiclassically Quantized Solitons of the One-Dimensional Easy-Axis Néel State. *Physical Review Letters*, 50(15):1153–1156, 1983.
- [12] Ian Affleck and F. D. M. Haldane. Critical theory of quantum spin chains. *Phys. Rev. B*, 36:5291–5300, Oct 1987.
- [13] F. D. M. Haldane. O(3) nonlinear σ model and the topological distinction between integer- and half-integer-spin antiferromagnets in two dimensions. *Phys. Rev. Lett.*, 61:1029–1032, Aug 1988.
- [14] N. Read and Subir Sachdev. Valence-bond and spin-peierls ground states of low-dimensional quantum antiferromagnets. *Phys. Rev. Lett.*, 62:1694–1697, Apr 1989.
- [15] N. Read and Subir Sachdev. Spin-peierls, valence-bond solid, and néel ground states of low-dimensional quantum antiferromagnets. *Phys. Rev. B*, 42:4568–4589, Sep 1990.
- [16] T. Senthil, Ashvin Vishwanath, Leon Balents, Subir Sachdev, and Matthew P. A. Fisher. Deconfined quantum critical points. *Science*, 303(5663):1490–1494, 2004.
- [17] V L Berezinskii. Destruction of long-range order in one-dimensional and two-dimensional systems having a continuous symmetry group i. classical systems. *Soviet Journal of Experimental and Theoretical Physics*, 32(3):493, 1971.
- [18] V L Berezinskii. Destruction of long-range order in one-dimensional and two-dimensional systems having a continuous symmetry group ii. classical systems. *Soviet Journal of Experimental and Theoretical Physics*, 34(3):610, 1972.

- [19] J M Kosterlitz and D J Thouless. Ordering, metastability and phase transitions in two-dimensional systems. Journal of Physics C: Solid State Physics, 6(7):1181, apr 1973.
- [20] J M Kosterlitz. The critical properties of the two-dimensional xy model. Journal of Physics C: Solid State Physics, 7(6):1046, mar 1974.
- [21] A.M. Polyakov. Interaction of goldstone particles in two dimensions. applications to ferromagnets and massive yang-mills fields. Physics Letters B, 59(1):79–81, 1975.
- [22] E. J. König, P. M. Ostrovsky, I. V. Protodopov, and A. D. Mirlin. Metal-insulator transition in two-dimensional random fermion systems of chiral symmetry classes. Physical Review B, 85(19):195130, 2012.
- [23] Pengwei Zhao and Ryuichi Shindou. Theory of anderson transition in three-dimensional chiral symmetry classes: Connection to type-ii superconductors. Phys. Rev. B, 112:174203, Nov 2025.
- [24] E. Brézin and J. Zinn-Justin. Spontaneous breakdown of continuous symmetries near two dimensions. Phys. Rev. B, 14:3110–3120, Oct 1976.
- [25] Franz Wegner. The mobility edge problem: Continuous symmetry and a conjecture. Zeitschrift für Physik B Condensed Matter, 35(3):207–210, 1979.
- [26] Franz Wegner. Supermathematics and Its Applications in Statistical Physics: Grassmann Variables and the Method of Supersymmetry. Springer, 2016.
- [27] K. B. Efetov, A. I. Larkin, and D. E. Kheml'nitskii. Interaction of diffusion modes in the theory of localization. Journal of Experimental and Theoretical Physics, 52(3):568–574, 1980.
- [28] Shinobu Hikami, Anatoly I. Larkin, and Yosuke Nagaoka. Spin-orbit interaction and magnetoresistance in the two dimensional random system. Progress of Theoretical Physics, 63(2):707–710, 02 1980.
- [29] Sudip Chakravarty, Bertrand I. Halperin, and David R. Nelson. Two-dimensional quantum heisenberg antiferromagnet at low temperatures. Phys. Rev. B, 39:2344–2371, Feb 1989.
- [30] Ferdinand Evers and Alexander D. Mirlin. Anderson transitions. Reviews of Modern Physics, 80(4):1355–1417, 2008.
- [31] Alexander Altland, Dmitry Bagrets, Lars Fritz, Alex Kamenev, and Hanno Schmiedt. Quantum Criticality of Quasi-One-Dimensional Topological Anderson Insulators. Physical Review Letters, 112(20):206602, 2014.
- [32] Pengwei Zhao, Zhenyu Xiao, Yeyang Zhang, and Ryuichi Shindou. Topological effect on the anderson transition in chiral symmetry classes. Phys. Rev. Lett., 133:226601, Nov 2024.
- [33] L Onsager. Statistical hydrodynamics. Nuovo Cimento Suppl, 6:279–287, March 1949.
- [34] R. P. Feynman. Chapter ii application of quantum mechanics to liquid helium. volume 1 of Progress in Low Temperature Physics, pages 17–53. Elsevier, 1955.
- [35] V. N. Popov. Quantum vortices and phase transitions in bose systems. Soviet Physics – JETP, 37:341, 1973.
- [36] Matthew P. A. Fisher, Peter B. Weichman, G. Grinstein, and Daniel S. Fisher. Boson localization and the superfluid-insulator transition. Phys. Rev. B, 40:546–570, Jul 1989.
- [37] V Emery and S Kivelson. Importance of phase fluctuations in superconductors with small superfluid density. Nature, 374:434–437, March 1995.
- [38] Path integrals. NATO advanced study institutes, pages 419–454. Springer, 1978.
- [39] Laurence Jacobs, Jorge V. José, and M. A. Novotny. First-order reentrant transition in granular superconducting films. Phys. Rev. Lett., 53:2177–2180, Nov 1984.
- [40] Igor Herbut. A Modern Approach to Critical Phenomena. Cambridge University Press, 2007.
- [41] Matthew P. A. Fisher and D. H. Lee. Correspondence between two-dimensional bosons and a bulk superconductor in a magnetic field. Phys. Rev. B, 39:2756–2759, Feb 1989.
- [42] Akihiro Tanaka and Shintaro Takayoshi. A short guide to topological terms in the effective theories of condensed matter. Science and Technology of Advanced Materials, 16(1):014404, 2015.
- [43] M. Ma, B. I. Halperin, and P. A. Lee. Strongly disordered superfluids: Quantum fluctuations and critical behavior. Phys. Rev. B, 34:3136–3143, Sep 1986.
- [44] T. Giamarchi and H. J. Schulz. Localization and interaction in one-dimensional quantum fluids. Europhysics Letters, 3(12):1287, jun 1987.
- [45] T. Giamarchi and H. J. Schulz. Anderson localization and interactions in one-dimensional metals. Phys. Rev. B, 37:325–340, Jan 1988.
- [46] Matteo Ciardi, Adriano Angelone, Fabio Mezzacapo, and Fabio Cinti. Quasicrystalline bose glass in the absence of disorder and quasidisorder. Phys. Rev. Lett., 131:173402, Oct 2023.
- [47] Zhaoxuan Zhu, Hepeng Yao, and Laurent Sanchez-Palencia. Thermodynamic phase diagram of two-dimensional bosons in a quasicrystal potential. Phys. Rev. Lett., 130:220402, May 2023.
- [48] T. Banks, R. Myerson, and J. Kogut. Phase transitions in abelian lattice gauge theories. Nuclear Physics B, 129(3):493–510, 1977.
- [49] Martin B. Einhorn and Robert Savit. Topological excitations in the abelian higgs model. Phys. Rev. D, 17:2583–2594, May 1978.
- [50] Robert Savit. Vortices and the low-temperature structure of the $x-y$ model. Phys. Rev. B, 17:1340–1350, Feb 1978.
- [51] Michael E Peskin. Mandelstam-'t hooft duality in abelian lattice models. Annals of Physics, 113(1):122–152, 1978.
- [52] Robert Savit. Duality in field theory and statistical systems. Rev. Mod. Phys., 52:453–487, Apr 1980.
- [53] Michael Kiometzis, Hagen Kleinert, and Adriaan M. J. Schakel. Dual description of the superconducting phase transition. Fortschritte der Physik/Progress of Physics, 43(8):697–732, 1995.
- [54] G. Blatter, M. V. Feigel'man, V. B. Geshkenbein, A. I. Larkin, and V. M. Vinokur. Vortices in high-temperature superconductors. Rev. Mod. Phys., 66:1125–1388, Oct 1994.
- [55] D. Huse, M. P. A. Fisher, and D. Fisher. Are superconductors really superconducting ? Nature, 358:553–559, Aug 1992.
- [56] Matthew P. A. Fisher. Vortex-glass superconductivity: A possible new phase in bulk high- t_c oxides. Phys. Rev. Lett., 62:1415–1418, Mar 1989.
- [57] A. A. Abrikosov. On the magnetic properties of superconductors of the second group. Soviet Phys. JETP, 5:1174, 1957.
- [58] A. I. Larkin. Effect of inhomogeneties on the structure of the mixed state of superconductors. Soviet Phys. JETP, 31:784, 1970.

- [59] David R. Nelson. Vortex entanglement in high- T_c superconductors. *Phys. Rev. Lett.*, 60:1973–1976, May 1988.
- [60] David R. Nelson and H. Sebastian Seung. Theory of melted flux liquids. *Phys. Rev. B*, 39:9153–9174, May 1989.
- [61] H. Safar, P. L. Gammel, D. A. Huse, D. J. Bishop, J. P. Rice, and D. M. Ginsberg. Experimental evidence for a first-order vortex-lattice-melting transition in untwinned, single crystal $\text{YBa}_2\text{Cu}_3\text{O}_7$. *Phys. Rev. Lett.*, 69:824–827, Aug 1992.
- [62] H. Pastoriza, M. F. Goffman, A. Arribère, and F. de la Cruz. First order phase transition at the irreversibility line of $\text{Bi}_2\text{Sr}_2\text{CaCu}_2\text{O}_8$. *Phys. Rev. Lett.*, 72:2951–2954, May 1994.
- [63] R. A. Doyle, D. Liney, W. S. Seow, A. M. Campbell, and K. Kadowaki. First-order decoupling transition in the vortex lattice of $\text{Bi}_2\text{Sr}_2\text{CaCu}_2\text{O}_8$ from local mutual inductance measurements. *Phys. Rev. Lett.*, 75:4520–4523, Dec 1995.
- [64] E. Zeldov, D. Majer, M. Konczykowski, V. B. Geshkenbein, V. M. Vinokur, and H. Shtrikman. Thermodynamic observation of first-order vortex-lattice melting transition. *Nature*, 375:373–376, 1995.
- [65] A. Schilling, R. A. Fisher, N. E. Phillips, U. Welp, D. Dasgupta, W. K. Kwok, and G. W. Crabtree. Calorimetric measurement of the latent heat of vortex-lattice melting in untwinned $\text{YBa}_2\text{Cu}_3\text{O}_{7-\delta}$. *Nature*, 382:791–793, Aug 1996.
- [66] R. E. Hetzel, A. Sudbø, and D. A. Huse. First-order melting transition of an abrikosov vortex lattice. *Phys. Rev. Lett.*, 69:518–521, Jul 1992.
- [67] Anh Kiet Nguyen, A. Sudbø, and R. E. Hetzel. Vortex-loop unbinding and flux-line lattice melting in superconductors. *Phys. Rev. Lett.*, 77:1592–1595, Aug 1996.
- [68] A. K. Nguyen and A. Sudbø. Onsager loop transition and first-order flux-line lattice melting in high- T_c superconductors. *Phys. Rev. B*, 57:3123–3143, Feb 1998.
- [69] A. K. Nguyen and A. Sudbø. Phase coherence and the boson analogy of vortex liquids. *Phys. Rev. B*, 58:2802–2815, Aug 1998.
- [70] Seungoh Ryu and David Stroud. Nature of the low-field transition in the mixed state of high-temperature superconductors. *Phys. Rev. B*, 57:14476–14497, Jun 1998.
- [71] A. K. Nguyen and A. Sudbø. Topological phase fluctuations, amplitude fluctuations, and criticality in extreme type-II superconductors. *Phys. Rev. B*, 60:15307–15331, Dec 1999.
- [72] F.W. Wiegel. Vortex-ring model of bose condensation. *Physica*, 65(2):321–336, 1973.
- [73] Vincent Kotsubo and Gary A. Williams. Superfluid transition of ^4He films adsorbed in porous materials. *Phys. Rev. B*, 33:6106–6122, May 1986.
- [74] Gary A. Williams. Vortex-ring model of the superfluid λ transition. *Phys. Rev. Lett.*, 59:1926–1929, Oct 1987.
- [75] Subodh R. Shenoy. Vortex-loop scaling in the three-dimensional xy ferromagnet. *Phys. Rev. B*, 40:5056–5068, Sep 1989.
- [76] Wolfhard Janke and Tetsuo Matsui. Crossover in the xy model from three to two dimensions. *Phys. Rev. B*, 42:10673–10681, Dec 1990.
- [77] Gary A. Williams. Vortex dynamics and superfluid relaxation near the ^4He λ transition. *Phys. Rev. Lett.*, 71:392–395, Jul 1993.
- [78] Biplab Chattopadhyay and Subodh R. Shenoy. Kosterlitz-thouless signatures from 3d vortex loops in layered superconductors. *Phys. Rev. Lett.*, 72:400–403, Jan 1994.
- [79] Gary A. Williams. Vortex-loop phase transitions in liquid helium, cosmic strings, and high- T_c superconductors. *Phys. Rev. Lett.*, 82:1201–1204, Feb 1999.
- [80] Gary A. Williams. Vortex fluctuations in the critical casimir effect of superfluid and superconducting films. *Phys. Rev. Lett.*, 92:197003, May 2004.
- [81] Paul M Goldbart and Florin Bora. Quantized vortices and superflow in arbitrary dimensions: structure, energetics and dynamics. *Journal of Physics A: Mathematical and Theoretical*, 42(18):185001, apr 2009.
- [82] See Supplemental Material for details of the vortex membrane model for the general D -dimensional $U(1)$ NLsM with temporal Berry phase χ , renormalization group (RG) analyses of the vortex membrane model, $\epsilon = D - 2$ expansion analysis of the vortex membrane model around $\chi = 0$, $D = 2$ RG analysis in the presence of χ , $D = 3$ RG analysis in the presence of χ , and further considerations on the vortex fugacity renormalization.
- [83] Ryuichi Shindou and Pengwei Zhao. Topological effect on order-disorder transitions in $u(1)$ sigma models. *Phys. Rev. B*, 111:224507, Jun 2025.
- [84] John Cardy. *Scaing and Renormalization in Statistical Physics*. Cambridge University Press, Cambridge, 1996.
- [85] Thierry Giamarchi. *Quantum Physics in One Dimension*. Oxford University Press, Oxford, 2003.
- [86] Igor F. Herbut and Zlatko Tešanović. Critical fluctuations in superconductors and the magnetic field penetration depth. *Phys. Rev. Lett.*, 76:4588–4591, Jun 1996.
- [87] Peter Olsson and S. Teitel. Critical behavior of the meissner transition in the lattice london superconductor. *Phys. Rev. Lett.*, 80:1964–1967, Mar 1998.
- [88] Theodore Frankel. *The Geometry of Physics, An Introduction (second edition)*. Cambridge University Press, 2004.

**SUPPLEMENTAL MATERIAL FOR “TEMPORAL BERRY PHASE AND THE EMERGENCE OF
BOSE-GLASS-ANALOG PHASE IN A CLEAN U(1) SUPERFLUID”**

U(1) nonlinear sigma model (NLSM) with a Berry phase term in $D = d + 1$ dimension describes a zero-temperature partition function for d -dim. phase-fluctuation-driven superfluid (SF) transitions, where SF phase fluctuates in space r and time τ , while SF amplitude is constrained around a finite value by a certain physical mechanism. The Berry phase term along the time direction originates from a quantum-mechanical commutation relation between SF amplitude and phase. An ordered-disordered phase transition of the model is driven by a spatial proliferation of vortex excitations, where the Berry phase term confers a complex phase factor upon the partition function with the vortex excitations, possibly altering a nature of the disordered phase through an interference effect caused by the complex phase factor. In this supplemental material, we map the U(1) NLSM into a D -dimensional generalization of the Maxwell action, whose electromagnetic field couples with vortex excitations, mediating the long-ranged $1/|x|^{D-2}$ Coulomb interaction between vortex hypersurface elements. Based on this dual model, we derive a renormalization group (RG) equation of the phase-fluctuation-driven SF transition, where the screening of smaller vortex hypersurfaces renormalizes the electromagnetic constitutive constant in the Maxwell action, and the short-range part of the Maxwell action renormalizes the vortex fugacity. By analyzing the scaling property of the RG equation around a saddle-fixed point using the authentic $\epsilon \equiv D - 2$ expansion, we obtain the critical exponent ν and scaling dimension y_χ of the Berry phase parameter χ around the phase transition at $\chi = 0$. Using the $D = 3$ RG equation, we clarify that the screening effect in the presence of the Berry phase term yields a space-time anisotropy in the constitutive constant of the Maxwell action, while the space-time anisotropy polarizes vortex lines locally along the τ direction. Our numerical solutions of the $D = 3$ RG equation demonstrate that the phase transition at $\chi \neq 0$ is driven by the proliferation of the vortex lines along τ , indicating the emergence of the quasi-disordered phase next to the ordered phase. In the quasi-disordered phase, the SF phase correlation time is divergent, while correlation length is finite.

I. U(1) NLSM AND ITS DUAL FORM

The U(1) NLSM with the 1-dimensional Berry phase term is given by

$$Z = \exp \left[-\frac{1}{2g} \int d^D \mathbf{x} \nabla \theta \cdot \nabla \theta - i\chi \int d^D \mathbf{x} \partial_\tau \theta \right]. \quad (\text{I.1})$$

with $\mathbf{x} = (\tau, \mathbf{r})$, $\nabla \equiv (\partial_\tau, \partial_\mathbf{r})$, and U(1) phase $\theta(\mathbf{x})$. The Berry phase term χ originates from a quantum-mechanical commutation relation between the amplitude and phase of the superfluid (SF) order parameter, while the SF amplitude is constrained to a finite value by a specific physical mechanism. Quantum fluctuation parameter g plays the role of a coupling constant in the model. The perturbative β function for the coupling constant has no disordering effect in general D , indicating that the phase transition to its disordered phase is entirely driven by the vortex proliferation associated with the U(1) phase. To analyze this topological phase transition for the general D dimension, we can decompose the phase gradient vector $\nabla \theta$ into a gradient field $\nabla \phi$ and a solenoidal field \mathbf{b} with $\nabla \cdot \mathbf{b} = 0$ and $\oint \nabla \phi \cdot d\mathbf{l} = 0$,

$$\nabla \theta = \mathbf{b} + \nabla \phi. \quad (\text{I.2})$$

The gradient and solenoidal fields constitute the spin-wave part Z_{sw} and the vortex part Z_{v} of the partition function, respectively.

$$\begin{aligned} Z &= Z_{\text{sw}} Z_{\text{v}}, \\ Z_{\text{sw}} &= \int \mathcal{D}\phi \exp \left[-\frac{1}{2g} \int d^D \mathbf{x} \nabla \phi \cdot \nabla \phi \right], \\ Z_{\text{v}} &= \int \mathcal{D}\mathbf{b} \exp \left[-\frac{1}{2g} \int d^D \mathbf{x} \mathbf{b} \cdot \mathbf{b} - i\chi \int d^D \mathbf{x} b_\tau \right]. \end{aligned} \quad (\text{I.3})$$

In the case of $D = 2$, the vortex excitation forms pairs of a vortex and an antivortex, and the space-time rotation of the solenoidal field is characterized by a dipole vector,

$$\partial_\tau b_1(\mathbf{x}) - \partial_1 b_\tau(\mathbf{x}) = 2\pi \sum_j (\delta^2(\mathbf{x} - \mathbf{R}_{j,\text{v}}) - \delta^2(\mathbf{x} - \mathbf{R}_{j,\text{av}})). \quad (\text{I.4})$$

Here $\mathbf{R}_{j,v}$ and $\mathbf{R}_{j,av}$ are the two-dimensional coordinates of the vortex and antivortex in the j th dipole vector. For $D = 3$, the vortex excitation forms a closed loop, and the rotation of the solenoidal field, $v_{\mu\nu}(\mathbf{x}) \equiv \partial_\mu b_\nu(\mathbf{x}) - \partial_\nu b_\mu(\mathbf{x})$, becomes nothing but a vortex field with a quantized flux line along the loop,

$$\begin{aligned} v_{\mu\nu}(\mathbf{x}) &\equiv \epsilon_{\mu\nu\lambda} J_\lambda(\mathbf{x}), \\ J_\lambda(\mathbf{x}) &= 2\pi \sum_j \int_{\partial\Gamma_j} ds \frac{\partial R_{j,\lambda}(s)}{ds} \delta^3(\mathbf{x} - \mathbf{R}_j(s)). \end{aligned} \quad (\text{I.5})$$

Here $\partial\Gamma_j$ is the j -th closed vortex loop, whose element is parameterized by the one-dimensional parameter s as $\mathbf{R}_j(s)$. The vortex excitation for $D \geq 4$ generally forms a $(D-2)$ -dimensional closed hyper-surface, and $\partial\Gamma_j$ becomes a j -th closed vortex hyper-surface, whose space-time coordinate $\mathbf{R}_j(\mathbf{s})$ is parameterized by $(D-2)$ variables $\mathbf{s} \equiv (s_1, s_2, \dots, s_{D-2})$. Thereby, the exterior derivative of the solenoidal field is given by an $(D-2)$ -dimensional \mathbf{s} -integral of the quantized flux over the vortex hyper-surface,

$$v_{\mu\nu}(\mathbf{x}) \equiv \epsilon_{\mu\nu\lambda\rho\cdots\sigma} \frac{J_{\lambda\rho\cdots\sigma}(\mathbf{x})}{(D-2)!}, \quad (\text{I.6})$$

$$J_{\lambda\rho\cdots\sigma}(\mathbf{x}) \equiv 2\pi \sum_j \int_{\partial\Gamma_j} d^{D-2}\mathbf{s} \epsilon_{ab\cdots c} \left(\frac{\partial R_{j,\lambda}(\mathbf{s})}{\partial s_a} \frac{\partial R_{j,\rho}(\mathbf{s})}{\partial s_b} \cdots \frac{\partial R_{j,\sigma}(\mathbf{s})}{\partial s_c} \right) \delta^D(\mathbf{x} - \mathbf{R}_j(\mathbf{s})). \quad (\text{I.7})$$

Here $\epsilon_{\mu\nu\cdots}$ and $\epsilon_{ab\cdots}$ are antisymmetric tensors in the D -dimensional and $(D-2)$ -dimensional spaces, respectively. The quantized flux for $D \geq 4$ takes the form of a D -dimensional antisymmetric tensor, and it is given by a product between the delta function, $\delta^D(\mathbf{x} - \mathbf{R}_j(\mathbf{s}))$, and an oriented volume $\mathbf{g}_j(\mathbf{s})$ of a parallelepiped at $\mathbf{R}_j(\mathbf{s})$,

$$\mathbf{g}_{j,\lambda\rho\cdots\sigma}(\mathbf{s}) \equiv \sum_{a,b,\cdots,c=1,2,\cdots,D-2} \epsilon_{ab\cdots c} \left(\frac{\partial R_{j,\lambda}(\mathbf{s})}{\partial s_a} \frac{\partial R_{j,\rho}(\mathbf{s})}{\partial s_b} \cdots \frac{\partial R_{j,\sigma}(\mathbf{s})}{\partial s_c} \right). \quad (\text{I.8})$$

Here, the parallelepiped is formed by the $(D-2)$ linearly independent vectors, $\partial\mathbf{R}_j(\mathbf{s})/\partial s_a$ ($a = 1, \dots, D-2$), that are tangential to the vortex hyper-surface at $\mathbf{R}_j(\mathbf{s})$. In this paper, we consider only vortex excitations with the 2π vorticity, as vortex excitations with higher vorticity can be expressed as a sum of vortex excitations with the 2π vorticity.

The vortex part of the partition function is given by a sum over possible space-time configurations of multiple vortex hyper-spheres. To this end, the \mathbf{b}^2 term is decomposed by a dual field $\boldsymbol{\varphi}$,

$$Z_v = \int \mathcal{D}\mathbf{b} \int \mathcal{D}\boldsymbol{\varphi} \exp \left[- \int d^D\mathbf{x} \left(\frac{1}{2} \varphi_\mu^2 + \frac{i}{\sqrt{g}} \varphi_\mu b_\mu + i\chi b_\tau \right) \right]. \quad (\text{I.9})$$

The solenoidal field is divergence free; so is the auxiliary field $\boldsymbol{\varphi}$. Such a one-form field can be derived from a two-form field by the Hodge star. Namely, the auxiliary field can be represented by an antisymmetric tensor $u_{\mu\nu} = -u_{\nu\mu}$ as $\varphi_\nu = \partial_\mu u_{\mu\nu}$.

$$Z_v = \int \mathcal{D}\mathbf{b} \int \mathcal{D}\mathbf{u} \exp \left[- \int d^D\mathbf{r} \left[\frac{1}{2} (\partial_\mu u_{\mu\nu})(\partial_\lambda u_{\lambda\nu}) - \frac{i}{2\sqrt{g}} u_{\mu\nu} (\partial_\mu b_\nu - \partial_\nu b_\mu) + i\chi b_\tau \right] \right]. \quad (\text{I.10})$$

For $D = 2$, the $u_{\mu\nu}$ reduces to a scalar potential, $u_{\tau 1} = -u_{1\tau} = \phi_E$, where the first term becomes an electric part $(\nabla\phi_E)^2$ of the Maxwell action, and the coupling between $u_{\mu\nu}$ and $v_{\mu\nu}$ becomes the electric coupling between the scalar potential and electric charge. For $D = 3$, the antisymmetric tensor reduces to a magnetic vector potential $u_{\mu\nu} = \epsilon_{\mu\nu\lambda} a_\lambda$, where the $(\partial u)^2$ term becomes a magnetic part of the Maxwell action, and the $u_{\mu\nu} v_{\mu\nu}$ term becomes the magnetic coupling between the vector potential and the electric current. These suggest that the antisymmetric tensor $u_{\mu\nu}$, the $(\partial u)^2$ term, and the coupling constant $e \equiv 1/\sqrt{g}$ can be regarded as higher-dimensional ($D \geq 4$) generalizations of the dual vector potentials, the Maxwell term, and the electric charge in electromagnetism, respectively.

In the presence of the vortex excitations, the Berry phase term endows the partition function with a complex phase factor. Namely, the integral over the imaginary time τ can be taken in $\int d^D\mathbf{x} \partial_\tau \theta(\mathbf{x})$, yielding the phase factor proportional to a $(D-1)$ -dimensional volume $\mathcal{A}_{\tau,j}$ inside the vortex hyper-surface *projected* to a $\tau = \text{constant}$ plane,

$$\mathcal{A}_{\tau,j} \equiv \int_{(\tau,\mathbf{r}) \in \Gamma_j} d^{D-1}\mathbf{r}, \quad (\text{I.11})$$

with $\int d^D \mathbf{x} b_\tau(\mathbf{x}) = 2\pi \sum_j \mathcal{A}_{\tau,j}$.

As the right hand side of Eq. (I.10) is given only by the space-time coordinates of the $(D-2)$ -dimensional vortex hyper-surface, the integral over $\mathbf{b}(\mathbf{x})$ can be rewritten into a sum over all possible space-time configurations of vortex hyper-surfaces,

$$Z_v = \int \mathcal{D}\mathbf{u} \exp \left[-\frac{1}{2} \int d^D \mathbf{x} (\partial_\mu u_{\mu\nu})(\partial_\lambda u_{\lambda\nu}) \right] \left\{ 1 + \sum_{N=1}^{\infty} \frac{1}{N!} \prod_{j=1}^N \left(\int \mathcal{D}^D \mathbf{X}_j \int \mathcal{D}^D \mathbf{Y}_j \int \mathcal{D}\mathbf{g}_j(\mathbf{s}) \exp [E_j] \right) \exp \left[-\frac{i}{2} e \int d^D \mathbf{x} u_{\mu\nu}(\mathbf{x}) v_{\mu\nu}(\mathbf{x}) - i2\pi\chi \sum_j \mathcal{A}_{\tau,j} \right] \right\}. \quad (\text{I.12})$$

Here $\exp[E_j]$ and \mathbf{X}_j denote the fugacity and the center of mass of the j th vortex hyper-surface, respectively, while $\mathbf{Y}_j/2$ is a vector connecting the center of mass and one of vortex hyper-surface elements, $\mathbf{R}_j(\mathbf{s}=0)$. The integral over the oriented volume $\mathbf{g}_j(\mathbf{s})$ of the parallelepiped element is taken at every \mathbf{s} on the j th hyper-surface. The integral over $\mathbf{g}_j(\mathbf{s})$ enumerates all shapes of the hyper-surface. We choose the surface element at $\mathbf{s}=0$ to be the closest to the center of mass, $|\mathbf{R}_j(\mathbf{s}) - \mathbf{X}_j| \geq |\mathbf{R}_j(\mathbf{s}=0) - \mathbf{X}_j| = |\mathbf{Y}_j|/2$. For typical vortex hyper-surfaces, $|\mathbf{Y}_j|$ can be regarded as a linear dimension of the hyper-surface size. Note that the integral over $\mathbf{g}_{j,\lambda\rho\dots\sigma}(\mathbf{s})$ has no scaling dimension, as both \mathbf{s} and $\mathbf{R}_j(\mathbf{s})$ have the length-scale dimension in Eq. (I.8). For $D=2$, $\mathbf{X}_j \pm \mathbf{Y}_j/2$ are the coordinates of vortex and antivortex in the j th pair, respectively, so that the configurational integral for $D=2$ is given only by $\prod_{j=1}^N (\int \mathcal{D}^2 \mathbf{X}_j \int \mathcal{D}^2 \mathbf{Y}_j)$. In order to make the right hand side to be dimensionless, we normalize \mathbf{X}_j and \mathbf{Y}_j by an ultraviolet (UV) cutoff length scale a_0 ,

$$\int \mathcal{D}^D \mathbf{X}_j \equiv \frac{1}{a_0^D} \int d^D \mathbf{X}_j, \quad \int \mathcal{D}^D \mathbf{Y}_j \equiv \frac{1}{a_0^D} \int d^D \mathbf{Y}_j. \quad (\text{I.13})$$

The symmetry factor of $1/N!$ in Eq. (I.12) accounts for the multiple counting of an identical configuration that comes from $\prod_{j=1}^N (\int \mathcal{D}^D \mathbf{X}_j \int \mathcal{D}^D \mathbf{Y}_j \int \mathcal{D}\mathbf{g}_j(\mathbf{s}))$.

In the case of $D=2$, a Gaussian integration over $u_{\mu\nu}$ leads to the 2D logarithmic Coulomb interaction between vortices. For $D \geq 3$, a Gaussian integration over the dual vector potential yields the $1/|\mathbf{x}-\mathbf{x}'|^{D-2}$ Coulomb interaction between two parallelepiped elements at \mathbf{x} and \mathbf{x}' on a closed vortex hyper-surface. When \mathbf{x}' is further integrated over the $(D-2)$ -dimensional surface, the interaction leads to a logarithmic divergence from $\mathbf{x}' \simeq \mathbf{x}$. To regularize these logarithmic ultraviolet (UV) divergences in $D \geq 2$, we introduce a UV cutoff in the momentum-energy integral for the Maxwell action and introduce a UV cutoff for the size of the j th vortex hyper-surface $|\mathbf{Y}_j|$:

$$\begin{aligned} \int d^D \mathbf{x} (\partial_\mu u_{\mu\nu}(\mathbf{x}))(\partial_\lambda u_{\lambda\nu}(\mathbf{x})) &= \int_{|\mathbf{k}| < \Lambda} \frac{d^D \mathbf{k}}{(2\pi)^D} k_\mu k_\lambda u_{\mu\nu}(\mathbf{k}) u_{\lambda\nu}(-\mathbf{k}), \\ \int d^D \mathbf{x} u_{\mu\nu}(\mathbf{x}) v_{\mu\nu}(\mathbf{x}) &= \int_{|\mathbf{k}| < \Lambda} \frac{d^D \mathbf{k}}{(2\pi)^D} u_{\mu\nu}(\mathbf{k}) v_{\mu\nu}(-\mathbf{k}), \\ \int \mathcal{D}^D \mathbf{Y}_j &= \int_{|\mathbf{Y}_j| > a_0} \mathcal{D}^D \mathbf{Y}_j. \end{aligned} \quad (\text{I.14})$$

The Coulomb interaction mediated by the vector potential with $|\mathbf{k}| > \Lambda$ is considered to be included in the vortex core energy E_j [see section II B].

The vortex excitations for $D=2$ are point defects, where the vortex fugacity is parameterized by a scalar constant: $E_j = w$. For $D \geq 3$, the vortex excitation has a finite $(D-2)$ -dimensional volume. Thereby, in addition to the constant w , the vortex core energy E_j must also have a term that depends on the volume and local geometry of the vortex hyper-surface. In the case of the space-time isotropic system without the Berry phase term [$\chi = 0$], the additional fugacity term is proportional to the $(D-2)$ -dimensional volume of the vortex hyper-surface, i.e.

$$E_j = w + t \int_{\partial\Gamma_j} d^{D-2} \mathbf{s} \sqrt{\det \hat{\mathbf{g}}_j(\mathbf{s})} \quad \text{for } \chi = 0. \quad (\text{I.15})$$

Here, $(D-2) \times (D-2)$ real symmetric matrix $\hat{\mathbf{g}}_j(\mathbf{s})$ is the first fundamental form,

$$[\hat{\mathbf{g}}_j(\mathbf{s})]_{ab} \equiv \sum_{\mu=\tau,1,2,\dots,D-1} \frac{\partial R_{j,\mu}(\mathbf{s})}{\partial s_a} \frac{\partial R_{j,\mu}(\mathbf{s})}{\partial s_b}, \quad (\text{I.16})$$

for $a, b = 1, \dots, D-2$. Note that the volume of a hyper-surface is generally given by the \mathbf{s} -integral of the square-root of the determinant of its first fundamental form [81, 88]. In the case of the space-time anisotropic case with finite χ , E_j is parameterized by a vortex core energy density, which is a function of time component $\hat{\mathbf{g}}_{j,\tau}$ and spatial component $\hat{\mathbf{g}}_{j,r}$ of the metric tensor,

$$E_j \equiv w + \int_{\partial\Gamma_j} d^{D-2}\mathbf{s} \, t(\hat{\mathbf{g}}_{j,\tau}(\mathbf{s}), \hat{\mathbf{g}}_{j,r}(\mathbf{s})), \quad \text{for } \chi \neq 0. \quad (\text{I.17})$$

These metric tensors take the $(D-2) \times (D-2)$ real symmetric matrices,

$$[\hat{\mathbf{g}}_{j,\tau}(\mathbf{s})]_{ab} \equiv \frac{\partial R_{j,\tau}(\mathbf{s})}{\partial s_a} \frac{\partial R_{j,\tau}(\mathbf{s})}{\partial s_b}, \quad [\hat{\mathbf{g}}_{j,r}(\mathbf{s})]_{ab} \equiv \sum_{\mu=1,2,\dots,D-1} \frac{\partial R_{j,\mu}(\mathbf{s})}{\partial s_a} \frac{\partial R_{j,\mu}(\mathbf{s})}{\partial s_b}, \quad (\text{I.18})$$

which are invariant under arbitrary $O(D-1)$ rotation of the spatial coordinate \mathbf{r} [$(\tau, \mathbf{r}) \rightarrow (\tau, \tilde{\mathbf{r}})$ with $\tilde{\mathbf{r}} = O(D-1) \cdot \mathbf{r}$] as well as under the mirror with respect to the time [$(\tau, \mathbf{r}) \rightarrow (-\tau, \mathbf{r})$]. Thus, the fugacity parameter E_j is also invariant under the spatial rotation and/or the mirror operation of the vortex hyper-surface. In Sec. IIB, we will justify Eqs. (I.15, I.17) by deriving the fugacity renormalization for these cases.

In the presence of the Berry phase term χ , the electromagnetic constitutive constant in the Maxwell action acquires the space-time anisotropy through the screening effect of smaller vortex excitations [see Sec. IIA]. Thus, we include the space-time anisotropy parameter γ_τ into the Maxwell action,

$$\begin{aligned} Z_v = & \int \mathcal{D}\mathbf{u} \exp \left[-\frac{1}{2} \int_{|\partial u| < \Lambda|u|} d^D\mathbf{x} \left\{ \gamma_\tau (\partial_\mu u_{\mu\tau}) (\partial_\lambda u_{\lambda\tau}) + \sum_{\nu=1}^{D-1} (\partial_\mu u_{\mu\nu}) (\partial_\lambda u_{\lambda\nu}) \right\} \right] \\ & \left\{ 1 + \sum_{N=1}^{\infty} \frac{1}{N!} \prod_{j=1}^N \left(\int \mathcal{D}^D\mathbf{X}_j \int_{|\mathbf{Y}_j| > a_0} \mathcal{D}^D\mathbf{Y}_j \int \mathcal{D}\mathbf{g}_j(\mathbf{s}) \exp[E_j] \right) \right. \\ & \left. \exp \left[-\frac{i}{2} e \int_{|\partial u| < \Lambda|u|} d^D\mathbf{x} \, u_{\mu\nu}(\mathbf{x}) v_{\mu\nu}(\mathbf{x}) - i2\pi\chi \sum_j \mathcal{A}_{\tau,j} \right] \right\}, \end{aligned} \quad (\text{I.19})$$

with

$$\begin{aligned} \int_{|\partial u| < \Lambda|u|} d^D\mathbf{x} (\partial_\mu u_{\mu\nu}(\mathbf{x})) (\partial_\lambda u_{\lambda\nu}(\mathbf{x})) & \equiv \int_{|\mathbf{k}| < \Lambda} \frac{d^D\mathbf{k}}{(2\pi)^D} k_\mu u_{\mu\nu}(\mathbf{k}) k_\lambda u_{\lambda\nu}(-\mathbf{k}), \\ \int_{|\partial u| < \Lambda|u|} d^D\mathbf{x} u_{\mu\nu}(\mathbf{x}) v_{\mu\nu}(\mathbf{x}) & \equiv \int_{|\mathbf{k}| < \Lambda} \frac{d^D\mathbf{k}}{(2\pi)^D} u_{\mu\nu}(\mathbf{k}) v_{\mu\nu}(-\mathbf{k}). \end{aligned} \quad (\text{I.20})$$

II. RENORMALIZATION GROUP THEORY

The partition function Eq. (I.19) can be studied using renormalization group (RG) analyses, where short-distance degrees of freedom are recursively integrated out. Since the tree-level scaling dimension of the electric constant e is $(D-2)/2$, and the RG equation for $\chi = 0$ has a stable fixed point at $e^2 \simeq \mathcal{O}(\epsilon)$ for $D = 2 + \epsilon$ [see section IIIA], we regard e as a small quantity and treat the coupling constant perturbatively in the renormalization group analysis. The perturbative treatment is justified for $D \gtrsim 2$.

A. one-loop renormalization to the constitutive constants and Berry phase term

In Eq. (I.19), the UV cutoff length appears in (i) the integral over the vortex surface size $|\mathbf{Y}_j|$, and in (ii) the momentum integral in the Maxwell term. Following the previous work [19, 20, 74, 75, 83], we first decompose the configuration sum over each vortex surface into a smallest vortex-surface case and larger vortex-surface case,

$$\int_{|\mathbf{Y}_j| > a_0} \mathcal{D}^D\mathbf{Y}_j = \int_{|\mathbf{Y}_j| > a_0 b} \mathcal{D}^D\mathbf{Y}_j + \int_{a_0 b > |\mathbf{Y}_j| > a_0} \mathcal{D}^D\mathbf{Y}_j. \quad (\text{II.1})$$

Here b stands for a renormalization scale parameter with $\ln b \gtrsim 1$. In the hyper-cubic lattice with the lattice constant a_0 , the vortex surface in the smallest vortex surface case becomes a $(D-2)$ -dimensional unit hyper-cubic plaquette.

To mimic such a hyper-cubic plaquette in the continuum model, we consider a symmetric $(D-2)$ -sphere with diameter a_0 as the smallest surface. Suppose that \mathbf{e}_0 is a unit vector normal to a plane in which the $(D-2)$ -sphere lies. Then, the configuration sum of the smallest vortex surface is given by an integral of its center of mass, and an integral of \mathbf{e}_0 over the $(D-1)$ -sphere S_{D-1} ,

$$\int \mathcal{D}^D \mathbf{X}_j \int_{a_0 < |\mathbf{Y}_j| < a_0 b} \mathcal{D}^D \mathbf{Y}_j \int \mathcal{D} \mathbf{g}_j(\mathbf{s}) \simeq a_0^{-2D} \int d^D \mathbf{X}_j \int_{a_0}^{a_0 b} Y_j^{D-1} dY_j \int_{S_{D-1}} \mathcal{D}^{D-1} \mathbf{e}_0. \quad (\text{II.2})$$

By substituting Eq. (II.1,II.2) into Eq. (I.19) and keeping only the first order in $\ln b$, we obtain

$$\begin{aligned} Z_v &= \int \mathcal{D} \mathbf{u} \exp \left[-\frac{1}{2} \int_{|\partial u| < \Lambda |u|} d^D \mathbf{x} \left\{ \gamma_\tau (\partial_\mu u_{\mu\tau}) (\partial_\lambda u_{\lambda\tau}) + \sum_{\nu=1}^{D-1} (\partial_\mu u_{\mu\nu}) (\partial_\lambda u_{\lambda\nu}) \right\} \right] \\ &\quad \left\{ 1 + \sum_{N=1}^{\infty} \frac{1}{N!} \prod_{j=1}^N \left(\int \mathcal{D}^D \mathbf{X}_j \int_{|\mathbf{Y}_j| > a_0 b} \mathcal{D}^D \mathbf{Y}_j \int \mathcal{D} \mathbf{g}_j(\mathbf{s}) \exp [E_j] \right) \right. \\ &\quad \left. \exp \left[-\frac{i}{2} e \int_{|\partial u| < \Lambda |u|} d^D \mathbf{x} u_{\mu\nu}(\mathbf{x}) v_{\mu\nu}(\mathbf{x}) - i2\pi\chi \sum_j \mathcal{A}_{\tau,j} \right] \right\} + \ln b Z'_v. \end{aligned} \quad (\text{II.3})$$

Here Z'_v contributes to the one-loop renormalization to Z_v , and it is given by

$$\begin{aligned} Z'_v &= \int \mathcal{D} \mathbf{u} \exp \left[-\frac{1}{2} \int_{|\partial u| < \Lambda |u|} d^D \mathbf{x} \left\{ \gamma_\tau (\partial_\mu u_{\mu\tau}) (\partial_\lambda u_{\lambda\tau}) + \sum_{\nu=1}^{D-1} (\partial_\mu u_{\mu\nu}) (\partial_\lambda u_{\lambda\nu}) \right\} \right] \\ &\quad \int \mathcal{D}^D \mathbf{X}_0 \int_{S_{D-1}} \mathcal{D}^{D-1} \mathbf{e}_0 \exp [E_0 - i2\pi\chi \mathcal{A}_{\tau,0}] \exp \left[-\frac{ie}{2} \int_{|\partial u| < \Lambda |u|} d^D \mathbf{x} u_{\mu\nu}(\mathbf{x}) v_{\mu\nu}^>(\mathbf{x}) \right] \\ &\quad \left\{ 1 + \sum_{N=2}^{\infty} \frac{1}{(N-1)!} \prod_{j=1}^{N-1} \left(\int \mathcal{D}^D \mathbf{X}_j \int_{|\mathbf{Y}_j| > a_0 b} \mathcal{D}^D \mathbf{Y}_j \int \mathcal{D} \mathbf{g}_j(\mathbf{s}) \exp [E_j] \right) \right. \\ &\quad \left. \exp \left[-\frac{i}{2} e \int_{|\partial u| < \Lambda |u|} d^D \mathbf{x} u_{\mu\nu}(\mathbf{x}) v_{\mu\nu}^<(\mathbf{x}) - i2\pi\chi \sum_{j=1}^{N-1} \mathcal{A}_{\tau,j} \right] \right\}. \end{aligned} \quad (\text{II.4})$$

\mathbf{X}_0 and E_0 are the center-of-mass coordinate and fugacity parameter of the smallest $(D-2)$ -sphere, respectively,

$$E_0 = \begin{cases} w & \text{for } D = 2, \\ w + \int_{|\mathbf{R}_0(\mathbf{s})|=a_0/2} d^{D-2} \mathbf{s} t(\mathbf{g}_{0,\tau}(\mathbf{s}), \mathbf{g}_{0,\tau}(\mathbf{s})) & \text{for } D > 2. \end{cases} \quad (\text{II.5})$$

$\mathcal{A}_{\tau,0}$ is the $(D-1)$ -dimensional volume inside the smallest sphere projected onto a τ -constant plane. In Eq. (II.4), the vortex field $v_{\mu\nu}(\mathbf{x})$ is decomposed into a vortex field $v_{\mu\nu}^>(\mathbf{x})$ of the smallest vortex surface with $a_0 < |\mathbf{Y}_0| < a_0 b$ and a vortex field $v_{\mu\nu}^<(\mathbf{x})$ of the others with $a_0 b < |\mathbf{Y}_j|$. For $D = 2$, they are given by

$$v_{\tau 1}^>(\mathbf{x}) = 2\pi \left(\delta^2(\mathbf{x} - \mathbf{X}_0 - \frac{a_0}{2} \mathbf{e}_1) - \delta^2(\mathbf{x} - \mathbf{X}_0 + \frac{a_0}{2} \mathbf{e}_1) \right), \quad (\text{II.6})$$

$$v_{\tau 1}^<(\mathbf{x}) = 2\pi \sum_{j=1}^{N-1} \left(\delta^2(\mathbf{x} - \mathbf{X}_j - \frac{\mathbf{Y}_j}{2}) - \delta^2(\mathbf{x} - \mathbf{X}_j + \frac{\mathbf{Y}_j}{2}) \right), \quad (\text{II.7})$$

respectively. Here, \mathbf{e}_1 in Eq. (II.6) is the unit vector perpendicular to \mathbf{e}_0 , and vortex and antivortex in the smallest vortex-antivortex pair are coordinated by $\mathbf{X}_0 \pm \frac{a_0}{2} \mathbf{e}_1$, respectively [$\{\mathbf{e}_0, \mathbf{e}_1\}$ forms the right-handed orthonormal basis in the 2-dimensional system]. For $D > 2$, $v_{\mu\nu}^>(\mathbf{x})$ and $v_{\mu\nu}^<(\mathbf{x})$ are given by,

$$v_{\mu\nu}^>(\mathbf{x}) \equiv \frac{2\pi \varepsilon_{\mu\nu\lambda\rho\cdots\sigma}}{(D-2)!} \int_{|\mathbf{R}_0(\mathbf{s})|=a_0/2} d^{D-2} \mathbf{s} \varepsilon_{a\cdots b} \left(\frac{\partial R_{0,\lambda}(\mathbf{s})}{\partial s_a} \cdots \frac{\partial R_{0,\sigma}(\mathbf{s})}{\partial s_b} \right) \delta^D(\mathbf{x} - \mathbf{X}_0 - \mathbf{R}_0(\mathbf{s})), \quad (\text{II.8})$$

$$v_{\mu\nu}^<(\mathbf{x}) \equiv \frac{2\pi \varepsilon_{\mu\nu\lambda\rho\cdots\sigma}}{(D-2)!} \sum_{j=1}^{N-1} \int_{\partial\Gamma_j} d^{D-2} \mathbf{s} \varepsilon_{a\cdots b} \left(\frac{\partial R_{j,\lambda}(\mathbf{s})}{\partial s_a} \cdots \frac{\partial R_{j,\sigma}(\mathbf{s})}{\partial s_b} \right) \delta^D(\mathbf{x} - \mathbf{R}_j(\mathbf{s})), \quad (\text{II.9})$$

where $\partial\Gamma_j$ is a larger vortex hyper-surface with $|\mathbf{Y}_j| > a_0 b$.

Suppose that the unit normal vector \mathbf{e}_0 has an angle θ with respect to the time τ direction,

$$\mathbf{e}_0 \equiv (\cos \theta, \sin \theta \cos \theta', \dots, \sin \theta \sin \theta' \dots \sin \theta''). \quad (\text{II.10})$$

Then, the fugacity parameter E_0 of the smallest vortex sphere in Eq. (II.5) is a function only of θ , and it is symmetric around $\theta = \pi/2$: $E_0 = E_0(\theta) = E_0(\pi - \theta)$. This is because both temporal and spatial components of the metric tensor, $\hat{\mathbf{g}}_{j,r}$ and $\hat{\mathbf{g}}_{j,\tau}$ are generally invariant under the spatial rotations around the τ axis as well as under the inversion of τ . The projected volume $\mathcal{A}_{\tau,0}$ inside the smallest $(D-2)$ -sphere is also given by a function of θ , while it is odd under $\theta \rightarrow \pi - \theta$,

$$\mathcal{A}_{\tau,0} = \cos \theta \int_0^{\frac{a_0}{2}} r^{D-2} dr \int_0^\pi (\sin \lambda_1)^{D-3} d\lambda_1 \dots \int_0^{2\pi} d\lambda_{D-2} = 2A \left(\frac{a_0}{2}\right)^{D-1} \cos \theta, \quad (\text{II.11})$$

with

$$A \equiv \frac{1}{D-1} \frac{\pi^{\frac{D-1}{2}}}{\Gamma(\frac{D-1}{2})} = \frac{1}{2} \frac{\pi^{\frac{D-1}{2}}}{\Gamma(\frac{D+1}{2})}. \quad (\text{II.12})$$

Note that Eq. (II.11) is also valid for $D = 2$.

Now that the vector potential $u_{\mu\nu}(\mathbf{x})$ changes slowly in space and time on the scale of a_0 , we use a gradient expansion to evaluate $\int_{|\partial u| < \Lambda|u|} d^D \mathbf{x} u_{\mu\nu}(\mathbf{x}) v_{\mu\nu}^>(\mathbf{x})$. In the following, we evaluate the expansion for $D > 2$ and $D = 2$ separately. In the end, we observe that the final results [Eqs. (II.24,II.25,II.26,II.28, II.27)] for general D are consistent with the results for the $D = 2$ case.

1. gradient expansion for general D

To exercise the expansion for general $D > 2$, we first introduce the spherical coordinate system for the symmetric $(D-2)$ -sphere. Suppose that the unit vector \mathbf{e}_0 is normal to the plane where the sphere lies, and $\{\mathbf{e}_0, \mathbf{e}_1, \dots, \mathbf{e}_{D-1}\}$ forms the right-handed orthonormal basis in the D -dimensional system. The parallelepiped element of the symmetric sphere can be parameterized by $(D-2)$ angle variables, $\boldsymbol{\lambda} \equiv (\lambda_1, \lambda_2, \dots, \lambda_{D-3}, \lambda_{D-2})$,

$$\begin{aligned} \mathbf{R}_0(\boldsymbol{\lambda}) = & \frac{a_0}{2} \left(\cos \lambda_1 \mathbf{e}_1 + \sin \lambda_1 \cos \lambda_2 \mathbf{e}_2 + \sin \lambda_1 \sin \lambda_2 \cos \lambda_3 \mathbf{e}_3 + \dots \right. \\ & \left. + \sin \lambda_1 \dots \sin \lambda_{D-3} \cos \lambda_{D-2} \mathbf{e}_{D-2} + \sin \lambda_1 \dots \sin \lambda_{D-3} \sin \lambda_{D-2} \mathbf{e}_{D-1} \right). \end{aligned} \quad (\text{II.13})$$

We set the integral domain as $\lambda_j \in [0, \pi]$ ($j = 1, \dots, D-3$), and $\lambda_{D-2} \in [0, 2\pi]$. By replacing \mathbf{s} in Eq. (II.8) by $\frac{a_0}{2} \boldsymbol{\lambda}$, we obtain the vortex field $v_{\mu\nu}^>(\mathbf{r})$ from the smallest sphere as follows,

$$\begin{aligned} v_{\mu\nu}^>(\mathbf{x}) = & 2\pi \left(\frac{a_0}{2}\right)^{D-3} \int_0^\pi (\sin \lambda_1)^{D-3} d\lambda_1 \int_0^\pi (\sin \lambda_2)^{D-4} d\lambda_2 \dots \int_0^\pi \sin \lambda_{D-3} d\lambda_{D-3} \\ & \int_0^{2\pi} d\lambda_{D-2} (\mathbf{e}_{0,\mu} \mathbf{R}_{0,\nu}(\boldsymbol{\lambda}) - \mathbf{e}_{0,\nu} \mathbf{R}_{0,\mu}(\boldsymbol{\lambda})) \delta^D(\mathbf{x} - \mathbf{X}_0 - \mathbf{R}_0(\boldsymbol{\lambda})). \end{aligned} \quad (\text{II.14})$$

The integral region of $\boldsymbol{\lambda}$ can be decomposed into a pair of two domains, which are transformed into each other by $\lambda_j \rightarrow \pi - \lambda_j$ ($j = 1, \dots, D-3$) and $\lambda_{D-2} \rightarrow \lambda_{D-2} + \pi$. Namely, we can rewrite also this in the following way,

$$\begin{aligned} v_{\mu\nu}^>(\mathbf{x}) = & 2\pi \left(\frac{a_0}{2}\right)^{D-3} \int_0^\pi (\sin \lambda_1)^{D-3} d\lambda_1 \int_0^\pi (\sin \lambda_2)^{D-4} d\lambda_2 \dots \int_0^\pi \sin \lambda_{D-3} d\lambda_{D-3} \int_0^\pi d\lambda_{D-2} \\ & (\mathbf{e}_{0,\mu} \mathbf{R}_{0,\nu}(\boldsymbol{\lambda}) - \mathbf{e}_{0,\nu} \mathbf{R}_{0,\mu}(\boldsymbol{\lambda})) \left(\delta^D(\mathbf{x} - \mathbf{X}_0 - \mathbf{R}_0(\boldsymbol{\lambda})) - \delta^D(\mathbf{x} - \mathbf{X}_0 + \mathbf{R}_0(\boldsymbol{\lambda})) \right). \end{aligned} \quad (\text{II.15})$$

Eq. (II.15) facilitates an expansion of $\int_{|\partial u| < |u|} d^D \mathbf{x} u_{\mu\nu}(\mathbf{x}) v_{\mu\nu}^>(\mathbf{x})$ in the power of the UV length scale a_0 ,

$$\begin{aligned}
\int_{|\partial u| < \Lambda|u|} d^D \mathbf{x} u_{\mu\nu}(\mathbf{x}) v_{\mu\nu}^>(\mathbf{x}) &= 2\pi \left(\frac{a_0}{2}\right)^{D-3} \int_0^\pi (\sin \lambda_1)^{D-3} d\lambda_1 \cdots \int_0^\pi d\lambda_{D-2} \\
&\quad \left(\mathbf{e}_{0,\mu} \mathbf{R}_{0,\nu}(\boldsymbol{\lambda}) - \mathbf{e}_{0,\nu} \mathbf{R}_{0,\mu}(\boldsymbol{\lambda}) \right) \left(u_{\mu\nu}(\mathbf{X}_0 + \mathbf{R}_0(\boldsymbol{\lambda})) - u_{\mu\nu}(\mathbf{X}_0 - \mathbf{R}_0(\boldsymbol{\lambda})) \right), \\
&= 4\pi \left(\frac{a_0}{2}\right)^{D-3} \int_0^\pi (\sin \lambda_1)^{D-3} d\lambda_1 \cdots \int_0^\pi d\lambda_{D-2} \\
&\quad \left(\mathbf{e}_{0,\mu} \mathbf{R}_{0,\nu}(\boldsymbol{\lambda}) - \mathbf{e}_{0,\nu} \mathbf{R}_{0,\mu}(\boldsymbol{\lambda}) \right) \left(\mathbf{R}_{0,\phi}(\boldsymbol{\lambda}) \partial_\phi u_{\mu\nu}(\mathbf{X}_0) + \mathcal{O}(\partial^3 u) \right) \\
&= 8\pi \left(\frac{a_0}{2}\right)^{D-1} A \mathbf{e}_{0,\mu} \partial_\nu u_{\mu\nu}(\mathbf{X}_0) + \mathcal{O}(\partial^3 u). \tag{II.16}
\end{aligned}$$

From the second to third lines, we used

$$\int_0^\pi (\sin \lambda_1)^{D-3} d\lambda_1 \cdots \int_0^\pi d\lambda_{D-2} \mathbf{R}_{0,\nu}(\boldsymbol{\lambda}) \mathbf{R}_{0,\phi}(\boldsymbol{\lambda}) = A \left(\frac{a_0}{2}\right)^2 (\delta_{\nu,\phi} - \mathbf{e}_{0,\nu} \mathbf{e}_{0,\phi}), \tag{II.17}$$

with Eq. (II.12). Substituting Eq. (II.16) into Eq. (II.4), and expanding the smallest vortex hyper-sphere term in the power of the electric coupling constant e , we obtain

$$\begin{aligned}
Z'_v &= \int \mathcal{D}\mathbf{u} \exp \left[-\frac{1}{2} \int_{|\partial u| < \Lambda|u|} d^D \mathbf{x} \left\{ \gamma_\tau (\partial_\mu u_{\mu\tau}) (\partial_\lambda u_{\lambda\tau}) + \sum_{\nu=1}^{D-1} (\partial_\mu u_{\mu\nu}) (\partial_\lambda u_{\lambda\nu}) \right\} \right] \\
&\quad \int \mathcal{D}^D \mathbf{X}_0 \int_{S_{D-1}} \mathcal{D}^{D-1} \mathbf{e}_0 \exp [E_0(\theta) - i4\pi \left(\frac{a_0}{2}\right)^{D-1} A \chi \cos \theta] \\
&\quad \left[1 - 4\pi i e \left(\frac{a_0}{2}\right)^{D-1} A \mathbf{e}_{0,\mu} \partial_\nu u_{\mu\nu}(\mathbf{X}_0) - 8\pi^2 e^2 \left(\frac{a_0}{2}\right)^{2(D-1)} A^2 (\mathbf{e}_{0,\mu} \partial_\nu u_{\mu\nu}(\mathbf{X}_0)) (\mathbf{e}_{0,\phi} \partial_\lambda u_{\phi\lambda}(\mathbf{X}_0)) + \mathcal{O}(\partial^3 u, \partial u \partial^3 u) \right] \\
&\quad \left\{ 1 + \sum_{N=1}^{\infty} \frac{1}{N!} \prod_{j=1}^N \left(\int \mathcal{D}^D \mathbf{X}_j \int_{|\mathbf{Y}_j| > a_0 b} \mathcal{D}^D \mathbf{Y}_j \int \mathcal{D}\mathbf{g}_j(\mathbf{s}) \exp [E_j] \right) \right. \\
&\quad \left. \exp \left[-\frac{i}{2} e \int_{|\partial u| < \Lambda|u|} d^D \mathbf{x} u_{\mu\nu}(\mathbf{x}) v_{\mu\nu}^<(\mathbf{x}) - i2\pi\chi \sum_{j=1}^N \mathcal{A}_{\tau,j} \right] \right\}. \tag{II.18}
\end{aligned}$$

From Eq. (II.4) to Eq. (II.18), we have changed N by one, $N_{\text{new}} = N_{\text{old}} - 1$, and replaced Eq. (II.9) by

$$v_{\mu\nu}^<(\mathbf{x}) = \frac{2\pi \varepsilon_{\mu\nu\lambda\rho\cdots\sigma}}{(D-2)!} \sum_{j=1}^N \int_{\partial\Gamma_j} d^{D-2} \mathbf{s} \varepsilon_{a\cdots b} \left(\frac{\partial R_{j,\lambda}(\mathbf{s})}{\partial s_a} \cdots \frac{\partial R_{j,\sigma}(\mathbf{s})}{\partial s_b} \right) \delta^D(\mathbf{x} - \mathbf{R}_j(\mathbf{s})).$$

From Eq. (II.10), the integral over \mathbf{e}_0 is given by,

$$\int_{S_{D-1}} \mathcal{D}^{D-1} \mathbf{e}_0 \equiv \int_0^\pi (\sin \theta)^{D-2} d\theta \int_0^\pi (\sin \theta')^{D-3} d\theta' \cdots \int_0^{2\pi} d\theta''. \tag{II.19}$$

The integral over \mathbf{e}_0 is calculated up to the second order in e ,

$$\int \mathcal{D}^D \mathbf{X}_0 \int \mathcal{D}^{D-1} \mathbf{e}_0 e^{E_0(\theta) - i4\pi\chi \left(\frac{a_0}{2}\right)^{D-1} A \cos \theta} = \frac{V}{a_0^D} \delta f, \tag{II.20}$$

$$\int \mathcal{D}^D \mathbf{X}_0 \int_{S_{D-1}} \mathcal{D}^{D-1} \mathbf{e}_0 e^{E_0(\theta) - i4\pi\chi \left(\frac{a_0}{2}\right)^{D-1} A \cos \theta} (-4\pi i e) \left(\frac{a_0}{2}\right)^{D-1} A \mathbf{e}_{0,\mu} \partial_\nu u_{\mu\nu}(\mathbf{X}_0) = -\delta\chi \int d^D \mathbf{x} \partial_\nu u_{\tau\nu}(\mathbf{x}), \tag{II.21}$$

$$\begin{aligned}
&\int \mathcal{D}^D \mathbf{X}_0 \int \mathcal{D}^{D-1} \mathbf{e}_0 e^{E_0(\theta) - i4\pi\chi \left(\frac{a_0}{2}\right)^{D-1} A \cos \theta} (8\pi^2 e^2) \left(\frac{a_0}{2}\right)^{2(D-1)} A^2 \mathbf{e}_{0,\mu} \mathbf{e}_{0,\phi} \partial_\nu u_{\mu\nu}(\mathbf{X}_0) \partial_\lambda u_{\phi\lambda}(\mathbf{X}_0) \\
&= \delta\gamma_\tau \int d^D \mathbf{x} \partial_\nu u_{\nu\tau}(\mathbf{x}) \partial_\lambda u_{\lambda\tau}(\mathbf{x}) + \delta\gamma_\mathbf{r} \int d^D \mathbf{x} \sum_{\mu=1, \dots, D-1} \partial_\nu u_{\nu\mu}(\mathbf{x}) \partial_\lambda u_{\lambda\mu}(\mathbf{x}), \tag{II.22}
\end{aligned}$$

with

$$\delta f \equiv \frac{D-1}{2} A \int_0^\pi d\theta e^{E_0(\theta)} \cos \left[4\pi\chi \left(\frac{a_0}{2} \right)^{D-1} A \cos \theta \right], \quad (\text{II.23})$$

$$\delta\chi \equiv 4\pi e \frac{a_0^{-1}}{2^{D-1}} A \int_{S_{D-1}} \mathcal{D}^{D-1} \mathbf{e}_0 e^{E_0(\theta)} \sin \left[4\pi\chi \left(\frac{a_0}{2} \right)^{D-1} A \cos \theta \right] \cos \theta, \quad (\text{II.24})$$

$$\delta\gamma_\tau \equiv 8\pi^2 e^2 \frac{a_0^{D-2}}{2^{2D-2}} A^2 \int_{S_{D-1}} \mathcal{D}^{D-1} \mathbf{e}_0 e^{E_0(\theta)} \cos \left[4\pi\chi \left(\frac{a_0}{2} \right)^{D-1} A \cos \theta \right] \cos^2 \theta, \quad (\text{II.25})$$

$$\delta\gamma_r \equiv 8\pi^2 e^2 \frac{a_0^{D-2}}{2^{2D-2}} A^2 \frac{1}{D-1} \int_{S_{D-1}} \mathcal{D}^{D-1} \mathbf{e}_0 e^{E_0(\theta)} \cos \left[4\pi\chi \left(\frac{a_0}{2} \right)^{D-1} A \cos \theta \right] \sin^2 \theta. \quad (\text{II.26})$$

Here $E_0(\theta)$ is given by Eq. (II.5) for $D \geq 3$,

$$E_0(\theta) = w + \int_{|\mathbf{R}_0(\mathbf{s})|=a_0/2} d^{D-2} \mathbf{s} t(\mathbf{g}_{0,\tau}(\mathbf{s}), \mathbf{g}_{0,r}(\mathbf{s})).$$

By substituting Eqs. (II.21,II.22) into Eq. (II.4,II.3), we finally obtain the one-loop renormalization of the electromagnetic constitutive constants,

$$Z_v = e^{V\delta f} \int \mathcal{D}\mathbf{u} \exp \left[-\frac{1}{2} \int_{|\partial u| < \Lambda|u|} d^D \mathbf{x} \left\{ \bar{\gamma}_\tau (\partial_\mu u_{\mu\tau}) (\partial_\lambda u_{\lambda\tau}) + \bar{\gamma}_r \sum_{\nu=1}^{D-1} (\partial_\mu u_{\mu\nu}) (\partial_\lambda u_{\lambda\nu}) - 2\delta\chi \ln b \partial_\mu u_{\mu\tau} \right\} \right] \left\{ 1 + \sum_{N=1}^{\infty} \frac{1}{N!} \prod_{j=1}^N \left(\int \mathcal{D}^D \mathbf{X}_j \int_{|\mathbf{Y}_j| > a_0 b} \mathcal{D}^D \mathbf{Y}_j \int \mathcal{D}\mathbf{g}_j(\mathbf{s}) e^{E_j} \right) e^{-\frac{i\epsilon}{2} \int_{|\partial u| < \Lambda|u|} d^D \mathbf{x} u_{\mu\nu}(\mathbf{x}) v_{\mu\nu}(\mathbf{x}) - i2\pi\chi \sum_{j=1}^N \mathcal{A}_{\tau,j}} \right\}, \quad (\text{II.27})$$

with

$$\bar{\gamma}_\tau = \gamma_\tau + 2\delta\gamma_\tau \ln b, \quad \bar{\gamma}_r = 1 + 2\delta\gamma_r \ln b. \quad (\text{II.28})$$

δf contributes to an inhomogeneous scaling relation of the free energy density. As we are primarily interested in renormalization equations for the coupling constants, we will not delve into the free energy renormalization in this paper.

2. gradient expansion for $D = 2$

For $D = 2$, Eq. (II.6) directly yields the gradient expansion of $\int_{|\partial u| < \Lambda|u|} d^D \mathbf{x} u_{\mu\nu}(\mathbf{x}) v_{\mu\nu}^>(\mathbf{x})$,

$$\begin{aligned} \int_{|\partial u| < \Lambda|u|} d^D \mathbf{x} u_{\mu\nu}(\mathbf{x}) v_{\mu\nu}^>(\mathbf{x}) &= 4\pi \int d^2 \mathbf{x} u_{\tau 1}(\mathbf{x}) \left(\delta^2(\mathbf{x} - \mathbf{X}_0 - \frac{a_0}{2} \mathbf{e}_1) - \delta^2(\mathbf{x} - \mathbf{X}_0 + \frac{a_0}{2} \mathbf{e}_1) \right), \\ &= 4\pi a_0 \mathbf{e}_{1,\lambda} \partial_\lambda u_{\tau 1}(\mathbf{X}_0) + \mathcal{O}(\partial^3 u) = 4\pi a_0 \mathbf{e}_{0,\mu} \partial_\nu u_{\mu\nu} + \mathcal{O}(\partial^3 u). \end{aligned} \quad (\text{II.29})$$

In fact, this is consistent with Eq. (II.16): A in Eq. (II.12) is equal to one for $D = 2$. Thus, Eqs. (II.24,II.25,II.26, II.27, II.28) are also valid for $D = 2$, where $E_0(\theta) = w$ and $\int D\mathbf{e}_0 = \int_0^{2\pi} d\theta$.

3. renormalization to Berry phase term

$\delta\chi \partial_\mu u_{\mu\tau}$ in Eq. (II.27) can be absorbed into the antisymmetric integral variable $u_{\mu\tau} = -u_{\tau\mu}$ by the following gauge transformation,

$$\begin{aligned} \partial_\mu u_{\mu\tau} - \frac{\delta\chi \ln b}{\bar{\gamma}_\tau} &\rightarrow \partial_\mu u_{\mu\tau}, \\ \partial_\mu u_{\mu\lambda} &\rightarrow \partial_\mu u_{\mu\lambda}, \end{aligned} \quad (\text{II.30})$$

with $\lambda = 1, \dots, D-1$. Here, the summation over $\mu = \tau, 1, \dots, D-1$ is assumed. For example, one can consider the following variable changes,

$$u_{\mu\tau}(\mathbf{x}) \rightarrow u_{\mu\tau}(\mathbf{x}) + \frac{\delta\chi \ln b}{\bar{\gamma}_r} \delta_{\mu 1} r_1, \quad u_{\tau\mu}(\mathbf{x}) \rightarrow u_{\tau\mu}(\mathbf{x}) - \frac{\delta\chi \ln b}{\bar{\gamma}_r} \delta_{\mu 1} r_1. \quad (\text{II.31})$$

This yields a one-loop renormalization of the Berry phase term,

$$\begin{aligned} \frac{ie}{2} \int d^D \mathbf{x} \ u_{\mu\nu}(\mathbf{x}) v_{\mu\nu}(\mathbf{x}) &\rightarrow \frac{ie}{2} \int d^D \mathbf{x} \ u_{\mu\nu}(\mathbf{x}) v_{\mu\nu}(\mathbf{x}) + \frac{ie\delta\chi \ln b}{\bar{\gamma}_r} \int d^D \mathbf{x} \ r_1 v_{1\tau}(\mathbf{x}), \\ &= \frac{ie}{2} \int d^D \mathbf{x} \ u_{\mu\nu}(\mathbf{x}) v_{\mu\nu}(\mathbf{x}) - \frac{ie\delta\chi \ln b}{\bar{\gamma}_r} \int d^D \mathbf{x} \ b_\tau(\mathbf{x}), \end{aligned} \quad (\text{II.32})$$

From the first line to the second line, we took partial integrals over r_1 and τ with $v_{1\tau} = \partial_{r_1} b_\tau - \partial_\tau b_1$, dropping the associated surface terms. The surface terms can be neglected because the boundary of the system is sufficiently far from any vortex excitations, and vortex excitations always take the form of closed hyper-surface (For $D = 2$, a pair of vortex and antivortex). To summarize, we reach the following partition function after the integration over the smallest vortex hyper-sphere degrees of freedom;

$$\begin{aligned} Z_v = \int \mathcal{D}\mathbf{u} \exp &\left[-\frac{1}{2} \int_{|\partial u| < \Lambda|u|} d^D \mathbf{x} \left\{ \bar{\gamma}_\tau (\partial_\mu u_{\mu\tau}) (\partial_\lambda u_{\lambda\tau}) + \bar{\gamma}_r \sum_{\nu=1}^{D-1} (\partial_\mu u_{\mu\nu}) (\partial_\lambda u_{\lambda\nu}) \right\} \right] \\ &\left\{ 1 + \sum_{N=1}^{\infty} \frac{1}{N!} \prod_{j=1}^N \left(\int \mathcal{D}^D \mathbf{X}_j \int_{|\mathbf{Y}_j| > a_0 b} \mathcal{D}^D \mathbf{Y}_j \int \mathcal{D}\mathbf{g}_j(\mathbf{s}) \ e^{E_j} \right) e^{-\frac{ie}{2} \int_{|\partial u| < \Lambda|u|} d^D \mathbf{x} \ u_{\mu\nu}(\mathbf{x}) v_{\mu\nu}(\mathbf{x}) - i2\pi\bar{\chi} \sum_{j=1}^N \mathcal{A}_{\tau,j}} \right\}. \end{aligned} \quad (\text{II.33})$$

with the renormalization to the Berry phase term,

$$\bar{\chi} \equiv \chi - \frac{e\delta\chi}{\gamma_\tau} \ln b. \quad (\text{II.34})$$

B. one-loop renormalization to vortex fugacity

The Maxwell term and the coupling between the vector potential fields and vortex excitations are given by the following action,

$$\frac{1}{2} \int_{|\partial u| < \Lambda|u|} d^D \mathbf{x} \left\{ \gamma_\tau (\partial_\mu u_{\mu\tau}) (\partial_\lambda u_{\lambda\tau}) + \sum_{\nu=1}^{D-1} (\partial_\mu u_{\mu\nu}) (\partial_\lambda u_{\lambda\nu}) \right\} + \frac{ie}{2} \int_{|\partial u| < \Lambda|u|} d^D \mathbf{x} \ u_{\mu\nu}(\mathbf{x}) v_{\mu\nu}(\mathbf{x}).$$

The integration over the fast component of the vector potential field yields the short-ranged part of the Coulomb interaction between vortex hyper-surface elements. The short-ranged part of the Coulomb interaction can be included as the renormalization to the vortex core energy density. For general D , the renormalization to the vortex core energy density is given by a function of the temporal and spatial components of the metric tensors defined in Eqs. (I.16, I.18), justifying Eq. (I.17, I.15) a posteriori.

1. vortex fugacity renormalization for general D

To determine the form of the short-ranged part of the Coulomb interaction for general $D (> 2)$ and $\gamma_\tau \neq 1$ cases, let us take the Fourier transform of the relevant parts of the action,

$$\begin{aligned}
& - \sum_{j=1}^N 2\delta E_j \equiv \\
& \int_{b^{-1}\Lambda < |\mathbf{k}| < \Lambda} \frac{d^D \mathbf{k}}{(2\pi)^D} \left\{ \gamma_\tau k_\mu u_{\mu\tau}(\mathbf{k}) k_\lambda u_{\lambda\tau}(-\mathbf{k}) + \sum_{\phi=1, \dots, D-1} k_\mu u_{\mu\phi}(\mathbf{k}) k_\lambda u_{\lambda\phi}(-\mathbf{k}) + \frac{ie}{2} (u_{\mu\nu}(\mathbf{k}) v_{\mu\nu}(-\mathbf{k}) + u_{\mu\nu}(-\mathbf{k}) v_{\mu\nu}(\mathbf{k})) \right\} \\
& = \int_{b^{-1}\Lambda < |\mathbf{k}| < \Lambda} \frac{d^D \mathbf{k}}{(2\pi)^D} \left\{ \gamma_\tau \varphi_\tau(\mathbf{k}) \varphi_\tau(-\mathbf{k}) + \sum_{\phi=1, \dots, D-1} \varphi_\phi(\mathbf{k}) \varphi_\phi(-\mathbf{k}) + ie \left(\frac{k_\mu}{k^2} \varphi_\nu(\mathbf{k}) v_{\mu\nu}(-\mathbf{k}) + \frac{k_\mu}{k^2} \varphi_\nu(-\mathbf{k}) v_{\mu\nu}(\mathbf{k}) \right) \right\} \\
& = e^2 \int_{b^{-1}\Lambda < |\mathbf{k}| < \Lambda} \frac{d^D \mathbf{k}}{(2\pi)^D} \frac{k_\mu k_\lambda}{k^4} v_{\mu\nu}(\mathbf{k}) v_{\lambda\nu}(-\mathbf{k}) [\mathbf{C}^{-1}]_{\nu\nu} + \text{const.} \tag{II.35}
\end{aligned}$$

To facilitate the Gaussian integration over the vector potential field for general dimension D , we chose a specific gauge in the right hand side [see also Sec. IV for the alternative choice], and express the vector potential in terms of the divergence-free auxiliary field φ ,

$$u_{\mu\nu}(\mathbf{k}) = \frac{1}{k^2} (k_\mu \varphi_\nu(\mathbf{k}) - k_\nu \varphi_\mu(\mathbf{k})). \tag{II.36}$$

$[\mathbf{C}]$ and its inverse are the $D \times D$ diagonal matrices,

$$[\mathbf{C}] = \begin{pmatrix} \gamma_\tau & \\ & \mathbf{1}_{(D-1) \times (D-1)} \end{pmatrix}, \quad [\mathbf{C}^{-1}] = \alpha_0 \mathbf{1}_{D \times D} + \alpha_1 \boldsymbol{\eta}, \tag{II.37}$$

with

$$\alpha_0 \equiv \frac{\gamma_\tau^{-1} + (D-1)}{D}, \quad \alpha_1 \equiv \frac{-\gamma_\tau^{-1} + 1}{D}, \quad \boldsymbol{\eta} \equiv \begin{pmatrix} -(D-1) & \\ & \mathbf{1}_{(D-1) \times (D-1)} \end{pmatrix}. \tag{II.38}$$

Then, take the sum over $\mu, \lambda, \nu = 0, \dots, D-1$ in Eq. (II.35),

$$\begin{aligned}
k_\mu k_\lambda v_{\mu\nu} v_{\lambda\nu} (\alpha_0 \delta_{\nu\nu} + \alpha_1 \boldsymbol{\eta}_{\nu\nu}) &= \left(\frac{1}{(D-2)!} \right)^2 (\alpha_0 \delta_{\nu\nu} + \alpha_1 \boldsymbol{\eta}_{\nu\nu}) k_\mu k_\lambda \varepsilon_{\mu\nu\sigma\phi\dots\psi} \varepsilon_{\lambda\nu\xi\rho\dots\eta} J_{\sigma\phi\dots\psi} J_{\xi\rho\dots\eta}, \\
&= \sum_{\sigma < \phi < \dots < \psi} J_{\sigma\phi\dots\psi} J_{\sigma\phi\dots\psi} \left(\alpha_0 k^2 - \alpha_1 \left(\sum_{\mu} \boldsymbol{\eta}_{\mu\mu} k_\mu^2 \right) - \alpha_1 k^2 (\boldsymbol{\eta}_{\sigma\sigma} + \boldsymbol{\eta}_{\phi\phi} + \dots + \boldsymbol{\eta}_{\psi\psi}) \right). \tag{II.39}
\end{aligned}$$

In the first line, the summations of the repeated indices over $\tau, 1, \dots, D-1$ are implicitly assumed. In the second line, the summations of $\sigma, \phi, \dots, \psi$ over $\tau, 1, \dots, D-1$ are taken in such a way that $\sigma < \phi < \dots < \psi$ is satisfied [$\tau = 0 < 1, \dots, D-1$], while the summation of μ over $0, 1, \dots, D-1$ is uncorrelated with $\sigma, \phi, \dots, \psi$. To derive Eq. (II.39), we used the following formula,

$$\sum_{\nu} \varepsilon_{\mu\nu\sigma\phi\dots\psi} \varepsilon_{\lambda\nu\xi\rho\dots\eta} = \begin{pmatrix} \mu & \sigma & \phi & \dots & \psi \\ \lambda & \xi & \rho & \dots & \eta \end{pmatrix}_{\mathbf{1}} \equiv \sum_P (-1)^P \delta_{\mu P(\lambda)} \delta_{\sigma P(\xi)} \dots \delta_{\psi P(\eta)}, \tag{II.40}$$

$$\begin{aligned}
\sum_{\nu} \boldsymbol{\eta}_{\nu\nu} \varepsilon_{\mu\nu\sigma\phi\dots\psi} \varepsilon_{\lambda\nu\xi\rho\dots\eta} &= - \begin{pmatrix} \mu & \sigma & \phi & \dots & \psi \\ \lambda & \xi & \rho & \dots & \eta \end{pmatrix}_{\boldsymbol{\eta}} \equiv - \sum_P (-1)^P \left\{ \boldsymbol{\eta}_{\mu P(\lambda)} \delta_{\sigma P(\xi)} \dots \delta_{\psi P(\eta)} \right. \\
&\quad \left. + \delta_{\mu P(\lambda)} \boldsymbol{\eta}_{\sigma P(\xi)} \dots \delta_{\psi P(\eta)} + \dots + \delta_{\mu P(\lambda)} \delta_{\sigma P(\xi)} \dots \boldsymbol{\eta}_{\psi P(\eta)} \right\}. \tag{II.41}
\end{aligned}$$

Here P stands for a permutation of the $(D-1)$ elements, a permutation from $(\lambda, \xi, \rho, \dots, \eta)$ to $(P(\lambda), P(\xi), P(\rho), \dots, P(\eta))$, and \sum_P is a sum over all the elements of the permutation group. $(-1)^P$ is $+1$ and -1 , respectively, when a permutation P consists of an even or odd number of transpositions. We also used a divergence-free condition for the vortex field [81],

$$\sum_{\lambda=0,1,\dots,D-1} \frac{\partial}{\partial x_\lambda} J_{\lambda\rho\dots\sigma}(\mathbf{x}) = \sum_{\rho} \frac{\partial}{\partial x_\rho} J_{\lambda\rho\dots\sigma}(\mathbf{x}) = \dots = \sum_{\sigma} \frac{\partial}{\partial x_\sigma} J_{\lambda\rho\dots\sigma}(\mathbf{x}) = 0. \tag{II.42}$$

The divergence-free condition is due to the fact that any closed vortex hyper-spheres have no boundaries. In the following, we will briefly explain the deduction of Eq. (II.39) for the memorandum. The α_0 term is calculated as follows:

$$\begin{aligned}
& \sum_{\nu} \sum_{\mu, \lambda, \sigma, \xi, \dots, \psi, \eta} k_{\mu} k_{\lambda} \varepsilon_{\mu\nu\sigma\phi\dots\psi} \varepsilon_{\lambda\nu\xi\rho\dots\eta} J_{\sigma\phi\dots\psi}(\mathbf{k}) J_{\xi\rho\dots\eta}(-\mathbf{k}) \\
&= \sum_{\mu, \lambda, \sigma, \xi, \dots, \psi, \eta} \left(\begin{array}{cccc} \mu & \sigma & \phi & \dots & \psi \\ \lambda & \xi & \rho & \dots & \eta \end{array} \right)_{\mathbf{1}} k_{\mu} k_{\lambda} J_{\sigma\phi\dots\psi}(\mathbf{k}) J_{\xi\rho\dots\eta}(-\mathbf{k}) \\
&= \sum_{\sigma, \xi, \dots, \psi, \eta} \sum_{\mu}^{\mu \neq \sigma, \phi, \dots, \psi} k_{\mu}^2 \left(\begin{array}{cccc} \sigma & \phi & \dots & \psi \\ \xi & \rho & \dots & \eta \end{array} \right)_{\mathbf{1}} J_{\sigma\phi\dots\psi} J_{\xi\rho\dots\eta} - (D-2)^2 \sum_{\phi, \rho, \dots, \psi, \eta} \sum_{\mu, \sigma}^{\mu \neq \sigma} k_{\mu} k_{\sigma} \left(\begin{array}{cccc} \phi & \dots & \psi \\ \rho & \dots & \eta \end{array} \right)_{\mathbf{1}} J_{\sigma\phi\dots\psi} J_{\mu\rho\dots\eta} \\
&= ((D-2)!)^2 \left\{ \sum_{\sigma < \phi < \dots < \psi} J_{\sigma\phi\dots\psi} J_{\sigma\phi\dots\psi} \sum_{\mu}^{\mu \neq \sigma, \phi, \dots, \psi} k_{\mu}^2 - \sum_{\phi < \dots < \psi} \sum_{\mu, \sigma}^{\mu \neq \sigma} k_{\mu} k_{\sigma} J_{\sigma\phi\dots\psi} J_{\mu\phi\dots\psi} \right\} \\
&= ((D-2)!)^2 \left\{ \sum_{\sigma < \phi < \dots < \psi} J_{\sigma\phi\dots\psi} J_{\sigma\phi\dots\psi} \sum_{\mu}^{\mu \neq \sigma, \phi, \dots, \psi} k_{\mu}^2 - \sum_{\phi < \dots < \psi} \sum_{\mu, \sigma} k_{\mu} k_{\sigma} J_{\sigma\phi\dots\psi} J_{\mu\phi\dots\psi} + \sum_{\phi < \dots < \psi} \sum_{\mu} k_{\mu}^2 J_{\mu\phi\dots\psi} J_{\mu\phi\dots\psi} \right\} \\
&= ((D-2)!)^2 \left\{ \sum_{\sigma < \phi < \dots < \psi} J_{\sigma\phi\dots\psi} J_{\sigma\phi\dots\psi} \sum_{\mu}^{\mu \neq \sigma, \phi, \dots, \psi} k_{\mu}^2 + \sum_{\mu < \phi < \dots < \psi} (k_{\mu}^2 + k_{\phi}^2 + \dots + k_{\psi}^2) J_{\mu\phi\dots\psi} J_{\mu\phi\dots\psi} \right\} \\
&= ((D-2)!)^2 k^2 \sum_{\sigma < \phi < \dots < \psi} J_{\sigma\phi\dots\psi} J_{\sigma\phi\dots\psi}. \tag{II.43}
\end{aligned}$$

From the fifth line to the sixth line, we used $\sum_{\mu} k_{\mu} J_{\mu\phi\dots\psi}(-\mathbf{k}) = 0$ from Eq. (II.42). We also used

$$\sum_{\mu} \sum_{\phi < \dots < \psi} k_{\mu}^2 J_{\mu\phi\dots\psi}(\mathbf{k}) J_{\mu\phi\dots\psi}(-\mathbf{k}) = \sum_{\mu < \phi < \dots < \psi} (k_{\mu}^2 + k_{\phi}^2 + \dots + k_{\psi}^2) J_{\mu\phi\dots\psi}(\mathbf{k}) J_{\mu\phi\dots\psi}(-\mathbf{k}). \tag{II.44}$$

Similarly, the α_1 term can be calculated,

$$\begin{aligned}
& \sum_{\nu} \sum_{\mu, \lambda, \sigma, \xi, \dots, \psi, \eta} k_{\mu} k_{\lambda} \boldsymbol{\eta}_{\nu\nu} \varepsilon_{\mu\nu\sigma\phi\dots\psi} \varepsilon_{\lambda\nu\xi\rho\dots\eta} J_{\sigma\phi\dots\psi}(\mathbf{k}) J_{\xi\rho\dots\eta}(-\mathbf{k}) \\
&= - \sum_{\mu, \lambda, \sigma, \xi, \dots, \psi, \eta} \left(\begin{array}{c} \mu \ \sigma \ \phi \ \dots \ \psi \\ \lambda \ \xi \ \rho \ \dots \ \eta \end{array} \right)_{\boldsymbol{\eta}} k_{\mu} k_{\lambda} J_{\sigma\phi\dots\psi}(\mathbf{k}) J_{\xi\rho\dots\eta}(-\mathbf{k}) \\
&= - \sum_{\sigma, \xi, \dots, \psi, \eta} \sum_{\mu}^{\mu \neq \sigma, \phi, \dots, \psi} k_{\mu}^2 \left(\boldsymbol{\eta}_{\mu\mu} \left(\begin{array}{c} \sigma \ \phi \ \dots \ \psi \\ \xi \ \rho \ \dots \ \eta \end{array} \right)_{\mathbf{1}} + \delta_{\mu\mu} \left(\begin{array}{c} \sigma \ \phi \ \dots \ \psi \\ \xi \ \rho \ \dots \ \eta \end{array} \right)_{\boldsymbol{\eta}} \right) J_{\sigma\phi\dots\psi} J_{\xi\rho\dots\eta} \\
&\quad + (D-2)^2 \sum_{\phi, \xi, \dots, \psi, \eta} \sum_{\mu, \sigma}^{\mu \neq \sigma} k_{\mu} k_{\sigma} \left(\boldsymbol{\eta}_{\mu\mu} \delta_{\sigma\sigma} \left(\begin{array}{c} \phi \ \dots \ \psi \\ \rho \ \dots \ \eta \end{array} \right)_{\mathbf{1}} + \delta_{\mu\mu} \boldsymbol{\eta}_{\sigma\sigma} \left(\begin{array}{c} \phi \ \dots \ \psi \\ \rho \ \dots \ \eta \end{array} \right)_{\mathbf{1}} \right. \\
&\quad \left. + \delta_{\mu\mu} \delta_{\sigma\sigma} \left(\begin{array}{c} \phi \ \dots \ \psi \\ \rho \ \dots \ \eta \end{array} \right)_{\boldsymbol{\eta}} \right) J_{\sigma\phi\dots\psi} J_{\mu\rho\dots\eta} \\
&= -((D-2)!)^2 \sum_{\sigma < \phi < \dots < \psi} J_{\sigma\phi\dots\psi} J_{\sigma\phi\dots\psi} \left(\sum_{\mu}^{\mu \neq \sigma, \phi, \dots, \psi} k_{\mu}^2 \boldsymbol{\eta}_{\mu\mu} + \sum_{\mu}^{\mu \neq \sigma, \phi, \dots, \psi} k_{\mu}^2 (\boldsymbol{\eta}_{\sigma\sigma} + \boldsymbol{\eta}_{\phi\phi} + \dots + \boldsymbol{\eta}_{\psi\psi}) \right) \\
&\quad + ((D-2)!)^2 \sum_{\phi < \dots < \psi} \sum_{\mu, \sigma}^{\mu \neq \sigma} k_{\mu} k_{\sigma} J_{\sigma\phi\dots\psi} J_{\mu\phi\dots\psi} (\boldsymbol{\eta}_{\mu\mu} + \boldsymbol{\eta}_{\sigma\sigma} + \boldsymbol{\eta}_{\phi\phi} + \dots + \boldsymbol{\eta}_{\psi\psi}) \\
&= -((D-2)!)^2 \sum_{\sigma < \phi < \dots < \psi} J_{\sigma\phi\dots\psi} J_{\sigma\phi\dots\psi} \left(\sum_{\mu}^{\mu \neq \sigma, \phi, \dots, \psi} k_{\mu}^2 \boldsymbol{\eta}_{\mu\mu} + \sum_{\mu}^{\mu \neq \sigma, \phi, \dots, \psi} k_{\mu}^2 (\boldsymbol{\eta}_{\sigma\sigma} + \boldsymbol{\eta}_{\phi\phi} + \dots + \boldsymbol{\eta}_{\psi\psi}) \right) \\
&\quad + ((D-2)!)^2 \sum_{\phi < \dots < \psi} \sum_{\mu, \sigma} k_{\mu} k_{\sigma} J_{\sigma\phi\dots\psi} J_{\mu\phi\dots\psi} (\boldsymbol{\eta}_{\mu\mu} + \boldsymbol{\eta}_{\sigma\sigma} + \boldsymbol{\eta}_{\phi\phi} + \dots + \boldsymbol{\eta}_{\psi\psi}) \\
&\quad - ((D-2)!)^2 \sum_{\phi < \dots < \psi} \sum_{\mu} k_{\mu}^2 J_{\mu\phi\dots\psi} J_{\mu\phi\dots\psi} (\boldsymbol{\eta}_{\mu\mu} + \boldsymbol{\eta}_{\mu\mu} + \boldsymbol{\eta}_{\phi\phi} + \dots + \boldsymbol{\eta}_{\psi\psi}) \\
&= -((D-2)!)^2 \sum_{\sigma < \phi < \dots < \psi} J_{\sigma\phi\dots\psi} J_{\sigma\phi\dots\psi} \left(\sum_{\mu}^{\mu \neq \sigma, \phi, \dots, \psi} k_{\mu}^2 \boldsymbol{\eta}_{\mu\mu} + \sum_{\mu}^{\mu \neq \sigma, \phi, \dots, \psi} k_{\mu}^2 (\boldsymbol{\eta}_{\sigma\sigma} + \boldsymbol{\eta}_{\phi\phi} + \dots + \boldsymbol{\eta}_{\psi\psi}) \right) \\
&\quad - ((D-2)!)^2 \sum_{\mu < \phi < \dots < \psi} (k_{\mu}^2 \boldsymbol{\eta}_{\mu\mu} + k_{\phi}^2 \boldsymbol{\eta}_{\phi\phi} + \dots + k_{\psi}^2 \boldsymbol{\eta}_{\psi\psi}) J_{\mu\phi\dots\psi} J_{\mu\phi\dots\psi} \\
&\quad - ((D-2)!)^2 \sum_{\mu < \phi < \dots < \psi} (k_{\mu}^2 + k_{\phi}^2 + \dots + k_{\psi}^2) J_{\mu\phi\dots\psi} J_{\mu\phi\dots\psi} (\boldsymbol{\eta}_{\mu\mu} + \boldsymbol{\eta}_{\phi\phi} + \dots + \boldsymbol{\eta}_{\psi\psi}) \\
&= -((D-2)!)^2 \sum_{\sigma < \phi < \dots < \psi} J_{\sigma\phi\dots\psi} J_{\sigma\phi\dots\psi} \left(\sum_{\mu} k_{\mu}^2 \boldsymbol{\eta}_{\mu\mu} \right) \\
&\quad - ((D-2)!)^2 \sum_{\sigma < \phi < \dots < \psi} J_{\sigma\phi\dots\psi} J_{\sigma\phi\dots\psi} (\boldsymbol{\eta}_{\sigma\sigma} + \boldsymbol{\eta}_{\phi\phi} + \dots + \boldsymbol{\eta}_{\psi\psi}) \left(\sum_{\mu} k_{\mu}^2 \right) \tag{II.45}
\end{aligned}$$

From the fifth line to the sixth line, we used the divergence-free condition for the vortex field. We also used

$$\sum_{\mu} \sum_{\phi < \dots < \psi} k_{\mu}^2 \boldsymbol{\eta}_{\mu\mu} J_{\mu\phi\dots\psi}(\mathbf{k}) J_{\mu\phi\dots\psi}(-\mathbf{k}) = \sum_{\mu < \phi < \dots < \psi} (k_{\mu}^2 \boldsymbol{\eta}_{\mu\mu} + k_{\phi}^2 \boldsymbol{\eta}_{\phi\phi} + \dots + k_{\psi}^2 \boldsymbol{\eta}_{\psi\psi}) J_{\mu\phi\dots\psi}(\mathbf{k}) J_{\mu\phi\dots\psi}(-\mathbf{k}), \tag{II.46}$$

as well as

$$\begin{aligned}
& \sum_{\mu} \sum_{\phi < \dots < \psi} k_{\mu}^2 J_{\mu\phi\dots\psi}(\mathbf{k}) J_{\mu\phi\dots\psi}(-\mathbf{k}) (\boldsymbol{\eta}_{\mu\mu} + \boldsymbol{\eta}_{\phi\phi} + \dots + \boldsymbol{\eta}_{\psi\psi}) \\
&= \sum_{\mu < \phi < \dots < \psi} (k_{\mu}^2 + k_{\phi}^2 + \dots + k_{\psi}^2) J_{\mu\phi\dots\psi}(\mathbf{k}) J_{\mu\phi\dots\psi}(-\mathbf{k}) (\boldsymbol{\eta}_{\mu\mu} + \boldsymbol{\eta}_{\phi\phi} + \dots + \boldsymbol{\eta}_{\psi\psi}). \tag{II.47}
\end{aligned}$$

Eqs. (II.43,II.45) give Eq. (II.39). With Eqs. (II.38), the short-ranged part of the Coulomb interaction between parallelepiped elements take a diagonal form,

$$\sum_j \delta E_j = -\frac{1}{(D-2)!} \sum_{\sigma, \phi, \dots, \psi} \frac{e^2}{2} \int_{b^{-1}\Lambda < |\mathbf{k}| < \Lambda} \frac{d^D \mathbf{k}}{(2\pi)^D} f_{\sigma\phi\dots\psi}(\mathbf{k}) J_{\sigma\phi\dots\psi}(\mathbf{k}) J_{\sigma\phi\dots\psi}(-\mathbf{k}). \quad (\text{II.48})$$

The Fourier-transform of the interaction potential is given by,

$$f_{\sigma\phi\dots\psi}(\mathbf{k}) = \begin{cases} \frac{\mathbf{q}^2 + (2 - \gamma_\tau^{-1})\omega^2}{k^4} & \text{if } \tau \in \{\sigma, \phi, \dots, \psi\}, \\ \frac{\gamma_\tau^{-1} \mathbf{q} + \omega^2}{k^4} & \text{if } \tau \notin \{\sigma, \phi, \dots, \psi\}, \end{cases} \quad (\text{II.49})$$

with $\mathbf{k} = (\omega, \mathbf{q})$ and $\mathbf{k} \cdot \mathbf{x} \equiv \mathbf{q} \cdot \mathbf{r} - \omega\tau$.

The short-ranged part of the interaction gives rise to a fugacity renormalization from the leading-order term in its gradient expansion. To this end, rewrite Eq. (II.48) in the space-time coordinate,

$$\begin{aligned} \sum_j \delta E_j &= -\frac{1}{(D-2)!} \sum_{\sigma, \phi, \dots, \psi} \frac{e^2}{2} \int d^D \mathbf{R}_1 \int d^D \mathbf{R}_2 F_{\sigma\phi\dots\psi}(|\mathbf{R}_1 - \mathbf{R}_2|) J_{\sigma\phi\dots\psi}(\mathbf{R}_1) J_{\sigma\phi\dots\psi}(\mathbf{R}_2), \\ &= -\frac{2\pi^2 e^2}{(D-2)!} \sum_j \sum_{\sigma, \phi, \dots, \psi} \int_{\partial\Gamma_j} d^{D-2} \mathbf{s}_1 \int_{\partial\Gamma_j} d^{D-2} \mathbf{s}_2 F_{\sigma\phi\dots\psi}(|\mathbf{R}(\mathbf{s}_1) - \mathbf{R}(\mathbf{s}_2)|) \mathbf{g}_{j, \sigma\phi\dots\psi}(\mathbf{s}_1) \mathbf{g}_{j, \sigma\phi\dots\psi}(\mathbf{s}_2) \end{aligned} \quad (\text{II.50})$$

where we used Eq. (I.7) with the oriented volume

$$\mathbf{g}_{j, \sigma\phi\dots\psi}(\mathbf{s}) \equiv \sum_{a, b, \dots, c=1}^{D-2} \varepsilon_{ab\dots c} \frac{\partial R_{j, \sigma}(\mathbf{s})}{\partial s_a} \frac{\partial R_{j, \phi}(\mathbf{s})}{\partial s_b} \dots \frac{\partial R_{j, \psi}(\mathbf{s})}{\partial s_c}. \quad (\text{II.51})$$

$F_{\sigma\phi\dots\psi}(\mathbf{x})$ stands for the short-ranged part of the anisotropic Coulomb interaction,

$$F_{\sigma\phi\dots\psi}(\mathbf{x}) = \int_{b^{-1}\Lambda < |\mathbf{k}| < \Lambda} \frac{d^D \mathbf{k}}{(2\pi)^D} e^{i\mathbf{q}\mathbf{r} - i\omega\tau} f_{\sigma\phi\dots\psi}(\mathbf{k}) \equiv \begin{cases} \ln b F_\tau(\mathbf{x}) & \text{if } \tau \in \{\sigma, \phi, \dots, \psi\}, \\ \ln b F_\mathbf{r}(\mathbf{x}) & \text{if } \tau \notin \{\sigma, \phi, \dots, \psi\}, \end{cases} \quad (\text{II.52})$$

$$\ln b F_\tau(\mathbf{x}) \equiv \int_{b^{-1}\Lambda < |\mathbf{k}| < \Lambda} \frac{d^D \mathbf{k}}{(2\pi)^D} e^{i\mathbf{q}\mathbf{r} - i\omega\tau} \frac{\mathbf{q}^2 + (2 - \gamma_\tau^{-1})\omega^2}{k^4}, \quad (\text{II.53})$$

$$\ln b F_\mathbf{r}(\mathbf{x}) \equiv \int_{b^{-1}\Lambda < |\mathbf{k}| < \Lambda} \frac{d^D \mathbf{k}}{(2\pi)^D} e^{i\mathbf{q}\mathbf{r} - i\omega\tau} \frac{\gamma_\tau^{-1} \mathbf{q} + \omega^2}{k^4}, \quad (\text{II.53})$$

with $\mathbf{k} = (\omega, \mathbf{q})$ and $\mathbf{x} = (\tau, \mathbf{r})$. Since $F_{\sigma\phi\dots\psi}(\mathbf{x})$ ranges only over the lattice constant length scale $[|\mathbf{x}| < \Lambda^{-1}]$, we kept only the interaction within the same vortex hyper-surface in Eq. (II.50). Thanks to the short-ranged nature of the interaction, we may also use a gradient expansion on the hyper-surface and keep the leading order in the expansion,

$$\delta E_j = -\frac{2\pi^2 e^2}{(D-2)!} \sum_{\sigma, \phi, \dots, \psi} \int_{\partial\Gamma_j} d^{D-2} \mathbf{s} \mathbf{g}_{j, \sigma\phi\dots\psi}^2(\mathbf{s}) \int d^{D-2} \Delta \mathbf{s} F_{\sigma\phi\dots\psi} \left(\sum_{a=1}^{D-2} \Delta s_a \frac{\partial \mathbf{R}_j(\mathbf{s})}{\partial s_a} \right) + \dots, \quad (\text{II.54})$$

with $\Delta \mathbf{s} \equiv \mathbf{s}_1 - \mathbf{s}_2$, and $\mathbf{s} \equiv (\mathbf{s}_1 + \mathbf{s}_2)/2$. Note that $f_{\sigma\phi\dots\psi}(\mathbf{k})$ are even functions of their arguments, so are $F_{\sigma\phi\dots\psi}(\mathbf{x})$ as well. Moreover, $f_{\sigma\phi\dots\psi}(\mathbf{k} = (\mathbf{q}, \omega))$ is symmetric under the $O(D-1)$ rotation of \mathbf{q} $[(\mathbf{q}, \omega) \rightarrow (\tilde{\mathbf{q}}, \omega)]$ with $\tilde{\mathbf{q}} = O(D-1) \cdot \mathbf{q}$. Therefore, $F_{\sigma\phi\dots\psi}(\mathbf{x})$ must be functions of τ^2 and $|\mathbf{r}|^2$ as well. The $\Delta \mathbf{s}$ -integration of such functions with $\mathbf{x} \equiv \sum_{a=1}^{D-2} \Delta s_a \partial_{s_a} \mathbf{R}_j(\mathbf{s})$ must yield functions only of $\hat{\mathbf{g}}_{j, \tau}(\mathbf{s})$ and $\hat{\mathbf{g}}_{j, \mathbf{r}}(\mathbf{s})$. Let us call the $\Delta \mathbf{s}$ -integral of $F_\tau(\mathbf{x})$ and $F_\mathbf{r}(\mathbf{x})$ with $\mathbf{x} = \sum_{a=1}^{D-2} \Delta s_a \partial_{s_a} \mathbf{R}(\mathbf{s})$ as f_τ and $f_\mathbf{r}$, respectively,

$$f_\tau(\hat{\mathbf{g}}_{j, \tau}(\mathbf{s}), \hat{\mathbf{g}}_{j, \mathbf{r}}(\mathbf{s})) \equiv \int d^{D-2} \Delta \mathbf{s} F_\tau \left(\sum_{a=1}^{D-2} \Delta s_a \frac{\partial \mathbf{R}_j(\mathbf{s})}{\partial s_a} \right), \quad (\text{II.55})$$

$$f_\mathbf{r}(\hat{\mathbf{g}}_{j, \tau}(\mathbf{s}), \hat{\mathbf{g}}_{j, \mathbf{r}}(\mathbf{s})) \equiv \int d^{D-2} \Delta \mathbf{s} F_\mathbf{r} \left(\sum_{a=1}^{D-2} \Delta s_a \frac{\partial \mathbf{R}_j(\mathbf{s})}{\partial s_a} \right). \quad (\text{II.56})$$

Importantly, the function *forms* of f_τ and f_r do not depend on the shapes of vortex surfaces, and the same function forms apply to all vortex surfaces. This is because Eqs. (II.52,II.53) apply to all vortex surfaces.

With the use of these functions together with $h_\tau \equiv f_r^{-\frac{D-3}{D-2}} f_\tau$ and $h_1 = h_2 = \dots = h_{D-1} \equiv f_r^{\frac{1}{D-2}}$, the leading-order gradient-expansion term can be expressed as a function of $\hat{\mathbf{g}}_{j,\tau}(\mathbf{s})$ and $\hat{\mathbf{g}}_{j,r}(\mathbf{s})$,

$$\begin{aligned} \delta E_j &= -\frac{2\pi^2 e^2}{(D-2)!} \ln b \int_{\partial\Gamma_j} d^{D-2} \mathbf{s} \sum_{a,\dots,c,a',\dots,c'=1}^{D-2} \varepsilon_{ab\dots c} \varepsilon_{a'b'\dots c'} \\ &\quad \sum_{\sigma} \left(\frac{\partial R_{j,\sigma}(\mathbf{s})}{\partial s_a} h_{\sigma} \frac{\partial R_{\sigma}(\mathbf{s})}{\partial s_{a'}} \right) \sum_{\phi} \left(\frac{\partial R_{j,\phi}(\mathbf{s})}{\partial s_b} h_{\phi} \frac{\partial R_{j,\phi}(\mathbf{s})}{\partial s_{b'}} \right) \dots \sum_{\psi} \left(\frac{\partial R_{j,\psi}(\mathbf{s})}{\partial s_c} h_{\psi} \frac{\partial R_{j,\psi}(\mathbf{s})}{\partial s_{c'}} \right) \\ &= -2\pi^2 e^2 \ln b \int_{\partial\Gamma_j} d^{D-2} \mathbf{s} \det \left[f_r^{-\frac{D-3}{D-2}} f_\tau \hat{\mathbf{g}}_{j,\tau} + f_r^{\frac{1}{D-2}} \hat{\mathbf{g}}_{j,r} \right]. \end{aligned} \quad (\text{II.57})$$

Here \det is a determinant of a $(D-2) \times (D-2)$ matrix $f_r^{-\frac{D-3}{D-2}} f_\tau \hat{\mathbf{g}}_{j,\tau} + f_r^{\frac{1}{D-2}} \hat{\mathbf{g}}_{j,r}$, and f_r and f_τ are scalar functions of the temporal and spatial components of the metric tensor, $\hat{\mathbf{g}}_{j,\tau}$ and $\hat{\mathbf{g}}_{j,r}$. The function forms can be determined by integrals in Eqs. (II.52,II.53, II.55, II.56). Note that Eq. (II.57) inductively justifies the assumption given in Eq. (I.17).

To put this vortex fugacity renormalization into Eq. (II.33), we finally obtain

$$\begin{aligned} Z_v &= \int \mathcal{D}\mathbf{u} \exp \left[-\frac{1}{2} \int_{|\partial u| < b^{-1}\Lambda|u|} d^D \mathbf{x} \left\{ \bar{\gamma}_\tau (\partial_\mu u_{\mu\tau}) (\partial_\lambda u_{\lambda\tau}) + \bar{\gamma}_r \sum_{\nu=1}^{D-1} (\partial_\mu u_{\mu\nu}) (\partial_\lambda u_{\lambda\nu}) \right\} \right] \\ &\quad \left\{ 1 + \sum_{N=1}^{\infty} \frac{1}{N!} \prod_{j=1}^N \left(\int \mathcal{D}^D \mathbf{X}_j \int_{|\mathbf{Y}_j| > a_0 b} \mathcal{D}^D \mathbf{Y}_j \int \mathcal{D}\mathbf{g}_j(\mathbf{s}) \exp[w] \exp \left[\int_{\partial\Gamma_j} d^{D-2} \mathbf{s} \bar{t}(\hat{\mathbf{g}}_{j,\tau}, \hat{\mathbf{g}}_{j,r}) \right] \right) \right\} \\ &\quad \exp \left[-\frac{ie}{2} \int_{|\partial u| < b^{-1}\Lambda|u|} d^D \mathbf{x} u_{\mu\nu}(\mathbf{x}) v_{\mu\nu}(\mathbf{x}) - i2\pi\bar{\chi} \sum_{j=1}^N \mathcal{A}_{\tau,j} \right], \end{aligned} \quad (\text{II.58})$$

with Eqs. (II.24,II.25,II.26,II.28,II.34), and

$$\bar{t}(\hat{\mathbf{g}}_\tau, \hat{\mathbf{g}}_r) = t(\hat{\mathbf{g}}_\tau, \hat{\mathbf{g}}_r) - 2\pi^2 e^2 \ln b \det \left[f_r^{-\frac{D-3}{D-2}} (\hat{\mathbf{g}}_\tau, \hat{\mathbf{g}}_r) f_\tau(\hat{\mathbf{g}}_\tau, \hat{\mathbf{g}}_r) \hat{\mathbf{g}}_\tau + f_r^{\frac{1}{D-2}} (\hat{\mathbf{g}}_\tau, \hat{\mathbf{g}}_r) \hat{\mathbf{g}}_r \right], \quad (\text{II.59})$$

with Eqs. (II.55,II.52,II.56,II.53).

2. $D = 2$

The fugacity renormalization for $D = 2$ and $\gamma_\tau \neq 1$ can be calculated from Eq. (II.35), where $v_{\mu\nu}$ reduces to a scalar quantity;

$$v_{1\tau}(\mathbf{x}) = -v_{\tau 1}(\mathbf{x}) = 2\pi \sum_j \left(\delta^2(\mathbf{x} - \mathbf{R}_{j,v}) - \delta^2(\mathbf{x} - \mathbf{R}_{j,av}) \right) \equiv J(\mathbf{x}). \quad (\text{II.60})$$

Since $v_{\mu\nu}$ is scalar for $D = 2$, instead of Eq. (II.39), we have

$$\begin{aligned} k_\mu k_\lambda v_{\mu\nu}(\mathbf{k}) v_{\lambda\nu}(-\mathbf{k}) (\alpha_0 \delta_{\nu\nu} + \alpha_1 \eta_{\nu\nu}) &= J(\mathbf{k}) J(-\mathbf{k}) \left(\alpha_0 k^2 - \alpha_1 \left(\sum_{\mu=\tau,1} \eta_{\mu\mu} k_\mu^2 \right) \right) \\ &= J(\mathbf{k}) J(-\mathbf{k}) \left(\gamma_\tau^{-1} q^2 + \omega^2 \right), \end{aligned} \quad (\text{II.61})$$

with $\mathbf{k} \equiv (\omega, q)$. The short-ranged part of the logarithmic Coulomb interaction can be readily calculated,

$$\begin{aligned}
\sum_j \delta E_j &= -\frac{e^2}{2} \ln b \int d^2 \mathbf{R}_1 \int d^2 \mathbf{R}_2 F_{2D}(\mathbf{R}_1 - \mathbf{R}_2) J(\mathbf{R}_1) J(\mathbf{R}_2) \\
&= -2e^2 \pi^2 \ln b \sum_{j,m} \int d^2 \mathbf{R}_1 \int d^2 \mathbf{R}_2 F_{2D}(\mathbf{R}_1 - \mathbf{R}_2) \\
&\quad \left(\delta^2(\mathbf{R}_1 - \mathbf{R}_{j,v}) - \delta^2(\mathbf{R}_1 - \mathbf{R}_{j,av}) \right) \left(\delta^2(\mathbf{R}_2 - \mathbf{R}_{m,v}) - \delta^2(\mathbf{R}_2 - \mathbf{R}_{m,av}) \right) \\
&\simeq -\sum_j 4\pi^2 e^2 F_{2D}(\mathbf{0}) \ln b,
\end{aligned} \tag{II.62}$$

with

$$F_{2D}(\mathbf{R}) = \int_{\Lambda b^{-1} < |\mathbf{k}| < \Lambda} \frac{d^2 \mathbf{k}}{(2\pi)^2} e^{i\mathbf{k} \cdot \mathbf{R}} \frac{\gamma_\tau^{-1} q^2 + \omega^2}{k^4}. \tag{II.63}$$

In Eq. (II.62), we only kept ‘‘intra-vortex interactions’’ ($\mathbf{R}_1 = \mathbf{R}_2$) mediated by the scalar potential $u_{\tau 1}$, while neglecting the inter-vortex interactions ($\mathbf{R}_1 \neq \mathbf{R}_2$), because $F_{2D}(\mathbf{R}_1 - \mathbf{R}_2)$ is a short-ranged function. The strength of the ‘‘intra-vortex interaction’’ $F_{2D}(\mathbf{0})$ can be evaluated with a soft UV cutoff Λ ,

$$F_{2D}(\mathbf{0}) \simeq -\Lambda^{-1} \frac{\partial}{\partial \Lambda^{-1}} \left(\int \frac{d^2 \mathbf{k}}{(2\pi)^2} e^{-\Lambda^{-1} |\mathbf{k}|} \frac{\gamma_\tau^{-1} q^2 + \omega^2}{k^4} \right) = \frac{\gamma_\tau^{-1} + 1}{4\pi}. \tag{II.64}$$

To put this into Eq. (II.33) for $D = 2$, we obtain,

$$\begin{aligned}
Z_v &= \int \mathcal{D}\mathbf{u} \exp \left[-\frac{1}{2} \int_{|\partial u| < b^{-1} \Lambda |u|} d^D \mathbf{x} \left\{ \bar{\gamma}_\tau (\partial_\mu u_{\mu\tau}) (\partial_\lambda u_{\lambda\tau}) + \bar{\gamma}_\tau \sum_{\nu=1}^{D-1} (\partial_\mu u_{\mu\nu}) (\partial_\lambda u_{\lambda\nu}) \right\} \right] \\
&\quad \left\{ 1 + \sum_{N=1}^{\infty} \frac{1}{N!} \prod_{j=1}^N \left(\int \mathcal{D}^D \mathbf{X}_j \int_{|\mathbf{Y}_j| > a_0 b} \mathcal{D}^D \mathbf{Y}_j \exp[\bar{w}] \right) \right. \\
&\quad \left. \exp \left[-\frac{ie}{2} \int_{|\partial u| < b^{-1} \Lambda |u|} d^D \mathbf{x} u_{\mu\nu}(\mathbf{x}) v_{\mu\nu}(\mathbf{x}) - i2\pi \bar{\chi} \sum_{j=1}^N \mathcal{A}_{\tau,j} \right] \right\},
\end{aligned} \tag{II.65}$$

with

$$\bar{w} = w - \pi e^2 (\bar{\gamma}_\tau^{-1} + 1) \ln b. \tag{II.66}$$

C. renormalization group equation

After the integrations over the short-distance degrees of freedom, the partition function reduces to the same form as the original partition function, except for the renormalization of the coupling constants and the enlarged UV cutoff length. To put the enlarged UV length $a_0 b$ back into the original UV length a_0 , we employ a length rescaling in terms of the RG scale factor b ,

$$\mathbf{x} \rightarrow \mathbf{x}' = \mathbf{x} b^{-1}, \mathbf{s} \rightarrow \mathbf{s}' = \mathbf{s} b^{-1}, \mathbf{Y}_j \rightarrow \mathbf{Y}'_j = \mathbf{Y}_j b^{-1}, \mathbf{X}_j \rightarrow \mathbf{X}'_j = \mathbf{X}_j b^{-1}, \mathcal{A}_{j,\tau} \rightarrow \mathcal{A}'_{j,\tau} = \mathcal{A}_{j,\tau} b^{-(D-1)}, \tag{II.67}$$

with $\partial \dots \rightarrow \partial' \dots = b \partial \dots$, $\hat{\mathbf{g}}_{j,\dots}(\mathbf{s}) \rightarrow \hat{\mathbf{g}}'_{j,\dots}(\mathbf{s}') = \hat{\mathbf{g}}_{j,\dots}(\mathbf{s})$, $\mathbf{g}_{j,\lambda\rho\dots\sigma}(\mathbf{s}) \rightarrow \mathbf{g}'_{j,\lambda\rho\dots\sigma}(\mathbf{s}') = \mathbf{g}_{j,\lambda\rho\dots\sigma}(\mathbf{s})$, and $v \dots(\mathbf{x}) \rightarrow v' \dots(\mathbf{x}') = b^2 v \dots(\mathbf{x})$. We choose the normalization of the dual vector potential $u_{\mu\nu}(\mathbf{x})$ in such a way that the space component $\bar{\gamma}_\tau$ of the electromagnetic constitutive constant is invariant after the renormalization, i.e. $\bar{\gamma}_\tau = 1$,

$$u \dots(\mathbf{x}) \rightarrow u' \dots(\mathbf{x}') = \bar{\gamma}_\tau^{\frac{1}{2}} b^{\frac{D-2}{2}} u \dots(\mathbf{x}). \tag{II.68}$$

This determines the partition function after renormalization as follows,

$$\begin{aligned}
Z_v = & \int \mathcal{D}\mathbf{u} \exp \left[-\frac{1}{2} \int_{|\partial' u'| < \Lambda |u'|} d^D \mathbf{x}' \left\{ \gamma'_\tau (\partial'_\mu u'_{\mu\tau}) (\partial'_\lambda u'_{\lambda\tau}) + \sum_{\nu=1}^{D-1} (\partial'_\mu u'_{\mu\nu}) (\partial'_\lambda u'_{\lambda\nu}) \right\} \right] \\
& \left\{ 1 + \sum_{N=1}^{\infty} \frac{1}{N!} \prod_{j=1}^N \left(\int \mathcal{D}^D \mathbf{X}'_j \int_{|\mathbf{Y}'_j| > a_0} \mathcal{D}^D \mathbf{Y}'_j \int \mathcal{D}\mathbf{g}'_j(\mathbf{s}') \exp[w'] \exp \left[\int_{\partial\Gamma_j} d^{D-2} \mathbf{s}' t'(\hat{\mathbf{g}}'_{j,\tau}, \hat{\mathbf{g}}'_{j,r}) \right] \right) \right. \\
& \left. \exp \left[-\frac{ie'}{2} \int_{|\partial' u'| < \Lambda |u'|} d^D \mathbf{x}' u'_{\mu\nu}(\mathbf{x}') v'_{\mu\nu}(\mathbf{x}') - i2\pi\chi' \sum_{j=1}^N \mathcal{A}'_{\tau,j} \right] \right\}, \tag{II.69}
\end{aligned}$$

with

$$\gamma'_\tau = \frac{\bar{\gamma}_\tau}{\bar{\gamma}_r}, \quad (e')^2 = e^2 b^{D-2} \frac{1}{\bar{\gamma}_r}, \quad \chi' = \bar{\chi} b^{D-1}, \tag{II.70}$$

and

$$\begin{cases} t'(\hat{\mathbf{g}}'_\tau, \hat{\mathbf{g}}'_r) = b^{D-2} \bar{t}(\hat{\mathbf{g}}_\tau, \hat{\mathbf{g}}_r), & w' = w + 2D \ln b, & \text{for } D > 2, \\ w' = \bar{w} + 4 \ln b = w + 4 \ln b - \pi e^2 (\gamma_\tau^{-1} + 1) \ln b, & & \text{for } D = 2. \end{cases} \tag{II.71}$$

From this, we obtain the coupled RG equations for $D > 2$,

$$\frac{dw}{d \ln b} = 2D, \tag{II.72}$$

$$\frac{dt}{d \ln b} = (D-2)t - 2\pi^2 e^2 \det \left[f_r^{-\frac{D-3}{D-2}} f_\tau \hat{\mathbf{g}}_\tau + f_r^{\frac{1}{D-2}} \hat{\mathbf{g}}_r \right], \tag{II.73}$$

$$\frac{d\gamma_\tau}{d \ln b} = 16\pi^2 e^2 \frac{a_0^{D-2}}{2^{2D-2}} A^2 \int_{S_{D-1}} \mathcal{D}^{D-1} \mathbf{e}_0 e^{E_0(\theta)} \cos \left[4\pi\chi \left(\frac{a_0}{2} \right)^{D-1} A \cos \theta \right] \left(\cos^2 \theta - \gamma_\tau \frac{\sin^2 \theta}{D-1} \right), \tag{II.74}$$

$$\frac{de^2}{d \ln b} = (D-2)e^2 - 16\pi^2 e^4 \frac{a_0^{D-2}}{2^{2D-2}} \frac{A^2}{D-1} \int_{S_{D-1}} \mathcal{D}^{D-1} \mathbf{e}_0 e^{E_0(\theta)} \cos \left[4\pi\chi \left(\frac{a_0}{2} \right)^{D-1} A \cos \theta \right] \sin^2 \theta, \tag{II.75}$$

$$\frac{d\chi}{d \ln b} = (D-1)\chi - 4\pi e^2 \frac{1}{\gamma_\tau} \frac{a_0^{-1}}{2^{D-1}} A \int_{S_{D-1}} \mathcal{D}^{D-1} \mathbf{e}_0 e^{E_0(\theta)} \sin \left[4\pi\chi \left(\frac{a_0}{2} \right)^{D-1} A \cos \theta \right] \cos \theta. \tag{II.76}$$

f_r , f_τ and t in Eq. (II.73) are scalar functions of the temporal and spatial components of the metric tensor, $\hat{\mathbf{g}}_\tau$ and $\hat{\mathbf{g}}_r$. As in Eq. (I.17), the vortex energy for each closed vortex surface is given by an \mathbf{s} -integral of $t(\hat{\mathbf{g}}_\tau(\mathbf{s}), \hat{\mathbf{g}}_r(\mathbf{s}))$ over the surface. The second term of Eqs. (II.75, II.76) stands for the screening of the smaller vortex surface on the long-ranged Coulomb interaction. As for the smaller vortex surface, we considered the coplanar $(D-2)$ -sphere, whose diameter is the lattice constant a_0 , and who resides in a $(D-2)$ -dimensional plane. \mathbf{e}_0 in Eqs. (II.74, II.75, II.76) is the unit vector perpendicular to the $(D-2)$ -dimensional plane. The \mathbf{e}_0 -integral over the $(D-1)$ -sphere in Eqs. (II.74, II.75, II.76) enumerates all possible coplanar $(D-2)$ -spheres. θ in Eqs. (II.74, II.75, II.76) stands for the angle between \mathbf{e}_0 and the τ -axis. As discussed in a text below Eq. (II.10), the fugacity $E_0(\theta)$ of the coplanar vortex sphere is given by a symmetric function of θ , $E_0(\theta) = E_0(\pi - \theta)$.

For $D = 2$, the RG equations for w and t should be unified into an equation for w ,

$$\frac{dw}{d \ln b} = 4 - \pi e^2 (\gamma_\tau^{-1} + 1), \tag{II.77}$$

while $E_0(\theta)$ in Eqs. (II.75, II.74, II.76) becomes a scalar quantity w . In the following section, we analyze these RG equations in a few relevant cases.

III. PHASES, PHASE TRANSITIONS, AND UNIVERSAL CRITICALITY

A. An $\epsilon = D - 2$ expansion analysis on the phase transition at $\chi = 0$

In the absence of the Berry phase term [$\chi = 0$], the theory becomes isotropic, where $\gamma_\tau = 1$ is invariant under renormalization, the fugacity of a vortex hyper-surface is proportional to the $(D-2)$ -dimensional volume of the

surface [Eq. (I.15)], and the fugacity $E_0(\theta)$ of the smallest coplanar vortex sphere becomes independent of θ . In fact, Eqs. (II.53, II.52) with $\gamma_\tau = 1$ dictate that $F_\tau(\mathbf{x}) = F_{\mathbf{r}}(\mathbf{x}) \equiv F(\mathbf{x})$ depends only on $|\mathbf{x}| = \sqrt{\tau^2 + |\mathbf{r}|^2}$, and Eqs. (II.56, II.55) indicate that $f_\tau = f_{\mathbf{r}} \equiv f$ depends only on $\hat{\mathbf{g}} = \hat{\mathbf{g}}_\tau + \hat{\mathbf{g}}_{\mathbf{r}}$ [see Eq. (I.16)]. By calculating the integrals with a soft UV cutoff [see section. IV A], one obtains,

$$f = f_\tau = f_{\mathbf{r}} = \frac{1}{2\pi} \frac{1}{\det[\hat{\mathbf{g}}]^{1/2}}. \quad (\text{III.1})$$

By substituting Eq. (III.1) into Eq. (II.73), one can see that the fugacity renormalization is given by $\pi e^2 \det[\hat{\mathbf{g}}]^{1/2}$, justifying Eq. (I.15): the fugacity of a vortex hyper-surface is proportional to the $(D-2)$ -dimensional volume of the surface. Therefore, Eq (II.73) reduces to a differential equation for a real-valued scalar parameter t ,

$$\frac{dt}{d \ln b} = (D-2)t - \pi e^2. \quad (\text{III.2})$$

According to Eq. (I.15), the fugacity for the smallest coplanar vortex sphere [$(D-2)$ -sphere] in Eq. (II.5) is independent of θ ,

$$E_0 = t \left(\frac{a_0}{2}\right)^{D-2} \frac{2\pi^{\frac{D-1}{2}}}{\Gamma(\frac{D-1}{2})}, \quad (\text{III.3})$$

so that the integral over \mathbf{e}_0 in Eqs. (II.75, II.74, II.76) can be easily calculated at $\chi = 0$,

$$\begin{aligned} \frac{de^2}{d \ln b} &= (D-2)e^2 - 16\pi^2 \exp[E_0] e^4 \frac{a_0^{D-2}}{2^{2D-2}} \frac{A^2}{D-1} \int_{S_{D-1}} \mathcal{D}^{D-1} \mathbf{e}_0 \sin^2 \theta, \\ &= (D-2)e^2 - 16\pi^2 \exp[E_0] e^4 \frac{a_0^{D-2}}{2^{2D-2}} \frac{\pi^{\frac{D}{2}}}{\Gamma(\frac{D+2}{2})} A^2, \end{aligned} \quad (\text{III.4})$$

with $d\gamma_\tau/d \ln b = 0$, and $d\chi/d \ln b = 0$. Here we used

$$\begin{aligned} \int_{S_{D-1}} \mathcal{D}^{D-1} \mathbf{e}_0 \sin^2 \theta &= \int_0^\pi (\sin \theta)^D d\theta \int_0^\pi (\sin \theta')^{D-3} d\theta' \dots \int_0^\pi \sin \theta'' d\theta'' \int_0^{2\pi} d\theta''' \\ &= \frac{\sqrt{\pi} \Gamma(\frac{D+1}{2})}{\Gamma(\frac{D+2}{2})} \frac{\sqrt{\pi} \Gamma(\frac{D-2}{2})}{\Gamma(\frac{D-1}{2})} \dots \frac{\sqrt{\pi} \Gamma(\frac{1+1}{2})}{\Gamma(\frac{1+2}{2})} 2\pi = (D-1) \frac{\pi^{\frac{D}{2}}}{\Gamma(\frac{D+2}{2})}. \end{aligned} \quad (\text{III.5})$$

$d\gamma_\tau/d \ln b = d\chi/d \ln b = 0$ justifies that $\gamma_\tau = 1$ and $\chi = 0$ are invariant under renormalization.

Let us normalize t and e^2 into dimensionless coupling constants,

$$t_{\text{new}} = t_{\text{old}} \left(\frac{a_0}{2}\right)^{D-2} \frac{2\pi^{\frac{D-1}{2}}}{\Gamma(\frac{D-1}{2})}, \quad e_{\text{new}}^2 = \pi e_{\text{old}}^2 \left(\frac{a_0}{2}\right)^{D-2} \frac{2\pi^{\frac{D-1}{2}}}{\Gamma(\frac{D-1}{2})}. \quad (\text{III.6})$$

We obtain

$$\frac{dt}{d \ln b} = (D-2)t - e^2, \quad \frac{de^2}{d \ln b} = (D-2)e^2 - \frac{4\sqrt{\pi}}{D-1} \frac{\left(\frac{\pi}{2}\right)^D}{\Gamma(\frac{D+1}{2})\Gamma(\frac{D+2}{2})} e^4 \exp[t]. \quad (\text{III.7})$$

With $D = 2 + \epsilon$ and $e^2 \equiv x$,

$$\frac{dt}{d \ln b} = \epsilon t - x, \quad \frac{dx}{d \ln b} = \epsilon x - (2\pi^2 - \Gamma\epsilon)x^2 \exp[t]. \quad (\text{III.8})$$

where $\Gamma \equiv \pi^2(3 - \gamma + \ln[4/\pi^2] + \psi^{(0)}(3/2)) = 15.36\dots$. The differential equation has a fixed-point solution at $x = x_* = \epsilon t_*$, $t = t_* = t_{(0),*} + \epsilon t_{(1),*} + \mathcal{O}(\epsilon^2)$. Here $t_{(0),*}$ and $t_{(1),*}$ satisfy

$$\begin{aligned} 1 &= 2\pi^2 t_{(0),*} e^{t_{(0),*}}, \\ t_{(1),*} &= \frac{\Gamma}{2\pi^2} \frac{t_{(0),*}}{1 + t_{(0),*}} = 0.0359\dots, \end{aligned}$$

with $t_{(0),*} = 0.0483\dots$. Around the fixed point, the differential equations can be linearized,

$$\frac{d}{d \ln b} \begin{pmatrix} \delta t \\ \delta x \end{pmatrix} = \begin{pmatrix} \epsilon & -1 \\ -\epsilon^2 t_* & -\epsilon \end{pmatrix} \begin{pmatrix} \delta t \\ \delta x \end{pmatrix}. \quad (\text{III.9})$$

The matrix has positive and negative eigenvalues,

$$\begin{aligned} \lambda_{\pm} &= \pm \epsilon \sqrt{1 + t_*} = \pm \left(\epsilon \sqrt{1 + t_{(0),*}} + \frac{1}{2} \epsilon^2 \frac{t_{(1),*}}{\sqrt{1 + t_{(0),*}}} + \mathcal{O}(\epsilon^3) \right) \\ &\simeq \pm (1.024\epsilon + 0.0175\epsilon^2), \end{aligned}$$

indicating that the fixed point is a saddle fixed point characterizing the universal criticality of the ordered-disordered transition. Eigenvectors that belong to λ_{\pm} are given by $(1 \pm \sqrt{1 + t_*}, -\epsilon t_*)$. This suggests that a relevant (thermal) scaling variable associated with λ_+ consists mostly of δt . A leading order estimate of the critical exponent for the ordered-disordered transition is

$$\nu = \frac{1}{\epsilon} \frac{1}{\sqrt{1 + t_{(0),*}}} - \frac{1}{2} \frac{t_{(1),*}}{(1 + t_{(0),*})^{\frac{3}{2}}} + \mathcal{O}(\epsilon) \simeq \frac{0.977}{\epsilon} - 0.0167. \quad (\text{III.10})$$

When $\epsilon = 1$ ($D = 3$), $\nu \simeq 0.960$. Note also that $x_* = \epsilon t_* = \mathcal{O}(\epsilon)$ at the saddle fixed point for $D = 2 + \epsilon$ justifies the perturbative treatment of $e \equiv \sqrt{x}$ in Sec. II A for small ϵ [$D \gtrsim 2$].

Apart from the thermal relevant scaling variable, the Berry phase parameter χ is also a relevant (magnetic) scaling variable whose scaling dimension y_{χ} determines other critical properties around the ordered-disordered transition point at $\chi = 0$. To determine the scaling dimension y_{χ} of the Berry phase parameter χ , let us linearize the RG equation for χ around the saddle-fixed point (t_*, x_*) on the non-magnetic [$\chi = 0$] plane;

$$\frac{d\chi}{d \ln b} = \left\{ (D-1) - 16\pi^2 e^2 \chi A^2 \left(\frac{a_0}{2} \right)^{D-2} \frac{1}{2^D} \frac{\pi^{\frac{D}{2}}}{\Gamma(\frac{D+2}{2})} \right\} \chi, \quad (\text{III.11})$$

where we used

$$\int_{S_{D-1}} d^{D-1} e_0 \cos \theta^2 = \frac{1}{D-1} \int_{S_{D-1}} d^{D-1} e_0 \sin \theta^2 = \frac{\pi^{\frac{D}{2}}}{\Gamma(\frac{D+2}{2})}. \quad (\text{III.12})$$

With Eq. (III.6), this becomes,

$$\frac{d\chi}{d \ln b} = \left\{ (D-1) - \frac{4\sqrt{\pi}}{D-1} \frac{\left(\frac{\pi}{2}\right)^D}{\Gamma(\frac{D+2}{2})\Gamma(\frac{D+1}{2})} e^2 \exp[t] \right\} \chi. \quad (\text{III.13})$$

Eqs. (III.13, III.7) indicates that the scaling dimension y_{χ} of the Berry phase parameter χ is always 1, being independent from the spatial dimension D ,

$$\frac{d\chi}{d \ln b} = \left\{ (D-1) - (D-2) \right\} \chi = \chi \quad @ \quad (e, t, \chi) = (e_*, t_*, 0). \quad (\text{III.14})$$

$y_{\chi} = 1$ at the fixed point $(e, t, \chi) = (e_*, t_*, 0)$ originates from the absence of the renormalization factor to the electric charge e . To see this point, let us first include χ into $\partial_{\mu} u_{\mu\tau}$, and rewrite it into a form of an external magnetic field χ_h in the Maxwell action. Namely, with $\chi_h \equiv \chi/e$ and $\partial_{\mu} u_{\nu\mu} + \chi_h \delta_{\nu\tau} \rightarrow \partial_{\mu} u_{\nu\mu}$, the Berry phase term in the partition function can be absorbed into the coupling term between the vector potential and vortex field,

$$\begin{aligned} \frac{ie}{2} \int d^D \mathbf{x} \left\{ u_{\mu\nu}(\mathbf{x}) v_{\mu\nu}(\mathbf{x}) + 2\chi_h b_{\tau}(\mathbf{x}) \right\} &= ie \int d^D \mathbf{x} \left\{ (\partial_{\mu} u_{\nu\mu}(\mathbf{x})) b_{\nu}(\mathbf{x}) + \chi_h b_{\tau}(\mathbf{x}) \right\} \\ &\rightarrow ie \int d^D \mathbf{x} (\partial_{\mu} u_{\nu\mu}(\mathbf{x})) b_{\nu}(\mathbf{x}), \end{aligned} \quad (\text{III.15})$$

while the transformation gives rise to the magnetic field term in the Maxwell action,

$$\frac{\gamma_{\tau}}{2} \int d^D \mathbf{x} (\partial_{\lambda} u_{\nu\lambda}) (\partial_{\mu} u_{\nu\mu}) \rightarrow \frac{\gamma_{\tau}}{2} \int d^D \mathbf{x} \left\{ (\partial_{\lambda} u_{\nu\lambda}) (\partial_{\mu} u_{\nu\mu}) - 2\chi_h \partial_{\lambda} u_{\tau\lambda} \right\}. \quad (\text{III.16})$$

Thereby, the partition function can be generally rewritten into another form as well:

$$\begin{aligned}
Z_v = & \int \mathcal{D}\mathbf{u} \exp \left[-\frac{1}{2} \int_{|\partial u| < \Lambda|u|} d^D \mathbf{x} \left\{ (\partial_\mu u_{\mu\nu})(\partial_\lambda u_{\lambda\nu}) + 2\chi_h(\partial_\lambda u_{\lambda\tau}) \right\} \right] \\
& \left\{ 1 + \sum_{N=1}^{\infty} \frac{1}{N!} \prod_{j=1}^N \left(\int \mathcal{D}^D \mathbf{X}_j \int_{|\mathbf{Y}_j| > a_0} \mathcal{D}^D \mathbf{Y}_j \int \mathcal{D}\mathbf{g}_j(\mathbf{s}) \exp [E_j] \right) \right. \\
& \left. \exp \left[-\frac{i}{2} e \int_{|\partial u| < \Lambda|u|} d^D \mathbf{x} u_{\mu\nu}(\mathbf{x}) v_{\mu\nu}(\mathbf{x}) \right] \right\}. \tag{III.17}
\end{aligned}$$

The partition function undergoes an ordered-disordered phase transition. When $\chi_h = 0$ [the space-time isotropic case], the universal criticality of the phase transition is characterized by the saddle-fixed point at $(e, t) = (e_*, t_*)$ with $E_j = w + t \int_{\partial\Gamma_j} d^{D-2} \mathbf{s} \{\det \hat{\mathbf{g}}_j(\mathbf{s})\}^{1/2}$. The form of Eq. (III.17) suggests that the scaling property of χ_h around the isotropic saddle fixed point is determined by the field renormalization Z_u of the dual vector potential at the fixed point;

$$\chi_h \rightarrow \chi'_h = b^{D-1} Z_u^{-\frac{1}{2}} b^{-\frac{D-2}{2}} \chi_h, \tag{III.18}$$

with

$$u_{\dots}(\mathbf{x}) \rightarrow u'_{\dots}(\mathbf{x}') = Z_u^{\frac{1}{2}} b^{\frac{D-2}{2}} u_{\dots}(\mathbf{x}). \tag{III.19}$$

Notice that $Z_u = b^{D-2}$ at the saddle fixed point. This is because the integration of the short-distance degrees of freedom at $\chi_h = 0$ yields only the renormalization to the electromagnetic constitutive constant and vortex fugacity, while keeping intact the electric charge e ,

$$\begin{aligned}
Z_v = & \int \mathcal{D}\mathbf{u} \exp \left[-\frac{1}{2} \int_{|\partial u| < \Lambda|u|} d^D \mathbf{x} (\partial_\mu u_{\mu\nu})(\partial_\lambda u_{\lambda\nu}) \right] \left\{ 1 + \sum_{N=1}^{\infty} \frac{1}{N!} \right. \\
& \prod_{j=1}^N \left(\int \mathcal{D}^D \mathbf{X}_j \int_{|\mathbf{Y}_j| > a_0} \mathcal{D}^D \mathbf{Y}_j \int \mathcal{D}\mathbf{g}_j(\mathbf{s}) \exp \left[t \int_{\partial\Gamma_j} d^{D-2} \mathbf{s} \sqrt{\det \hat{\mathbf{g}}(\mathbf{s})} \right] \right) \\
& \left. \exp \left[-\frac{i}{2} e \int_{|\partial u| < \Lambda|u|} d^D \mathbf{x} u_{\mu\nu}(\mathbf{x}) v_{\mu\nu}(\mathbf{x}) \right] \right\} \\
= & \int \mathcal{D}\mathbf{u} \exp \left[-\frac{1}{2} \int_{|\partial u| < \Lambda b^{-1}|u|} d^D \mathbf{x} (1 + \delta\gamma)(\partial_\mu u_{\mu\nu})(\partial_\lambda u_{\lambda\nu}) \right] \left\{ 1 + \sum_{N=1}^{\infty} \frac{1}{N!} \right. \\
& \prod_{j=1}^N \left(\int \mathcal{D}^D \mathbf{X}_j \int_{|\mathbf{Y}_j| > a_0 b} \mathcal{D}^D \mathbf{Y}_j \int \mathcal{D}\mathbf{g}_j(\mathbf{s}) \exp \left[(t + \delta t) \int_{\partial\Gamma_j} d^{D-2} \mathbf{s} \sqrt{\det \hat{\mathbf{g}}(\mathbf{s})} \right] \right) \\
& \left. \exp \left[-\frac{i}{2} e \int_{|\partial u| < \Lambda b^{-1}|u|} d^D \mathbf{x} u_{\mu\nu}(\mathbf{x}) v_{\mu\nu}(\mathbf{x}) \right] \right\}. \tag{III.20}
\end{aligned}$$

As a result, the scaling property of the electric charge e is entirely determined by Z_u ,

$$e \rightarrow e' = \frac{b^{\frac{D-2}{2}}}{\sqrt{Z_u}} e, \tag{III.21}$$

with $Z_u = 1 + \delta\gamma$. This yields the following identity at the fixed point with $e' = e = e_*$,

$$Z_u|_{e^2=e_*^2, t=t_*} = b^{D-2}. \tag{III.22}$$

Then, from Eq. (III.18), the scaling dimension of χ_h around the saddle fixed point must always be one,

$$\chi'_h = b\chi_h. \tag{III.23}$$

The scaling dimension y_χ of the Berry phase parameter χ is also 1 as well, being independent of the space-time dimension D ,

$$\chi' \equiv \chi'_h e' = b\chi_h e = b\chi. \tag{III.24}$$

B. $D = 2$ in the presence of the Berry phase term ($\chi \neq 0$)

Let us next analyze the $\chi \neq 0$ RG equation in $D = 2$. At $D = 2$, $A = 1$, and $E_0 = w$, and $\int D\mathbf{e}_0 = \int_0^{2\pi} d\theta$. With a change of variables, $y \equiv e^w$ and $\nu \equiv 2\pi a_0 \chi$, this leads to

$$\frac{dy}{d \ln b} = (4 - \pi(\gamma_\tau^{-1} + 1)e^2)y, \quad (\text{III.25})$$

$$\begin{aligned} \frac{d\gamma_\tau}{d \ln b} &= 4\pi^2 e^2 y \int_0^{2\pi} d\theta \cos(\nu \cos \theta) \left(\frac{1 - \gamma_\tau}{2} + \frac{1 + \gamma_\tau}{2} \cos 2\theta \right), \\ &= 8\pi^3 e^2 y \left(\frac{1 - \gamma_\tau}{2} J_0(\nu) + \frac{1 + \gamma_\tau}{2} J_2(\nu) \right), \end{aligned} \quad (\text{III.26})$$

$$\frac{de^2}{d \ln b} = -4\pi^2 e^4 y \int_0^{2\pi} d\theta \cos(\nu \cos \theta) \frac{1 - \cos 2\theta}{2} = -8\pi^3 e^4 y \frac{J_0(\nu) + J_2(\nu)}{2}, \quad (\text{III.27})$$

$$\frac{d\nu}{d \ln b} = \nu - 4\pi^2 e^2 \frac{y}{\gamma_\tau} \int_0^{2\pi} \sin(\nu \cos \theta) \cos \theta = \nu - 8\pi^3 e^2 \frac{y}{\gamma_\tau} J_1(\nu), \quad (\text{III.28})$$

with the Bessel function of the first kind $J_n(x)$. On the non-magnetic plane [$\gamma_\tau = 1$ and $\nu = 0$], the RG equation shows the celebrated phase diagram of the Berezinskii-Kosterlitz-Thouless (BKT) phase transition:

$$\frac{dy}{d \ln b} = (4 - 2\pi e^2)y, \quad \frac{de^2}{d \ln b} = -4\pi^3 e^4 y, \quad (\text{III.29})$$

with the universal KT transition ‘temperature’; $1/e_{\text{KT}}^2 = \pi/2$. A phase boundary between KT and disordered phases is given by the following separatrix,

$$y = \frac{1}{2\pi^2} \ln \left(\frac{\pi}{2} e^2 \right) - \frac{1}{2\pi^2} + \frac{1}{\pi^3} \frac{1}{e^2}, \quad (\text{III.30})$$

with $e^2 > e_{\text{KT}}^2$.

The e^4 term in the right hand side of Eq. (III.27) represents the screening onto the 2D Coulomb interaction, which shows an oscillatory behavior as a function of the Berry phase parameter ν . The unphysical oscillation of the screening is an artifact of the sharp UV cut-off in Eqs. (II.1,II.2). In fact, the oscillation disappears when one uses a soft UV cut-off in these equations [85],

$$\begin{aligned} \int D^2 \mathbf{X}_0 \int_{a_0 < |\mathbf{Y}_0| < a_0 b} D^2 \mathbf{Y}_0 &= a_0^{-4} \int d^2 \mathbf{X}_0 \int_{a_0}^{a_0 b} Y_0 dY_0 \int_0^{2\pi} d\theta \\ &\rightarrow \frac{1}{2} a_0^{-4} \int d^2 \mathbf{X}_0 a_0 \ln b \frac{\partial}{\partial a_0} \left(\int_0^\infty dY_0 Y_0 e^{-Y_0/a_0} \right) \int_0^{2\pi} d\theta \\ &= \frac{1}{2} a_0^{-2} \ln b \int d^2 \mathbf{X}_0 \int_0^\infty dy_0 y_0^2 e^{-y_0} \int_0^{2\pi} d\theta, \end{aligned} \quad (\text{III.31})$$

with $y_0 \equiv Y_0/a_0$. Thereby, the soft UV cut-off modifies the renormalization factors to the constitutive constants and the 1D Berry phase term in Eqs. (II.24,II.25,II.26,II.28,II.34),

$$\begin{aligned} \bar{\gamma}_\tau &= \gamma_\tau + 2\pi^3 \ln b e^w e^2 \int_0^\infty dy_0 y_0^4 e^{-y_0} (J_0(\nu y_0) - J_2(\nu y_0)), \\ \bar{\gamma}_r &= 1 + 2\pi^3 \ln b e^w e^2 \int_0^\infty dy_0 y_0^4 e^{-y_0} (J_0(\nu y_0) + J_2(\nu y_0)), \\ \bar{\chi} &= \chi - 2\pi^2 \ln b \frac{e^2}{\gamma_\tau} e^w a_0^{-1} \int_0^\infty dy_0 y_0^3 e^{-y_0} J_1(\nu y_0). \end{aligned} \quad (\text{III.32})$$

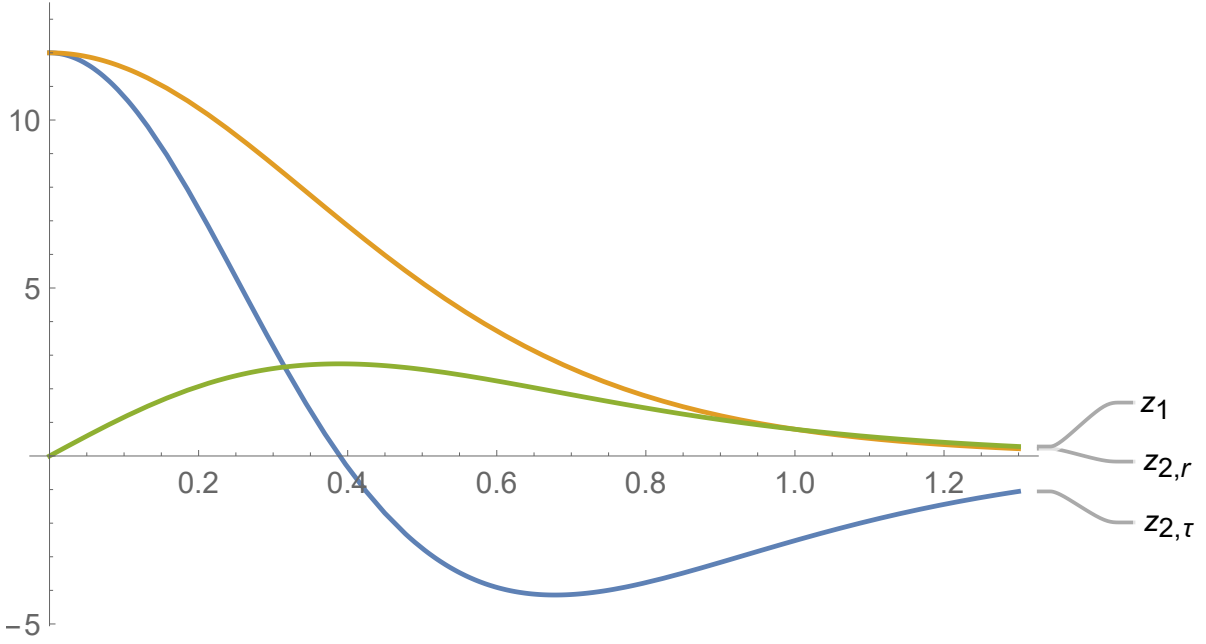


FIG. 4. $z_1(\nu)$ (green), $z_{2,\tau}(\nu)$ (blue) and $z_{2,r}(\nu)$ (orange) as functions of ν

With $y \equiv e^w$, $\nu \equiv 2\pi a_0 \chi$ and $e_{\text{new}}^2 = 4\pi^2 e_{\text{old}}^2$, we finally obtain $\chi \neq 0$ RG equations for $D = 2$ as follows,

$$\frac{d\gamma_\tau}{d\ln b} = \pi y e^2 \frac{12 - 81\nu^2 + 12\nu^4 - \gamma_\tau(12 + 9\nu^2 - 3\nu^4)}{(\nu^2 + 1)^{\frac{9}{2}}} \equiv \pi y e^2 (z_{2,\tau}(\nu) - \gamma_\tau z_{2,r}(\nu)), \quad (\text{III.33})$$

$$\frac{de^2}{d\ln b} = -\pi y e^4 \frac{12 + 9\nu^2 - 3\nu^4}{(\nu^2 + 1)^{\frac{9}{2}}} \equiv -\pi y e^4 z_{2,r}(\nu), \quad (\text{III.34})$$

$$\frac{d\nu}{d\ln b} = \nu - \frac{\pi y e^2}{\gamma_\tau} \frac{3\nu(4 - \nu^2)}{(\nu^2 + 1)^{\frac{7}{2}}} \equiv \nu - \frac{\pi y e^2}{\gamma_\tau} z_1(\nu), \quad (\text{III.35})$$

$$\frac{dy}{d\ln b} = \left(4 - \frac{\gamma_\tau^{-1} + 1}{4\pi} e^2\right) y, \quad (\text{III.36})$$

with

$$\begin{aligned} z_1(\nu) &\equiv \int_0^\infty dy y^3 e^{-y} J_1(\nu y) = \frac{3\nu(4 - \nu^2)}{(\nu^2 + 1)^{\frac{7}{2}}}, \\ z_{2,\tau}(\nu) &\equiv \frac{1}{2} \int_0^\infty dy y^4 e^{-y} (J_0(\nu y) - J_2(\nu y)) = \frac{12 - 81\nu^2 + 12\nu^4}{(\nu^2 + 1)^{\frac{9}{2}}}, \\ z_{2,r}(\nu) &\equiv \frac{1}{2} \int_0^\infty dy y^4 e^{-y} (J_0(\nu y) + J_2(\nu y)) = \frac{12 + 9\nu^2 - 3\nu^4}{(\nu^2 + 1)^{\frac{9}{2}}} = \frac{z_1(\nu)}{\nu}. \end{aligned}$$

$z_{2,\tau}(\nu)$, and $z_{2,r}(\nu)$ are even functions of ν , while $z_1(\nu)$ is an odd function of ν [Fig. 4].

The RG equation has an anisotropic weak-coupling fixed line with finite e^2 and $\gamma_\tau < 1$, around which the screening onto e^2 , $\gamma_\tau^{-1}e^2$ and ν are vanishingly small. The weak coupling fixed line characterizes a similar critical phase as the Kosterlitz-Thouless phase. The strong coupling fixed point of Eqs. (III.33,III.34,III.35,III.36) turns out to be identical to the isotropic strong coupling fixed point on the non-magnetic plane [$\nu = 0$] with $\gamma_\tau = 1$, divergent fugacity parameter y , and vanishing e^2 and ν , around which the screening effects reduce both e^2 and ν to zero. The strong coupling fixed point represents the conventional 2D disordered phase. An ordered-disordered phase transition from the weak-coupling KT-like phase to the strong-coupling conventional disordered phase is characterized by a saddle fixed point with an *infinite* space-time anisotropy [$\gamma_\tau = 0$] together with $e^2 = 0$, and finite universal values of y , ν , and e^2/γ_τ . In the following, we will explain them in details.

The weak-coupling fixed line is characterized by the absence of the screening, divergent Berry phase parameter ν , and finite (non-universal) values of e^2 and $\gamma_\tau^{-1}e^2$. When the value of $(\gamma_\tau^{-1} + 1)e^2$ is greater than 16π , the fugacity

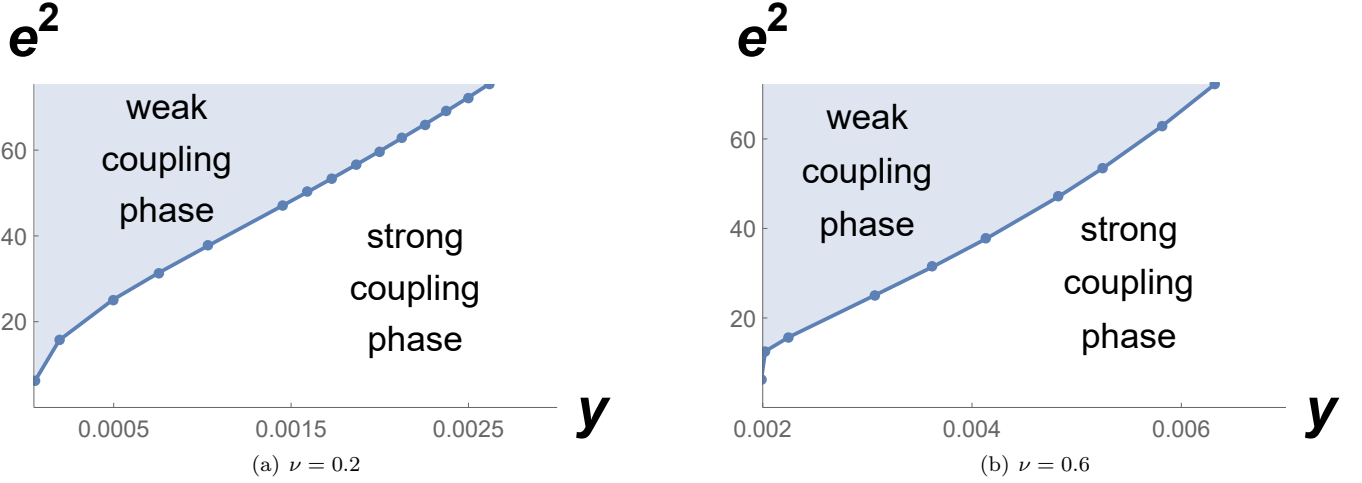


FIG. 5. numerical RG phase diagram with initial values of $\gamma_\tau = 1$ and $\nu = 0.2$ (left) and $\nu = 0.6$ (right). The horizontal and vertical axes are initial values of y , and e^2 , respectively. When the initial parameters are in the blue and white-colored regions, the RG equations drive them into the weak-coupling fixed line and strong-coupling fixed point, respectively.

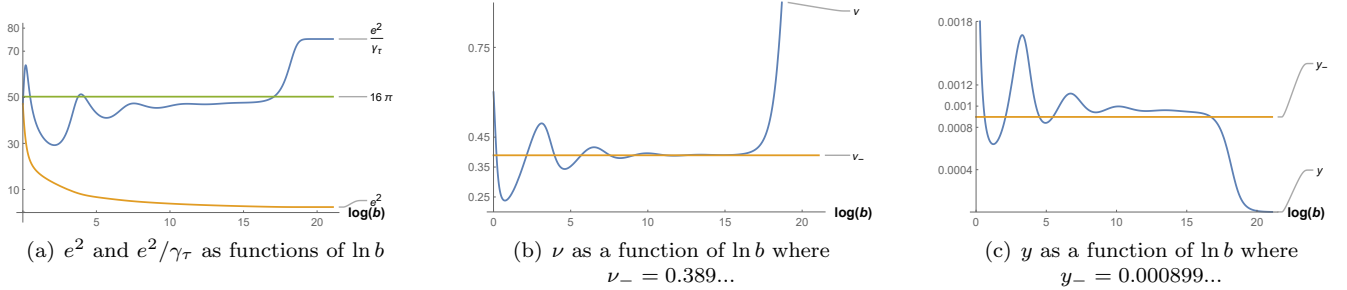


FIG. 6. Numerical solutions of e^2/γ_τ , e^2 , ν and y as functions of the RG scale $\ln b$ for a set of initial parameters closed to the phase boundary between ordered and disordered phases. The initial parameters are chosen in the ordered phase side of the phase boundary: $e^2/\gamma_\tau = e^2 = 15\pi$ and $\nu = 0.6$ and $y \lesssim y_c$ where $y_c = 0.004824\dots$

parameter y vanishes exponentially in the large $\ln b$ limit. Otherwise, y diverges exponentially in the large $\ln b$ limit, $y \propto b^\alpha$ with $\alpha < 4$. In either case, the quenching of screening in Eqs. (III.33,III.34,III.35) is induced by the divergent $\nu \propto b$, where a vanishingly small $z_{2,\tau(r)}(\nu) \propto \nu^{-5} \propto b^{-5}$ in the large $\ln b$ limit suppresses the second terms in Eqs. (III.34,III.35) irrespective of whether y is divergent or vanishing. Thereby, around the weak-coupling fixed line, the RG equation reduces to $d\gamma_\tau/d\ln b = de^2/d\ln b = 0$, $d\nu/d\ln b = \nu$, and $dy/d\ln b = (4 - (\gamma_\tau^{-1} + 1)e^2/4\pi)y$. Note that $z_{2,\tau}(\nu)$ is mostly smaller than $z_{2,r}(\nu)$, so that γ_τ is mostly decreasing and the convergent value of γ_τ is usually less than 1.

The strong coupling fixed point on the non-magnetic plane is a stable fixed point with $ye^2 = 1/(3\pi)$, $\nu = 0$, $\gamma_\tau = 1$, $e^2 = 0$ and divergent y . To see this stability, note first that when linearized around the fixed point, the RG equation for ye^2 has an IR stable fixed point at $ye^2 = 1/(3\pi)$ in the limit of $e^2 \rightarrow 0$,

$$\frac{d(ye^2)}{d\ln b} = 4ye^2 - 12\pi(ye^2)^2 - \frac{e^2}{2\pi}ye^2 \rightarrow 4ye^2 - 12\pi(ye^2)^2. \quad (\text{III.37})$$

The stability of the fixed point in the four-dimensional parameter space can be confirmed by a full set of linearized

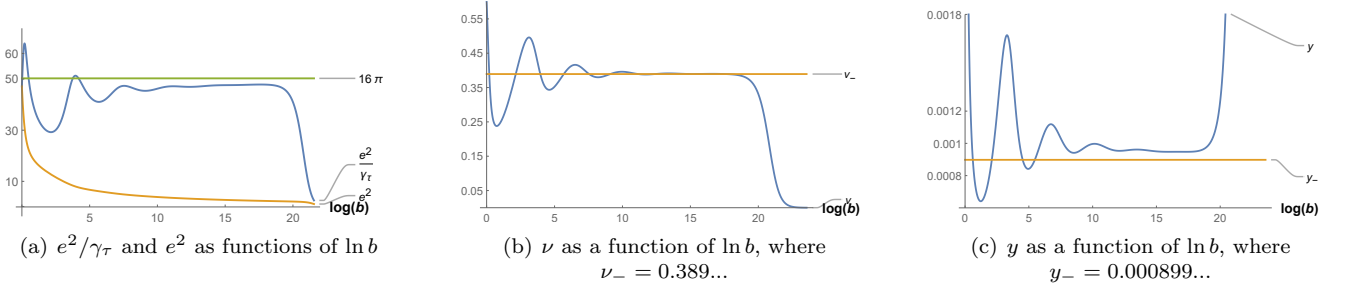


FIG. 7. Numerical solutions of e^2/γ_τ , e^2 , ν and y as functions of the RG scale $\ln b$ for a set of initial parameters closed to the phase boundary between ordered and disordered phases. The initial parameters are chosen in the disordered phase side of the phase boundary: with $e^2/\gamma_\tau = e^2 = 15\pi$ and $\nu = 0.6$ and $y \gtrsim y_c$ (strong-coupling ordered phase).

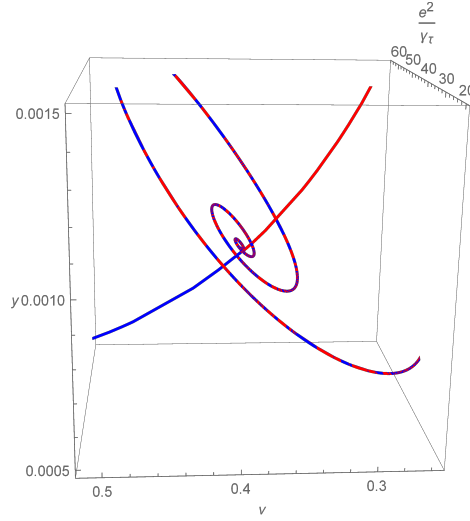


FIG. 8. Two RG flow trajectories near the saddle-fixed point in the three-dimensional parameter space. The saddle fixed point is at $(e^2/\gamma_\tau, \nu, y) = (16\pi, \nu_-, y_-) = (50.2\dots, 0.389\dots, 0.00899\dots)$. The blue (red) curve denotes the RG flow trajectory when the initial parameters are chosen in the ordered (disordered) phase side of the phase boundary: $e^2/\gamma_\tau = e^2 = 15\pi$ and $\nu = 0.6$ and $y \lesssim y_c$ ($y \gtrsim y_c$) respectively. The RG flow trajectories show swirling curves, when it is attracted toward the saddle fixed point. The RG flow trajectories show a rather straight curves, when they are repelled from the saddle fixed point. These behaviors are consistent with the linearization analysis of the RG equation around the fixed point: see Eq. (III.44) and texts below the equation.

RG equations,

$$\begin{aligned} \frac{d\delta(e^2)}{d\ln b} &= -\pi \left(\frac{1}{3\pi} + \delta(ye^2) \right) \delta(e^2) \left(z_{2,r}(0) + \mathcal{O}(\nu^2) \right) = -4\delta(e^2), \\ \frac{d\delta(ye^2)}{d\ln b} &= -4\delta(ye^2) - \frac{1}{6\pi^2} \delta(e^2), \\ \frac{d\delta\nu}{d\ln b} &= \delta\nu - \frac{\pi}{1 + \delta\gamma_\tau} \left(\frac{1}{3\pi} + \delta(ye^2) \right) \left(\frac{\partial z_1}{\partial \nu} \right)_{\nu=0} \delta\nu = \delta\nu - 4\delta\nu = -3\delta\nu, \\ \frac{d\delta\gamma_\tau}{d\ln b} &= \pi \left(\frac{1}{3\pi} + \delta(ye^2) \right) \left(12 - (1 + \delta\gamma_\tau)12 + \mathcal{O}(\delta\nu^2) \right) = -4\delta\gamma_\tau. \end{aligned}$$

with $\delta(ye^2) \equiv ye^2 - 1/(3\pi)$, $\delta\gamma_\tau \equiv \gamma_\tau - 1$, $\delta\nu \equiv \nu$, and $\delta(e^2) \equiv e^2$. The equations show an attractive nature of the fixed point in the four-dimensional parameter space.

The ordered-disordered phase transition between the weak-coupling phase and strong coupling phases is controlled by a saddle fixed point with an infinite space-time anisotropy $\gamma_\tau = 0$. To elaborate the nature of this fixed point, let

us rewrite the RG equations in terms of γ_τ/e^2 , y , ν and e^2 ;

$$\frac{d(\gamma_\tau/e^2)}{d \ln b} = \pi y z_{2,\tau}(\nu), \quad (\text{III.38})$$

$$\frac{de^2}{d \ln b} = -\pi y e^4 z_{2,r}(\nu), \quad (\text{III.39})$$

$$\frac{d\nu}{d \ln b} = \nu \left(1 - \frac{\pi y e^2}{\gamma_\tau} z_{2,r}(\nu) \right), \quad (\text{III.40})$$

$$\frac{dy}{d \ln b} = \left(4 - \frac{\gamma_\tau^{-1} + 1}{4\pi} e^2 \right) y, \quad (\text{III.41})$$

Note that $z_{2,\tau}(\nu)$ has a pair of zeros at $\nu_\pm^2 = (27 \pm \sqrt{665})/(2\sqrt{2})$ [Fig. 4], where $e^2 = 0$, $e^2/\gamma_\tau = 16\pi$, $y = y_\pm$ with

$$y_\pm = \frac{\gamma_\tau}{\pi e^2 z_{2,r}(\nu_\pm)} = \frac{1}{16\pi^2} \frac{1}{z_{2,r}(\nu_\pm)} \quad (\text{III.42})$$

could be possible fixed points of the RG equations. A negative value of $z_{2,r}(\nu_+)$ denies this possibility for the $\nu = \nu_+$ case.

The fixed point with $e^2 = 0$, $e^2/\gamma_\tau = 16\pi$, $y = y_- = 0.000898\dots$, and $\nu = \nu_- = 0.389\dots$ is a saddle fixed point with a relevant scaling variable, a marginally irrelevant scaling variable, and two irrelevant scaling variables. e^2 plays role of the marginally irrelevant scaling variable around the fixed point:

$$\frac{de^2}{d \ln b} = -\frac{1}{16\pi} e^4 + \mathcal{O}(e^4 \delta y, e^4 \delta \nu), \quad (\text{III.43})$$

with $\delta y \equiv y - y_-$, $\delta \nu \equiv \nu - \nu_-$ and $\delta(\gamma_\tau/e^2) \equiv \gamma_\tau/e^2 - 1/(16\pi)$. The relevant scaling variable and two other irrelevant scaling variables consist of the other three variables. The RG equations for the others are linearized around the fixed point,

$$\frac{d}{d \ln b} \begin{pmatrix} \delta(\frac{\gamma_\tau}{e^2}) \\ \delta \nu \\ \delta y \end{pmatrix} = \begin{pmatrix} 0 & \pi y_- \left(\frac{dz_{2,\tau}(\nu)}{d\nu} \right)_{|\nu=\nu_-} & 0 \\ 16\pi \nu_- & 1 & -\frac{\nu_-}{y_-} \\ 64\pi y_- & 0 & 0 \end{pmatrix} \begin{pmatrix} \delta(\frac{\gamma_\tau}{e^2}) \\ \delta \nu \\ \delta y \end{pmatrix}. \quad (\text{III.44})$$

The 3 by 3 matrix has eigenvalues of 1.95, $-0.475 \pm 1.84i$, where an eigenvector for the real positive eigenvalue y_t is given by

$$\left(\delta\left(\frac{\gamma_\tau}{e^2}\right) \delta \nu \delta y \right) = \left(-0.04616\dots \quad 0.999\dots \quad -0.00428\dots \right). \quad (\text{III.45})$$

This indicates that the RG flow to the strong/weak-coupling side of the fixed point increases/decreases y , while decreasing/increasing ν and increasing/decreasing $\delta(\gamma_\tau/e^2)$. A pair of two complex conjugate eigenvalues with a negative real part suggests that the RG flow streams into the saddle fixed point with a swirling trajectory [Fig. 8]. In the following, we name as \mathfrak{t} a scaling variable for the real positive eigenvalue y_t .

The numerical RG phase diagrams are shown in a two-dimensional parameter space subtended by initial values of y and e^2 for given initial values of ν and $\gamma_\tau = 1$ [Fig. 5]. The numerical phase diagrams generally show that larger (smaller) initial values of y and smaller (larger) initial values of e^2 lead to the strong-coupling disordered phase (weak-coupling ordered phase). Numerical solutions of e^2/γ_τ , e^2 , ν and y as functions of the RG scale $\ln b$ are shown in Figs. 6, 7. When the initial parameters are on the weak-coupling side of the phase boundary, both e^2/γ_τ and e^2 approach finite non-universal values in the IR limit [$\ln b \rightarrow \infty$], while ν diverges and y vanishes [Fig. 6]. When the initial parameters are on the strong-coupling side of the boundary, both e^2/γ_τ and e^2 approach zero, while γ_τ converges to 1, ν approaches zero, and y diverges [Fig. 7]. In either case, the parameters make a detour around the saddle fixed point: they first flow into the saddle fixed point before being repelled from the saddle fixed point to strong/weak coupling regions [Figs. 8, 6,7]. This clearly suggests that the ordered-disordered phase transition is of the second-order, and its universal criticality is controlled by the saddle fixed point at $(y, \nu, e^2/\gamma_\tau, e^2) = (y_-, \nu_-, 16\pi, 0)$. For example, the correlation-length exponent is estimated by the scaling dimension of the relevant scaling variable \mathfrak{t} : $1/y_{\mathfrak{t}} = 1/1.95\dots = 5.14\dots$

The divergence of γ_τ at the saddle fixed point suggests that the correlation time near the critical point acquires an additional logarithmic divergence compared to the divergent correlation length. To see this point, let us start from a scaling relation between the relevant scaling variable \mathfrak{t} before and after the renormalization, $\mathfrak{t}' = \mathfrak{t} b^{y_{\mathfrak{t}}}$. $\mathfrak{t} = 0$ corresponds to the critical point, while \mathfrak{t} is either negative (ordered phase) or positive (disordered phase), and $|\mathfrak{t}|$ can

be regarded as a ‘distance’ from the critical point. When an initial \mathbf{t} is infinitesimally small [the system is proximate to the critical point], one needs large b to bring the renormalized \mathbf{t}' away from a critical point : $b = (\mathbf{t}/\mathbf{t}_0)^{-1/y_c} \gg 1$ for $\mathbf{t}' = \mathbf{t}_0$. For such large b , the renormalized e^2 must be tiny: In fact, one solves Eq. (III.43) for the renormalized e^2 ,

$$\frac{1}{e_0^2} \simeq \frac{\ln b}{16\pi}. \quad (\text{III.46})$$

Since the renormalized e^2/γ_τ is around 16π , the renormalized space-time anisotropy parameter γ_τ must be tiny as well

$$\gamma_{\tau,0} \simeq \frac{y_c}{|\ln \mathbf{t}|}. \quad (\text{III.47})$$

The space-time anisotropy appears in a ratio between time and length scales. The form of the Maxwell action suggests that after the renormalization, the time scale $\xi_{\tau,0}$ becomes larger than the length scale $\xi_{r,0}$ by a factor $1/\sqrt{\gamma_{\tau,0}}$:

$$\xi_{\tau,0} = \xi_0 \frac{1}{\sqrt{\gamma_{\tau,0}}}, \quad \xi_{r,0} = \xi_0. \quad (\text{III.48})$$

Since these scales after the renormalization are related to the respective scales before the renormalization by a factor b , we finally obtain the correlation time ξ_τ and length ξ_r near the critical point as follows,

$$\xi_\tau = b\xi_{\tau,0} \sim |\mathbf{t}|^{-\frac{1}{y_c}} \sqrt{|\ln \mathbf{t}|}, \quad (\text{III.49})$$

$$\xi_r = b\xi_{r,0} \sim |\mathbf{t}|^{-\frac{1}{y_c}}. \quad (\text{III.50})$$

C. $D = 3$ in the presence of Berry phase term ($\chi \neq 0$)

In the presence of the Berry phase term, the fugacity renormalization in general D case takes complicated functions of space and time components of the metric tensor, $\hat{\mathbf{g}}_\tau$ and $\hat{\mathbf{g}}_r$. In $D = 3$, however, these components reduce to scalar quantities,

$$\begin{aligned} \hat{\mathbf{g}}_{j,\tau}(\mathbf{s}) &\rightarrow g_{j,\tau}(s) \equiv \left(\frac{dR_{j,\tau}(s)}{ds} \right)^2, \\ \hat{\mathbf{g}}_{j,r}(\mathbf{s}) &\rightarrow g_{j,r}(s) \equiv \sum_{\sigma=1,2} \left(\frac{dR_{j,\sigma}(s)}{ds} \right)^2, \end{aligned}$$

with $g_{j,\tau}(s) + g_{j,r}(s) = 1$, where the fugacity renormalization in Eq. (II.57) becomes simpler,

$$\delta E_j = -2\pi^2 e^2 \ln b \int_{\partial\Gamma_j} ds \left\{ f_\tau(g_{j,\tau}(s), g_{j,r}(s)) g_{j,\tau}(s) + f_r(g_{j,\tau}(s), g_{j,r}(s)) g_{j,r}(s) \right\}. \quad (\text{III.51})$$

Thereby, the fugacity for each closed vortex loop is given by the s -integral of the vortex core energy density $t(g_\tau(s))$ defined in the finite region $0 \leq g_\tau(s) \leq 1$, $E_j = \int_{\partial\Gamma_j} ds t(g_{j,\tau}(s))$, and the renormalization group equation for the vortex core energy density is given by,

$$\frac{dt(g_\tau)}{d \ln b} = t(g_\tau) - 2\pi^2 e^2 \left(f_\tau(g_\tau, 1 - g_\tau) g_\tau + f_r(g_\tau, 1 - g_\tau) (1 - g_\tau) \right). \quad (\text{III.52})$$

For simplicity, we characterize the vortex core energy density function by its two endpoint values, $t_\tau \equiv t(g_\tau = 1)$ and $t_r \equiv t(g_\tau = 0)$, while interpolating its middle values by $t(g_\tau) = t_\tau g_\tau + t_r g_r$, i.e.

$$E_j = w + \int_{\partial\Gamma_j} ds (t_\tau g_{j,\tau}(s) + t_r g_{j,r}(s)) = w + \int_{\partial\Gamma_j} ds \left(t_\tau \left(\frac{dR_{j,\tau}(s)}{ds} \right)^2 + t_r \sum_{\sigma=1,2} \left(\frac{dR_{j,\sigma}(s)}{ds} \right)^2 \right). \quad (\text{III.53})$$

From Eq. (III.52), the renormalization group equation for the two endpoint values is evaluated by

$$\frac{dt_\tau}{d \ln b} = t_\tau - 2\pi^2 e^2 f_\tau(g_\tau = 1, g_r = 0) = t_\tau - \pi e^2, \quad (\text{III.54})$$

$$\frac{dt_r}{d \ln b} = t_r - 2\pi^2 e^2 f_r(g_\tau = 0, g_r = 1) = t_r - \pi e^2 \frac{\gamma_\tau^{-1} + 1}{2}, \quad (\text{III.55})$$

[see sec. IV B for the evaluation]. Eqs. (III.54,III.55,III.53) with $t_\tau = t_r = t$ and $\gamma_\tau = 1$ become consistent with Eqs. (III.2,I.15) in the isotropic limit, upholding the validity of the simplification. In $D = 3$, the smallest vortex hyper-sphere becomes a coplanar vortex circle whose diameter is a_0 . From Eq. (III.53), the fugacity $E_0(\theta)$ for the vortex circle is given by

$$\begin{aligned} E_0(\theta) &= t_\tau \frac{a_0}{2} \int_0^{2\pi} d\alpha \sin^2 \theta \sin^2 \alpha + t_r \frac{a_0}{2} \int_0^{2\pi} d\alpha (\cos^2 \theta \sin^2 \alpha + \cos^2 \alpha) \\ &= \frac{a_0}{2} \pi (t_\tau (1 - \cos^2 \theta) + t_r (1 + \cos^2 \theta)), \end{aligned} \quad (\text{III.56})$$

where θ is the angle between a plane with the vortex circle and the time (τ) axis. From Eq. (II.19,II.74,II.75,II.76,III.56), the $D = 3$ RG equations for the other coupling constants are given by:

$$\frac{d\gamma_\tau}{d \ln b} = \frac{\pi^5}{2} e^2 a_0 \int_{-1}^1 ds e^{\frac{a_0}{2} \pi (t_\tau (1-s^2) + t_r (1+s^2))} e^{-i \frac{\pi^2 a_0^2}{2} \chi s} \left(s^2 - \gamma_\tau \frac{1-s^2}{2} \right), \quad (\text{III.57})$$

$$\frac{de^2}{d \ln b} = e^2 - \frac{\pi^5}{2} e^4 a_0 \int_{-1}^1 ds e^{\frac{a_0}{2} \pi (t_\tau (1-s^2) + t_r (1+s^2))} e^{-i \frac{\pi^2 a_0^2}{2} \chi s} \frac{1-s^2}{2}, \quad (\text{III.58})$$

$$\frac{d\chi}{d \ln b} = 2\chi - \pi^3 e^2 \frac{1}{\gamma_\tau} a_0^{-1} \int_{-1}^1 ds e^{\frac{a_0}{2} \pi (t_\tau (1-s^2) + t_r (1+s^2))} e^{-i \frac{\pi^2 a_0^2}{2} \chi s} i s, \quad (\text{III.59})$$

where $s = \cos \theta$ and $A = \frac{\pi}{2}$ at $D = 3$ in Eqs. (II.74,II.75,II.76). With proper normalization of the constants,

$$e_{\text{old}}^2 a_0 \equiv e_{\text{new}}^2, \quad \frac{\pi^2 a_0^2}{2} \chi \equiv \nu, \quad t_{\tau(r),\text{old}} a_0 \equiv t_{\tau(r),\text{new}}, \quad (\text{III.60})$$

the equations are simplified,

$$\frac{de^2}{d \ln b} = e^2 - \frac{\pi^5}{2} e^4 Z_{2,r}(\mathbf{t}, \nu), \quad (\text{III.61})$$

$$\frac{d\nu}{d \ln b} = 2\nu - \frac{\pi^5}{2} e^2 \gamma_\tau^{-1} Z_1(\mathbf{t}, \nu), \quad (\text{III.62})$$

$$\frac{d\gamma_\tau}{d \ln b} = \frac{\pi^5}{2} e^2 \left(Z_{2,\tau}(\mathbf{t}, \nu) - \gamma_\tau Z_{2,r}(\mathbf{t}, \nu) \right), \quad (\text{III.63})$$

$$\frac{dt_\tau}{d \ln b} = t_\tau - \pi e^2, \quad (\text{III.64})$$

$$\frac{dt_r}{d \ln b} = t_r - \pi e^2 \frac{\gamma_\tau^{-1} + 1}{2}, \quad (\text{III.65})$$

with $\mathbf{t} \equiv (t_\tau, t_r)$ and

$$Z_{2,\tau}(\mathbf{t}, \nu) \equiv \int_{-1}^1 ds s^2 e^{\frac{\pi}{2} (t_\tau (1-s^2) + t_r (1+s^2))} e^{-i\nu s}, \quad (\text{III.66})$$

$$Z_{2,r}(\mathbf{t}, \nu) \equiv \int_{-1}^1 ds \frac{1-s^2}{2} e^{\frac{\pi}{2} (t_\tau (1-s^2) + t_r (1+s^2))} e^{-i\nu s}, \quad (\text{III.67})$$

$$Z_1(\mathbf{t}, \nu) \equiv \int_{-1}^1 ds i s e^{\frac{\pi}{2} (t_\tau (1-s^2) + t_r (1+s^2))} e^{-i\nu s}. \quad (\text{III.68})$$

On the non-magnetic isotropic plane [$\nu = 0$, $\gamma_\tau = 1$ and $t_\tau = t_r = t$], the RG equation describes the ordered-disordered phase transition:

$$\frac{de^2}{d \ln b} = e^2 - \frac{\pi^5}{3} e^{\pi t} e^4, \quad \frac{dt}{d \ln b} = t - \pi e^2, \quad (\text{III.69})$$

with a saddle fixed point at (e_*^2, t_*) [$\pi e_*^2 = t_*$ and $1 = \frac{\pi^4}{3} e^{\pi t_*} \pi t_*$]. In the large b limit, parameters in the ordered phase flow into a weak coupling fixed point with divergent $e^2 \sim b$ and negatively divergent $t \sim -b \ln b$, while those in the disordered phase go to a strong coupling fixed point with vanishing $e^2 \sim b \exp[-A b]$ ($A > 0$), and positively divergent $t \sim b$.

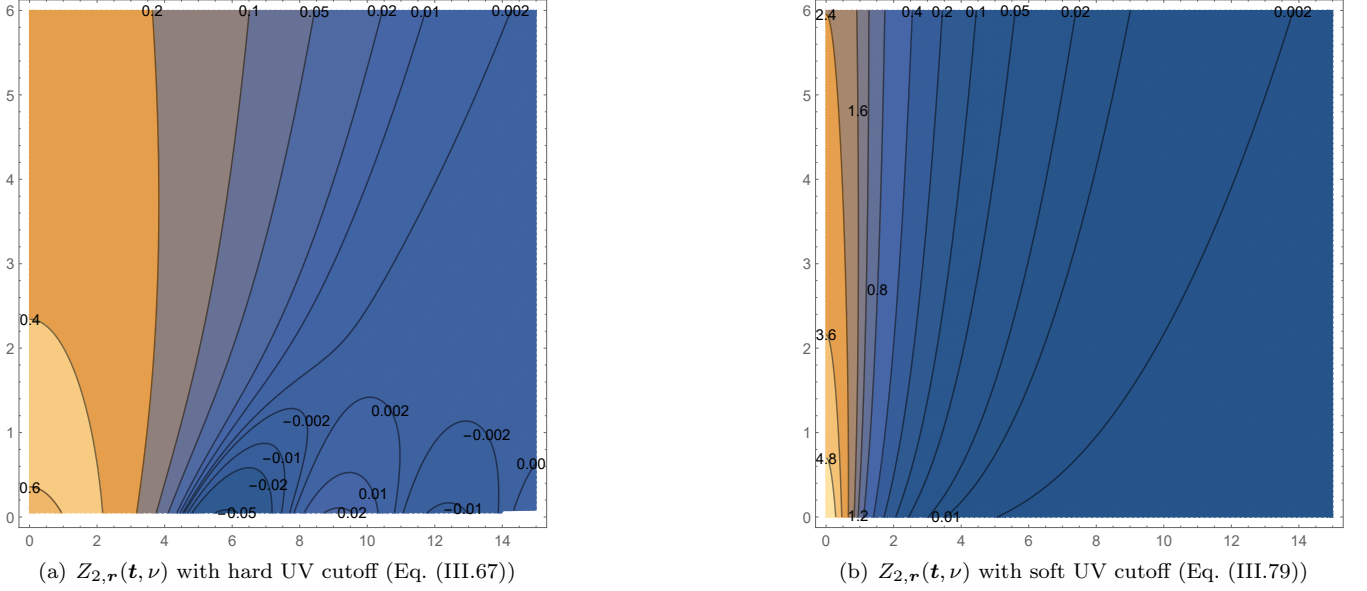


FIG. 9. Contour plots of $Z_{2,r}(t, \nu)$ as a function of $t_r = -t_r \equiv t_-/2$ and ν with the hard UV cutoff [Eq. (III.67)] and with the soft UV cutoff [Eq. (III.79)]. The horizontal and vertical axes are ν and t_- , respectively. Eq. (III.67) shows an oscillatory behavior as a function of the Berry phase parameter ν , while Eq. (III.79) does not.

Note that the e^4 term on the right hand side of Eq. (III.61) represents the screening effect, which shows an unphysical oscillatory behavior as a function of the 1D Berry phase parameter ν [Fig. 9(a)]. As in the 2D case, the oscillatory behavior is an artifact of a sharp UV cutoff in Eqs. (II.1,II.2), and it can be removed by using the soft UV cutoff [see Fig. 9(b)],

$$\begin{aligned}
\int D^3 \mathbf{X}_0 \int_{a_0 < |\mathbf{Y}_0| < a_0 b} D^3 \mathbf{Y}_0 \int D \mathbf{g}_0(\mathbf{s}) &= a_0^{-6} \int d^3 \mathbf{X}_0 \int_{a_0}^{a_0 b} Y_0^2 dY_0 \int_{S_2} d^2 \Omega \\
&\rightarrow \frac{1}{\mathcal{N}} a_0^{-6} \int d^3 \mathbf{X}_0 a_0 \ln b \frac{\partial}{\partial a_0} \left(\int_0^\infty dY_0 Y_0^2 e^{-Y_0^2/a_0^2} \right) \int_{S_2} d^2 \Omega \\
&= \frac{2}{\mathcal{N}} a_0^{-3} \ln b \int d^3 \mathbf{X}_0 \int_0^\infty dy_0 y_0^4 e^{-y_0^2} \int_{S_2} d^2 \Omega
\end{aligned} \tag{III.70}$$

with $y_0 \equiv Y_0/a_0$ and a normalization factor $\mathcal{N} = \int_0^\infty dy_0 2y_0^4 e^{-y_0^2} = 3\sqrt{\pi}/4$. With the soft UV cutoff, the renormalization of the consecutive constants and the Berry phase term in Eqs. (II.24,II.25,II.26) are modified,

$$\delta\chi = \frac{2\pi^3}{\mathcal{N}} e a_0^{-1} \int_0^\infty dy_0 y_0^6 e^{-y_0^2} \int_{-1}^1 ds e^{\frac{\pi y_0}{2} (t_r(1-s^2) + t_r(1+s^2))} s \sin(\nu y_0^2 s), \tag{III.71}$$

$$\begin{pmatrix} \delta\gamma_\tau \\ \delta\gamma_r \end{pmatrix} = \frac{\pi^5}{2\mathcal{N}} e^2 a_0 \int_0^\infty dy_0 y_0^8 e^{-y_0^2} \int_{-1}^1 ds e^{\frac{\pi y_0}{2} (t_r(1-s^2) + t_r(1+s^2))} \begin{pmatrix} s^2 \\ \frac{1-s^2}{2} \end{pmatrix} \cos(\nu y_0^2 s). \tag{III.72}$$

Accordingly, $Z_1(t, \nu)$, $Z_{2,r}(t, \nu)$ and $Z_{2,\tau}(t, \nu)$ in Eqs. (III.61,III.62,III.63) are modified into,

$$Z_1(t, \nu) \rightarrow \frac{2}{\mathcal{N}} \int_0^\infty dy y^6 e^{-y^2} \int_{-1}^1 ds i s e^{\frac{\pi y}{2} (t_r(1-s^2) + t_r(1+s^2))} e^{-i\nu y^2 s}, \tag{III.73}$$

$$\begin{pmatrix} Z_{2,\tau}(t, \nu) \\ Z_{2,r}(t, \nu) \end{pmatrix} \rightarrow \frac{2}{\mathcal{N}} \int_0^\infty dy y^8 e^{-y^2} \int_{-1}^1 ds \begin{pmatrix} s^2 \\ \frac{1-s^2}{2} \end{pmatrix} e^{\frac{\pi y}{2} (t_r(1-s^2) + t_r(1+s^2))} e^{-i\nu y^2 s}. \tag{III.74}$$

To evaluate these double integrals approximately, we replace y in the fugacity term $E_0(\theta)$ by 1;

$$\begin{aligned} Z_1(\mathbf{t}, \nu) &\simeq \frac{2}{\mathcal{N}} \int_{-1}^1 ds \, i s e^{\frac{\pi}{2}(t_\tau(1-s^2)+t_r(1+s^2))} \int_0^\infty dy y^6 e^{-y^2} e^{-i\nu y^2 s} \\ &= \frac{5}{2} \int_{-1}^1 ds \, i s e^{\frac{\pi}{2}(t_\tau(1-s^2)+t_r(1+s^2))} \frac{1}{(1+i\nu s)^{\frac{7}{2}}}, \end{aligned} \quad (\text{III.75})$$

$$\begin{aligned} \begin{pmatrix} Z_{2,\tau}(\mathbf{t}, \nu) \\ Z_{2,r}(\mathbf{t}, \nu) \end{pmatrix} &\simeq \frac{2}{\mathcal{N}} \int_{-1}^1 ds \begin{pmatrix} s^2 \\ \frac{1-s^2}{2} \end{pmatrix} e^{\frac{\pi}{2}(t_\tau(1-s^2)+t_r(1+s^2))} \int_0^\infty dy y^8 e^{-y^2} e^{-i\nu y^2 s} \\ &= \frac{35}{4} \int_{-1}^1 ds \begin{pmatrix} s^2 \\ \frac{1-s^2}{2} \end{pmatrix} e^{\frac{\pi}{2}(t_\tau(1-s^2)+t_r(1+s^2))} \frac{1}{(1+i\nu s)^{\frac{9}{2}}}, \end{aligned} \quad (\text{III.76})$$

where the following are used,

$$\int_0^\infty dy y^6 e^{-\alpha y^2} = \frac{5\mathcal{N}}{4} \frac{1}{\alpha^{\frac{7}{2}}}, \quad \int_0^\infty dy y^8 e^{-\alpha y^2} = \frac{35\mathcal{N}}{8} \frac{1}{\alpha^{\frac{9}{2}}}. \quad (\text{III.77})$$

Z_1 and $Z_{2,\tau(r)}$ can be numerically evaluated by the integral over $s \in [-1, 1]$,

$$Z_1(\mathbf{t}, \nu) = \frac{5}{2} e^{\frac{\pi}{2}(t_\tau+t_r)} \int_{-1}^1 ds e^{-\frac{\pi}{2}(t_\tau-t_r)s^2} \frac{s \sin\left(\frac{7}{2} \tan^{-1}(\nu s)\right)}{(1+\nu^2 s^2)^{\frac{7}{4}}}, \quad (\text{III.78})$$

$$\begin{pmatrix} Z_{2,\tau}(\mathbf{t}, \nu) \\ Z_{2,r}(\mathbf{t}, \nu) \end{pmatrix} = \frac{35}{4} e^{\frac{\pi}{2}(t_\tau+t_r)} \int_{-1}^1 ds e^{-\frac{\pi}{2}(t_\tau-t_r)s^2} \begin{pmatrix} s^2 \\ \frac{1-s^2}{2} \end{pmatrix} \frac{\cos\left(\frac{9}{2} \tan^{-1}(\nu s)\right)}{(1+\nu^2 s^2)^{\frac{9}{4}}}. \quad (\text{III.79})$$

These functions show similar behaviors to $z_1(\nu)$, $z_{2,\tau}(\nu)$, and $z_{2,r}(\nu)$ in 2D, respectively. They do not have the oscillatory behaviors as a function of ν [Fig. 9(b)]. In the following, we study the RG phase diagram obtained from Eqs. (III.61,III.62,III.63,III.65,III.64) with Eqs. (III.78,III.79).

In the large b limit, the RG equation drives the coupling constants into a weak coupling region for the ordered phase, an intermediate coupling region for the quasi-disordered phase or a strong coupling region for the disordered phase. The weak-coupling region is characterized by the vanishing screening effect, where $e^2 \sim b$, $\nu \sim b^2$, while γ_τ converges to a finite positive value less than 1. From Eqs. (III.64,III.65) with $e^2 \sim b$ and a constant γ_τ , both t_τ and t_r in the large b limit diverge negatively: $t_\tau, t_r \sim -b \ln b$. Due to the negatively divergent t_τ and t_r , $Z_{2,r}$, $Z_{2,\tau}$ and Z_1 in the large b limit vanish exponentially in b , resulting in the vanishing screening on the right hand sides of Eqs. (III.61, III.62,III.63).

The strong coupling region is characterized by the divergent screening effect, where $t_\tau + t_r$ diverges positively with $t_\tau + t_r \sim A_+ b$ ($A_+ > 0$), e^2 vanishes with $e^2 \sim b^{\frac{3}{2}} \exp[-\frac{\pi}{2} A_+ b]$, ν vanishes with $\nu \sim b^2 \exp[-\frac{\pi}{2} A_+ b]$, and the space-time anisotropy parameter diverges with $\gamma_\tau^{-1} \sim b$. Thereby, the temporal component t_τ of the vortex-loop fugacity always diverges positively with $t_\tau \sim A_\tau b$ ($A_\tau > 0$), while the spatial component t_r diverges either positively or negatively, depending on its initial value. The distinction between t_τ and t_r comes from the enhanced space-time anisotropy parameter ($\gamma_\tau^{-1} \sim b$), which selectively suppresses t_r through the fugacity renormalization: the second term of Eq. (III.65). The suppression of t_r by the enhanced space-time anisotropy always results in the positively divergent $t_\tau - t_r \sim A_- b$ ($A_- > 0$). With the divergent $t_\tau - t_r$, the s -integrals in Eqs. (III.78,III.79) are dominated by the contributions around $s = 0$, allowing asymptotic estimates of $Z_{2,\tau}(\mathbf{t}, \nu)$, $Z_{2,r}(\mathbf{t}, \nu)$, and $Z_1(\mathbf{t}, \nu)$:

$$\begin{pmatrix} Z_{2,\tau} \\ Z_{2,r} \end{pmatrix} \simeq \frac{35\sqrt{\pi}}{8} \exp\left[\frac{\pi}{2}(t_\tau + t_r)\right] \frac{1}{\sqrt{\frac{\pi}{2}(t_\tau - t_r)}} \begin{pmatrix} \frac{1}{\frac{\pi}{2}(t_\tau - t_r)} + \mathcal{O}(1/(t_\tau - t_r)^2) \\ 1 + \mathcal{O}(1/(t_\tau - t_r)) \end{pmatrix}, \quad (\text{III.80})$$

$$Z_1 \simeq \frac{35\sqrt{\pi}}{8} \nu \exp\left[\frac{\pi}{2}(t_\tau + t_r)\right] \left(\frac{1}{\left(\frac{\pi}{2}(t_\tau - t_r)\right)^{3/2}} + \mathcal{O}(1/(t_\tau - t_r)^{5/2}) \right). \quad (\text{III.81})$$

Eqs. (III.61,III.63,III.62,III.80,III.81) together with $t_\tau \pm t_r \sim A_\pm b$ lead to the strong-coupling asymptotics of e^2 , γ_τ and ν ;

$$e^2 \simeq \frac{A_+}{C_+} b^{\frac{3}{2}} \exp\left[-\frac{\pi}{2} A_+ b\right], \quad \gamma_\tau \simeq \frac{2}{\pi A_- b}, \quad \nu \simeq \text{const} \cdot b^2 \exp\left[-\frac{\pi}{2} A_+ b\right], \quad (\text{III.82})$$

with $C_+ = \frac{35\pi^4}{32} \sqrt{2/A_-}$.

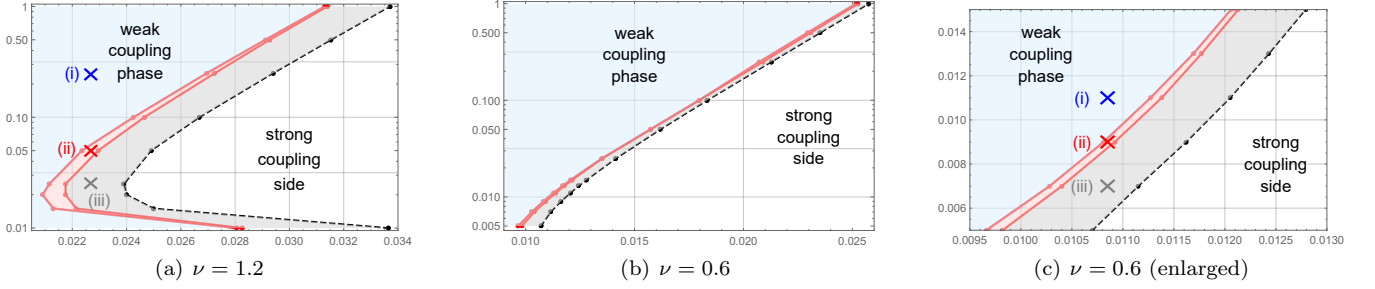


FIG. 10. Phase diagrams obtained from numerical solutions of the RG equations [Eqs. (III.61,III.62,III.63,III.65,III.64) together with Eqs. (III.78,III.79)] with initial values of e^2 , $t_\tau = t_r \equiv t$, $\gamma_\tau = 1$ and $\nu = 1.2$ (left) and 0.6 (middle, and right). The vertical and horizontal axes are initial values of e^2 and t , respectively. The light blue, light red, and light gray (white) regions stand for ordered, quasi-disordered, and disordered phases, respectively. A set of initial parameters in the light blue region goes to the weak-coupling region with divergent e^2 and ν , and negatively divergent t_τ and t_r , and constant γ_τ [see Figs. 11(a), 11(b), 11(c) for how the parameters evolve from the blue cross point “(i)” in Fig. 10(a); see Figs.12(a), 12(b), 12(c) for how the parameters evolves from the blue cross point “(i)” in Fig. 10(c)]. Initial parameters in the light gray (white) region go to the strong-coupling regions with vanishing e^2 and ν , positively divergent t_τ , and negatively (positively) divergent t_r , and divergent γ_τ^{-1} [see Figs. 11(g), 11(h), 11(i) for how the parameters evolve from the gray cross point “(iii)” in Fig. 10(a); see Figs.12(g), 12(h), 12(i) for how the parameters evolves from the gray cross point “(iii)” in Fig. 10(c)]. Initial parameters in the light red region go to the intermediate coupling region, where γ_τ^{-1} diverges at a finite value of the RG scale $\ln b$ [see Fig. 11(f) for how γ_τ^{-1} evolves from the red cross point “(ii)” in Fig. 10(a); see Fig.12(f) for how γ_τ^{-1} evolves from the red cross point “(ii)” in Fig. 10(c)].

For several initial values of ν and $\gamma_\tau = 1$, the phase diagrams of the RG equation are numerically obtained in a two-dimensional parameter space subtended by various initial values of $t = t_\tau = t_r$, and e^2 [Figs. 10(a), 10(b)]. The phase diagrams usually show that larger (smaller) initial values of t and smaller (larger) e^2 tend to be in the strong-coupling (weak-coupling) regions. For these regions, numerical solutions of e^2 , ν , γ_τ , and $t_\tau + t_r$ as functions of $\ln b$ are consistent with the previous arguments [Fig. 11]. Namely, when the initial parameters are in the weak-coupling region [light blue region], both e^2 and ν diverge with $e^2 \sim b$ and $\nu \sim b^2$ in the large b limit [Figs. 11(a),12(a)], while $t_\tau + t_r$ diverges negatively [Figs. 11(b),12(b)], and γ_τ converges to a finite non-universal constant [Figs. 11(c),12(c)]. When the initial parameters are in the strong-coupling region [gray or white regions], both e^2 and ν vanish exponentially in the large b limit [Figs. 11(g),12(g)], while $t_\tau + t_r$ diverges positively [Figs. 11(h),12(h)], and γ_τ goes to zero as $\gamma_\tau \sim 2/(\pi(t_\tau - t_r))$ [Figs. 11(i),12(i)].

Importantly, when the initial parameters are in the intermediate coupling region [light red region], γ_τ^{-1} diverges at a finite RG scale b [Figs. 11(f),12(f)] where e^2 and t_τ remain finite positive values [Figs. 11(d),12(d), Figs. 11(e),12(e)]. This numerical observation suggests a certain type of “Landau-pole” instability in the intermediate coupling region. To clarify the nature of the instability, note first that the large γ_τ^{-1} with finite e^2 generally polarizes vortex loops along the τ direction. Namely, with larger γ_τ^{-1} , the anisotropic Coulomb interaction energy between “neighboring” vortex loop elements favors vortex loop polarized along τ . From the analogy to 3-dimensional magnetostatics, the Coulomb energy $E_{\text{Coul}}(C, \gamma_\tau)$ of a vortex loop C is given by

$$\exp[-E_{\text{Coul}}(C, \gamma_\tau)] \equiv \int D\mathbf{a}(\mathbf{x}) \exp \left[-\frac{1}{2} \int d^3\mathbf{x} (\nabla \times \mathbf{a})^T \cdot \begin{pmatrix} \gamma_\tau & 0 \\ 0 & \mathbf{1}_{2 \times 2} \end{pmatrix} \cdot (\nabla \times \mathbf{a}) - 2\pi i e \oint_C d\mathbf{l} \cdot \mathbf{a}(\mathbf{l}) \right],$$

with $\mathbf{x} \equiv (\tau, \mathbf{r})$, $\nabla \equiv (\nabla_\tau, \nabla_{\mathbf{r}})$, $\mathbf{l} \equiv (l_\tau, \mathbf{l}_r)$, and $\mathbf{a} \equiv (\mathbf{a}_\tau, \mathbf{a}_r)$. To see how $E_{\text{Coul}}(C, \gamma_\tau)$ depends on the shape of the loop C , consider the following scale transformation,

$$\begin{aligned} \tau' &= \tau, \quad \mathbf{r}' = \mathbf{r} \frac{1}{\sqrt{\gamma_\tau}}, \quad \mathbf{a}'_\tau = \mathbf{a}_\tau, \quad \mathbf{a}'_r = \sqrt{\gamma_\tau} \mathbf{a}_r, \\ \nabla'_\tau &= \nabla_\tau, \quad \nabla'_r = \sqrt{\gamma_\tau} \nabla_r, \quad l'_\tau = l_\tau, \quad \mathbf{l}'_r = \mathbf{l}_r \frac{1}{\sqrt{\gamma_\tau}}, \end{aligned} \quad (\text{III.83})$$

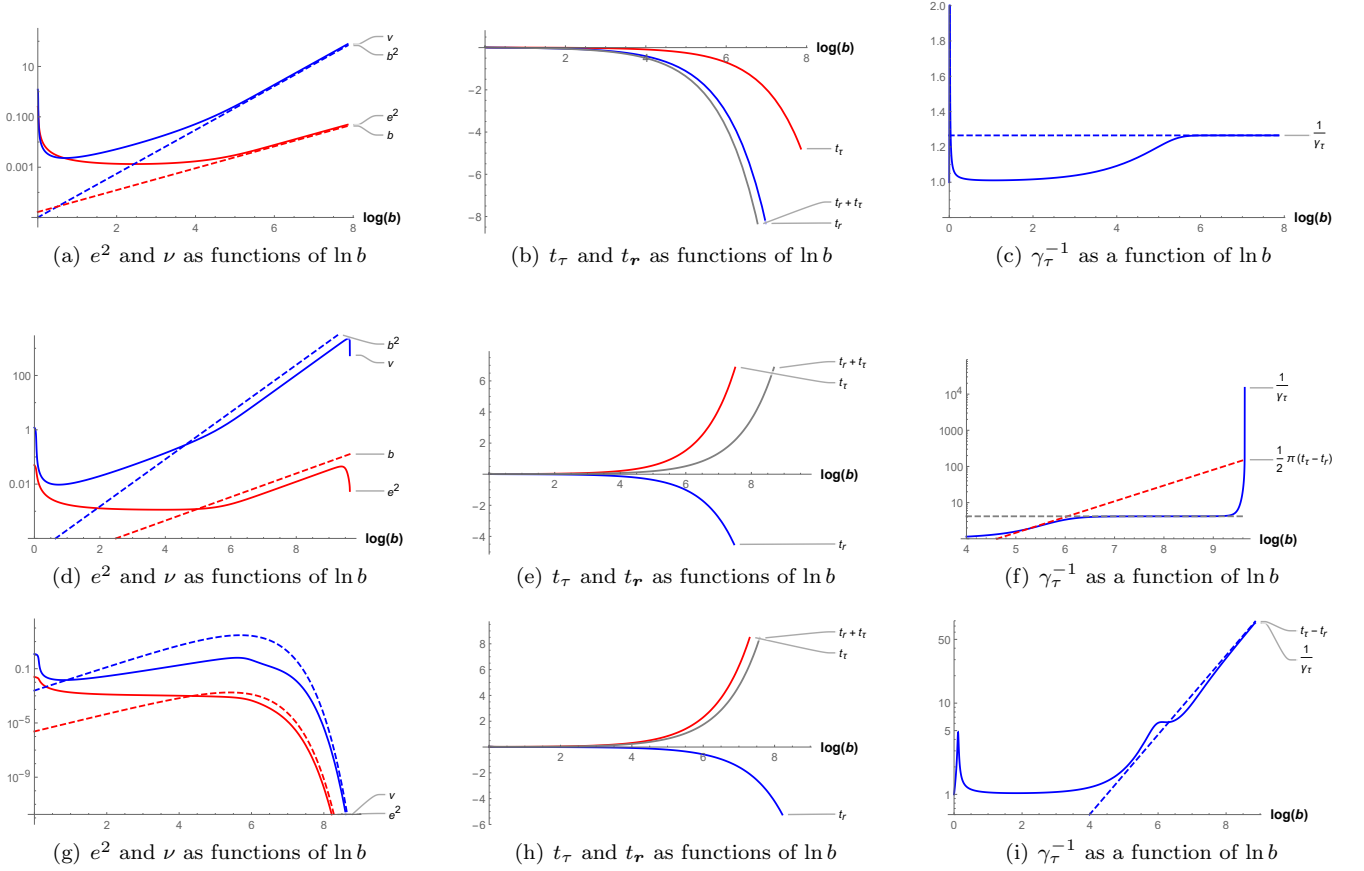


FIG. 11. Plots of e^2 , ν , t_τ , t_r and γ_τ^{-1} as functions of the RG scale $\ln b$. The plots are obtained from numerical solutions of the RG equations [Eqs. (III.61,III.62,III.63,III.65,III.64) together with Eqs. (III.78,III.79)]. The initial value of ν and γ_τ^{-1} are 1.2 and 1, respectively. As for the initial values of e^2 and $t_\tau = t_r = t$, we chose $(e^2, t)|_{\ln b=0} = (0.25, 0.02265)$ [denoted by blue cross mark in Fig. 10(a)] for Figs. 11(a),11(b),11(c), $(e^2, t)|_{\ln b=0} = (0.05, 0.02265)$ [denoted by red cross mark in Fig. 10(a)] for Figs. 11(d),11(e),11(f), and $(e^2, t)|_{\ln b=0} = (0.025, 0.02265)$ [denoted by gray cross mark in Fig. 10(a)] for Figs. 11(g),11(h),11(i). Dashed lines in Figs. 11(g), 11(i) are from Eq. (III.82).

which brings the Maxwell action with $\gamma_\tau \neq 1$ into the action with $\gamma_\tau = 1$,

$$\begin{aligned}
& \int Da(\mathbf{x}) \exp \left[-\frac{1}{2} \int d^3\mathbf{x} (\nabla \times \mathbf{a})^T \cdot \begin{pmatrix} \gamma_\tau & 0 \\ 0 & \mathbf{1}_{2 \times 2} \end{pmatrix} \cdot (\nabla \times \mathbf{a}) - 2\pi i e \oint_C d\mathbf{l} \cdot \mathbf{a}(\mathbf{l}) \right] \\
&= \text{const.} \int Da'(\mathbf{x}') \exp \left[-\frac{1}{2} \int d^3\mathbf{x}' (\nabla' \times \mathbf{a}')^T \cdot \begin{pmatrix} 1 & 0 \\ 0 & \mathbf{1}_{2 \times 2} \end{pmatrix} \cdot (\nabla' \times \mathbf{a}') - 2\pi i e \oint_{C'} d\mathbf{l}' \cdot \mathbf{a}'(\mathbf{l}') \right], \\
&= \text{const.} \exp[-E_{\text{Coul}}(C', \gamma_\tau = 1)].
\end{aligned} \tag{III.84}$$

The scale transformation deforms C into C' by stretching the loop in the \mathbf{r} direction by a factor of $1/\sqrt{\gamma_\tau}$. The transformation relates the anisotropic Coulomb interaction energy $E_{\text{Coul}}(C, \gamma_\tau)$ of C to the isotropic Coulomb interaction energy $E_{\text{Coul}}(C', \gamma_\tau = 1)$ of the stretched loop C' .

$$E_{\text{Coul}}(C, \gamma_\tau) = E_{\text{Coul}}(C', \gamma_\tau = 1) + \text{const.} \tag{III.85}$$

Here ‘const.’ on the right-hand sides is independent of the loops. Note that the Coulomb interaction energy of a vortex loop is generally dominated by its short-ranged part with the UV logarithmic divergence, $|\log a_0|$. In the isotropic limit, the coefficient of the UV logarithmic divergence is given by a vortex loop length,

$$E_{\text{Coul}}(C', \gamma_\tau = 1) = \frac{\pi e^2}{2} L(C') |\log a_0| + \dots \tag{III.86}$$

Thus, when $\gamma_\tau^{-1} \gg 1$, the dominant part of the anisotropic Coulomb energy $E_{\text{Coul}}(C, \gamma_\tau)$ disfavors vortex loops with finite projections in the \mathbf{r} direction. Namely, by the stretch, a loop C_1 with a finite projection in \mathbf{r} results in a longer loop than a loop C_2 without any projection in \mathbf{r} : in the limit of $\gamma_\tau^{-1} \rightarrow \infty$, $L(C_1) \gg L(C_2)$. The vortex loops without any projection to \mathbf{r} are nothing but vortex lines parallel to the τ axis.

Upon the divergence of γ_τ^{-1} with finite e^2 , the vortex excitations take the form of vortex lines fully polarized along τ , where the 3D partition function reduces to the 2D isotropic partition function for the BKT transition;

$$\begin{aligned} \lim_{\gamma_\tau \rightarrow 0} Z = & \int \mathcal{D}\mathbf{a} \exp \left[-\frac{1}{2} \int d^3\mathbf{x} \sum_{\mu=1,2} (\partial_\tau \mathbf{a}_\mu - \partial_\mu \mathbf{a}_\tau)^2 \right] \\ & \left\{ 1 + \sum_{N=1}^{\infty} \frac{1}{N!} \prod_{j=1}^N \left(\int \mathcal{D}^2 \mathbf{r}_{2j-1} e^{w+L_\tau t_\tau} \int \mathcal{D}^2 \mathbf{r}_{2j} e^{w+L_\tau t_\tau} \right) \right. \\ & \left. \exp \left[-i2\pi e \sum_{j=1}^{2N} (-1)^j \int_0^{L_\tau} d\tau \mathbf{a}_\tau(\mathbf{r}_j, \tau) \right] \right\}. \end{aligned} \quad (\text{III.87})$$

Here we take the inverse temperature L_τ [a ‘system size’ along the time direction] to be finite for bookkeeping purposes. \mathbf{r}_j ($j = 1, \dots, 2N$) denotes the two-dimensional spatial coordinate of the j th vortex line within the 1-2 plane, $e^{w+L_\tau t_\tau}$ is the fugacity of each vortex line, and $(-1)^j = \pm 1$ denotes the vorticity of the j th vortex line. As the vortex line is polarized along τ , only the temporal component \mathbf{a}_τ of the vector potential couples with the vortex excitations.

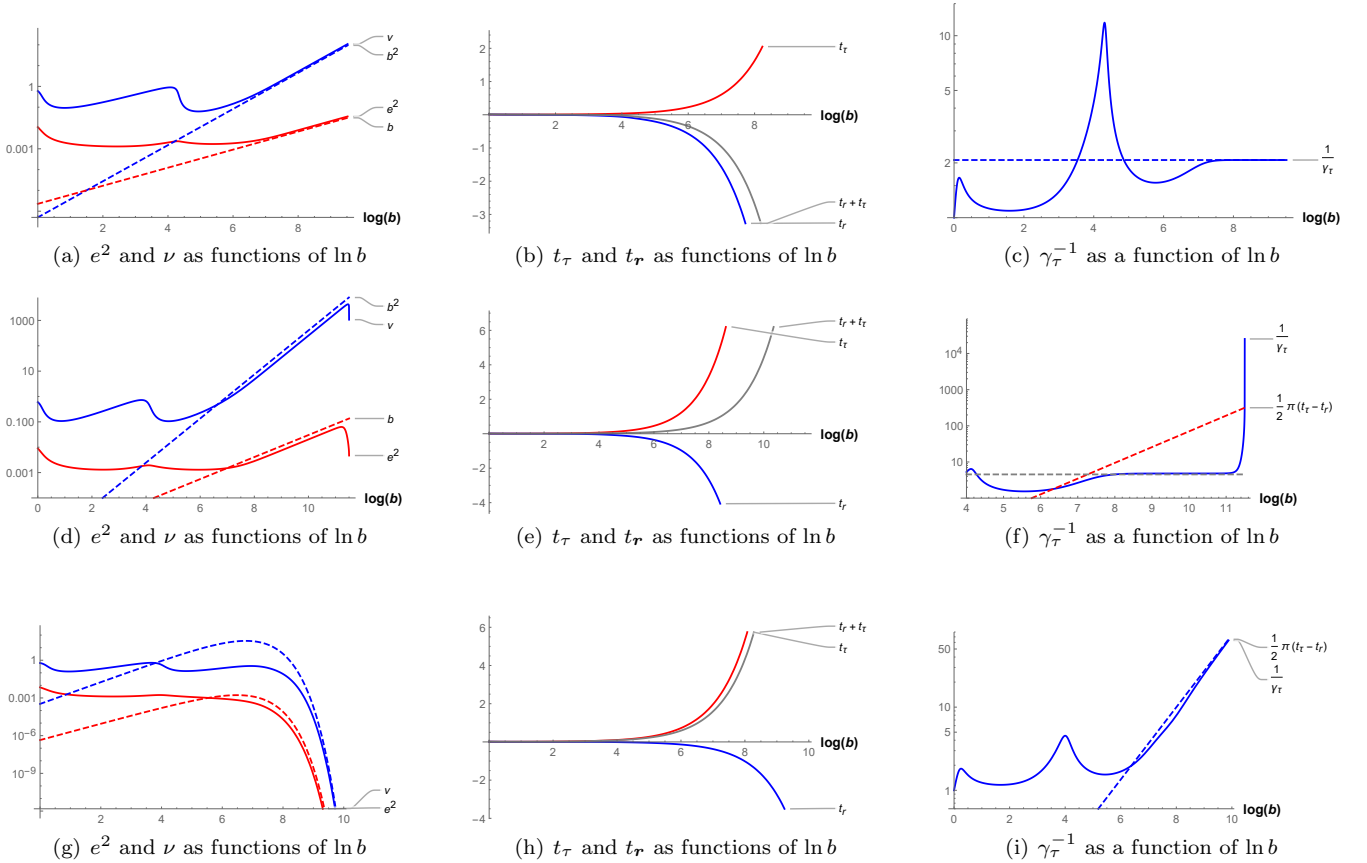


FIG. 12. Plots of e^2 , ν , t_τ , t_r and γ_τ^{-1} as functions of the RG scale $\ln b$. The plots are obtained from numerical solutions of the RG equations [Eqs. (III.61,III.62,III.63,III.65,III.64) together with Eqs. (III.78,III.79)]. The initial value of ν and γ_τ^{-1} are 0.6 and 1, respectively. As for the initial values of e^2 and $t_\tau = t_r = t$, we chose $(e^2, t)|_{\ln b=0} = (0.011, 0.01085)$ [denoted by blue cross mark in Fig. 10(c)] for Figs. 12(a),12(b),12(c), $(e^2, t)|_{\ln b=0} = (0.009, 0.01085)$ [denoted by red cross mark in Fig. 10(c)] for Figs. 12(d),12(e),12(f), and $(e^2, t)|_{\ln b=0} = (0.007, 0.01085)$ [denoted by gray cross mark in Fig. 10(c)] for Figs. 12(g),12(h),12(i). Dashed lines in Figs. 12(g), 12(i) are from Eq. (III.82).

Namely, the partition function in the momentum-frequency representation is given by

$$\begin{aligned} \lim_{\gamma_\tau \rightarrow 0} Z &= \int \mathcal{D}\mathbf{a} \exp \left[-\frac{1}{2} \frac{1}{L_\tau} \sum_{\omega} \int \frac{d^2\mathbf{q}}{(2\pi)^2} \sum_{\mu=1,2} |\omega \mathbf{a}_\mu(\omega, \mathbf{q}) - q_\mu \mathbf{a}_\tau(\omega, \mathbf{q})|^2 \right] \\ &\quad \left\{ 1 + \sum_{N=1}^{\infty} \frac{1}{N!} \prod_{j=1}^N \left(\int \mathcal{D}^2 \mathbf{r}_{2j-1} e^{L_\tau t_\tau} \int \mathcal{D}^2 \mathbf{r}_{2j} e^{L_\tau t_\tau} \right) \right. \\ &\quad \left. \exp \left[-i2\pi e \sum_{j=1}^{2N} \sigma_j \int \frac{d^2\mathbf{q}}{(2\pi)^2} e^{i\mathbf{q}\cdot\mathbf{r}_j} \mathbf{a}_\tau(\omega=0, \mathbf{q}) \right] \right\}, \end{aligned} \quad (\text{III.88})$$

with the Fourier transform,

$$\mathbf{a}_\mu(\tau, \mathbf{r}) = \frac{1}{L_\tau} \sum_{\omega} \int \frac{d^2\mathbf{q}}{(2\pi)^2} e^{i\mathbf{q}\mathbf{r} - i\omega\tau} \mathbf{a}_\mu(\omega, \mathbf{q}), \quad (\text{III.89})$$

and $\omega = \frac{2\pi}{L_\tau} n$ ($n = 1, 2, \dots$). In the right hand side, only $\mathbf{a}_\tau(\omega = 0, \mathbf{q})$ couples with the vortex excitations, while $\mathbf{a}_\tau(0, \mathbf{q})$ is decoupled from the spatial components $\mathbf{a}_\mu(0, \mathbf{q})$ of the gauge field ($\mu = 1, 2$) in the Maxwell action. Thus, by integrating out $\mathbf{a}_\tau(\omega \neq 0, \mathbf{q})$ and $\mathbf{a}_\mu(\omega \neq 0, \mathbf{q})$ ($\mu = 1, 2$), we reach the 2D isotropic partition function,

$$\begin{aligned} \lim_{\gamma_\tau \rightarrow 0} Z &= \text{const.} \int \mathcal{D}\mathbf{a}(0, \mathbf{q}) \exp \left[-\frac{1}{2} \frac{1}{L_\tau} \int \frac{d^2\mathbf{q}}{(2\pi)^2} q^2 |\mathbf{a}_\tau(0, \mathbf{q})|^2 \right] \\ &\quad \left\{ 1 + \sum_{N=1}^{\infty} \frac{1}{N!} \prod_{j=1}^N \left(\int \mathcal{D}^2 \mathbf{r}_{2j-1} e^{L_\tau t_\tau} \int \mathcal{D}^2 \mathbf{r}_{2j} e^{L_\tau t_\tau} \right) \right. \\ &\quad \left. \exp \left[-i2\pi e \sum_{j=1}^{2N} \sigma_j \int \frac{d^2\mathbf{q}}{(2\pi)^2} e^{i\mathbf{q}\cdot\mathbf{r}_j} \mathbf{a}_\tau(0, \mathbf{q}) \right] \right\}. \end{aligned} \quad (\text{III.90})$$

Eq. (III.90) is identical to Eq. (I.19) with $D = 2$, $\gamma_\tau = 1$, and $\chi = 0$, where $\mathbf{a}_\tau(\omega = 0, \mathbf{r})/\sqrt{L_\tau}$ plays the role of the 2D electrostatic potential $u_{\tau 1}(\mathbf{r})$, and the relevant parameters in the two equations are related by,

$$y \equiv e^\omega \text{ (2D } \gamma_\tau = 1, \chi = 0) \Leftrightarrow e^{2L_\tau t_\tau} \text{ (3D } \gamma_\tau = 0), \quad (\text{III.91})$$

$$e^2 \text{ (2D } \gamma_\tau = 1, \chi = 0) \Leftrightarrow e^2 L_\tau \text{ (3D } \gamma_\tau = 0). \quad (\text{III.92})$$

By substituting Eqs. (III.91, III.92) into Eq. (III.30), we can readily see that $\lim_{L_\tau \rightarrow \infty} \lim_{\gamma_\tau \rightarrow 0} Z$ with positive t_τ and a finite e^2 is in a quasi-disordered phase, while $\lim_{L_\tau \rightarrow \infty} \lim_{\gamma_\tau \rightarrow 0} Z$ with negative t_τ and a finite e^2 is in the ordered phase. In the quasi-disordered phase, the SF phase correlation becomes short-ranged in the spatial direction due to the proliferation of vortex lines, while the SF phase correlation remains long-ranged in the time direction. In the ordered phase, the fugacity of vortex lines vanishes, going far below the separatrix of the KT transition, and the SF phase correlation remains long-ranged in any directions. Numerical solutions of the RG equations show that the divergence of γ_τ^{-1} at the finite RG scale always comes with positive t_τ [Figs. 11(e), 12(e)] and finite e^2 [Figs. 11(d), 12(d)]. Thus, we conclude that the intermediate coupling region is unstable to a formation of the quasi-disordered phase with short-range spatial correlation but persistent temporal correlation.

The intermediate coupling region appears universally in the RG phase diagram upon a transformation from the weak coupling region to the strong coupling region. In the weak coupling side, $t_\tau + t_r$ diverges negatively, and ν increases with $\nu \sim b^2$, where $Z_{2,t}(\mathbf{t}, \nu)$ is vanishingly small, taking a negative value for the larger ν [Figs. 13(b), 13(c)]. In the strong coupling side, $t_\tau + t_r$ diverges positively, and ν becomes vanishingly small, where $Z_{2,t}(\mathbf{t}, \nu)$ gets exponentially larger, taking a positive value for the smaller ν [Fig. 13(b)]. The transformation of parameters between these two regions necessitates passage through an intermediate region where $Z_{2,t}(\mathbf{t}, \nu)$ attains large negative values. This arises from a causal constraint: the parameter ν begins to decrease only after $t_\tau + t_r$ diverges to large positive values. Consequently, by the time ν enters the negative ‘gorge’ of $Z_{2,t}(\mathbf{t}, \nu)$ (Fig. 13(c)), $t_\tau + t_r$ has already grown significantly positive. From the first term on the right hand side of Eq. (III.63), the large negative $Z_{2,t}(\mathbf{t}, \nu)$ reduces γ_τ to zero at a finite RG scale $\ln b$.

The ordered-quasi-disordered transition must be the first order, as the correlation length ξ_r on the strong-coupling side of the boundary remains finite, not showing any critical divergence. Namely, in the large L_τ limit, the substitution of Eqs. (III.91, III.92) into Eq. (III.30) always brings the relevant parameters into a 2D disordered phase region far above the separatrix of the KT transition, where the correlation length ξ_r must be fairly small.

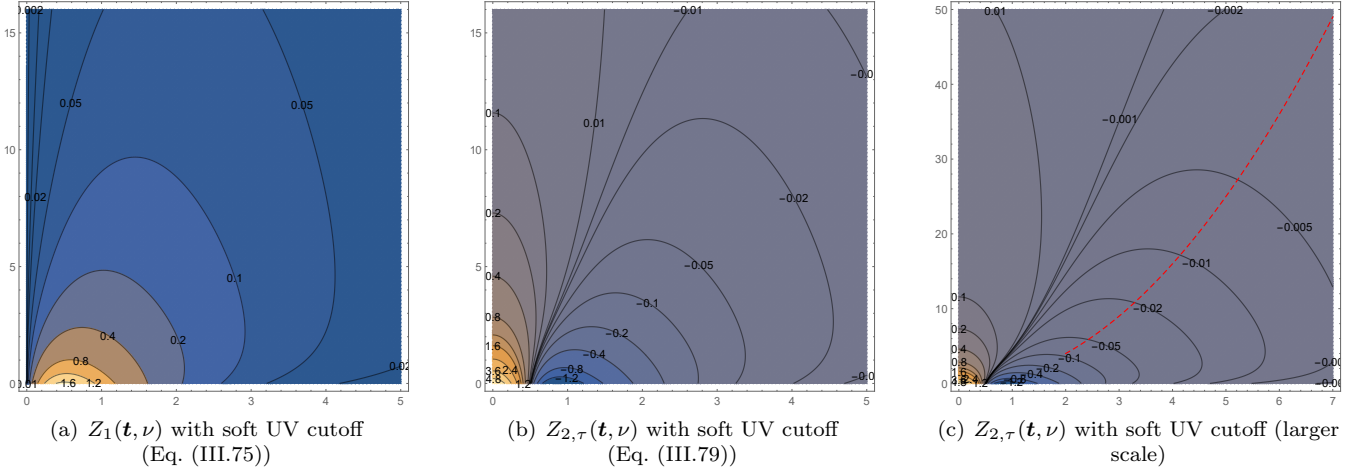


FIG. 13. Contour plots of $Z_{2,\tau}(\mathbf{t}, \nu) \equiv \partial_\nu Z_1(\mathbf{t}, \nu)$ and $Z_1(\mathbf{t}, \nu)$ as functions of $t_\tau = -t_r \equiv t_-/2$ and ν with the soft UV cutoff [Eq. (III.79)]. The horizontal and vertical axes are ν and t_- , respectively. $Z_1(\mathbf{t}, \nu)$ for $\nu > 0$ has a positive ‘ridge’ along $t_- \sim \nu$, while $Z_{2,\tau}(\mathbf{t}, \nu)$ has a negative ‘gorge’ along $t_- \sim \nu^2$ [dashed red line in Fig. 13(c)]

IV. FUGACITY RENORMALIZATION : FURTHER CONSIDERATIONS

A. Derivation of Eq. (III.1)

In the isotropic and general D case, we take $\gamma_\tau = 1$ in Eqs. (II.52,II.53) and calculate $F_\tau(\mathbf{x}) = F_r(\mathbf{x})$ with a soft ultraviolet (UV) cutoff for the momentum integral,

$$\begin{aligned} F(\mathbf{x}) \equiv F_\tau(\mathbf{x}) &= F_r(\mathbf{x}) = \Lambda \frac{\partial}{\partial \Lambda} \left[\int \frac{d^D \mathbf{k}}{(2\pi)^D} \frac{e^{i\mathbf{k} \cdot \mathbf{x}}}{k^2} e^{-\Lambda^{-1}k} \right] \\ &= \frac{2\pi^{\frac{D}{2}}}{\Lambda} \left[\int_0^\infty \frac{dk}{(2\pi)^D} k^{D-2} e^{-\Lambda^{-1}k} {}_0\tilde{F}_1\left(\frac{D}{2}, -\frac{k^2 x^2}{4}\right) \right], \end{aligned} \quad (\text{IV.1})$$

where ${}_0\tilde{F}_1(a, b)$ stands for the regularized hypergeometric function. Following a reference [81], we further calculate the $\Delta \mathbf{s}$ -integral in Eqs. (II.55,II.56) for $f \equiv f_\tau = f_r$,

$$f = \int d^{D-2} \Delta \mathbf{s} F\left(\sum_{a=1}^{D-2} \Delta s_a \frac{\partial \mathbf{R}_j(\mathbf{s})}{\partial s_a}\right) = \frac{1}{\sqrt{\det \hat{\mathbf{g}}_j}} \int d^{D-2} \boldsymbol{\xi} F(\boldsymbol{\xi}). \quad (\text{IV.2})$$

In the first line, the $(D-2)$ -dimensional vector $\Delta \mathbf{s}$ is transformed into a $(D-2)$ -dimensional vector $\boldsymbol{\xi}$ associated with the first fundamental form $\hat{\mathbf{g}}_j(\mathbf{s})$,

$$\hat{\mathbf{g}}_{j,ab}(\mathbf{s}) \equiv \sum_{\mu=\tau,1,\dots,D-1} \frac{\partial \mathbf{R}_{j,\mu}}{\partial s_a} \frac{\partial \mathbf{R}_{j,\mu}}{\partial s_b} \quad (\text{IV.3})$$

($a, b = 1, 2, \dots, D-2$). Firstly, this $(D-2) \times (D-2)$ real symmetric matrix $\hat{\mathbf{g}}_j$ is diagonalized by an orthogonal matrix with real positive eigenvalues η_a ($a = 1, \dots, D-2$). Then, $\Delta \mathbf{s}$ is linearly transformed into a $(D-2)$ -dimensional vector $\boldsymbol{\zeta}$ by the orthogonal matrix, while $\boldsymbol{\xi}$ is related to $\boldsymbol{\zeta}$ by a dilatation transformation with the positive eigenvalues, $\xi_a \equiv \zeta_a \sqrt{\eta_a}$ ($a = 1, \dots, D-2$). $\boldsymbol{\xi}$ thus introduced can be substituted for the argument of the integrand of Eq. (IV.2), as $F(\mathbf{x})$ depends only on $|\mathbf{x}|^2$, and

$$\sum_{\mu=\tau,1,\dots,D-1} \left(\sum_{a=1}^{D-2} \Delta s_a \frac{\partial \mathbf{R}_{j,\mu}(\mathbf{s})}{\partial s_a} \right)^2 = \sum_{a,b=1}^{D-2} \Delta s_a \Delta s_b \hat{\mathbf{g}}_{j,ab} = \sum_{a=1}^{D-2} \zeta_a^2 \eta_a = \sum_{a=1}^{D-2} \xi_a^2 \equiv |\boldsymbol{\xi}|^2. \quad (\text{IV.4})$$

When the $\Delta \mathbf{s}$ -integral is rewritten by the $\boldsymbol{\xi}$ -integral, the Jacobian gives $1/\sqrt{\det \hat{\mathbf{g}}_j}$,

$$\int d^{D-2} \Delta \mathbf{s} = \int d^{D-2} \boldsymbol{\zeta} = \left(\prod_{a=1}^{D-2} \sqrt{\eta_a} \right)^{-1} \int d^{D-2} \boldsymbol{\xi} = \frac{1}{\sqrt{\det \hat{\mathbf{g}}_j}} \int d^{D-2} \boldsymbol{\xi}. \quad (\text{IV.5})$$

The ξ -integral of $F(\xi)$ in the right hand side of Eq. (IV.2) yields a universal constant,

$$\begin{aligned}
\int d^{D-2}\xi F(\xi) &= \frac{1}{\Lambda} \frac{2\pi^{\frac{D}{2}}}{(2\pi)^D} \int d^{D-2}\xi \int_0^\infty k^{D-2} dk e^{-\Lambda^{-1}k} {}_0\tilde{F}_1\left(\frac{D}{2}, -\frac{k^2\xi^2}{4}\right) \\
&= \frac{1}{\Lambda} \frac{2^{D-1}\pi^{\frac{D-1}{2}}}{(2\pi)^D} \int d^{D-2}\xi \frac{\Gamma(\frac{D-1}{2})}{(\Lambda^{-2} + \xi^2)^{\frac{D-1}{2}}} \\
&= \frac{1}{\Lambda} \frac{2^{D-1}\pi^{\frac{D-1}{2}}}{(2\pi)^D} \frac{2\pi^{\frac{D-2}{2}}}{\Gamma(\frac{D-2}{2})} \int_0^\infty \xi^{D-3} d\xi \frac{\Gamma(\frac{D-1}{2})}{(\Lambda^{-2} + \xi^2)^{\frac{D-1}{2}}} \\
&= \frac{1}{\Lambda} \frac{1}{\pi^{\frac{3}{2}}} \frac{\Gamma(\frac{D-1}{2})}{\Gamma(\frac{D-2}{2})} \frac{\sqrt{\pi}}{2\Lambda^{-1}} \frac{\Gamma(\frac{D-2}{2})}{\Gamma(\frac{D-1}{2})} = \frac{1}{2\pi}.
\end{aligned} \tag{IV.6}$$

Eqs. (IV.2,IV.6) give Eq. (III.1).

B. Derivation of Eqs. (III.54,III.55)

As we discussed in Section II B, the short-range part of the Coulomb interaction gives rise to a fugacity renormalization. In the general D case, the fugacity renormalization is given by a rather complicated function of the temporal and spatial components of the metric tensor, $\hat{\mathbf{g}}_\tau$ and $\hat{\mathbf{g}}_\mathbf{r}$ [see Eqs. (II.57)]. In $D = 3$, however, the components reduce to scalar quantities, and the function reduces to a simpler form. To see this, let us start from the gradient expansion of the short-range part of the 3D Coulomb interaction within the same vortex loop $\partial\Gamma_j$,

$$\begin{aligned}
\sum_j \delta E_j &= \ln b \frac{e^2}{2} \sum_{\sigma=\tau,1,2} \int d^3\mathbf{R}_1 \int d^3\mathbf{R}_2 F_\sigma(|\mathbf{R}_1 - \mathbf{R}_2|) J_\sigma(\mathbf{R}_1) J_\sigma(\mathbf{R}_2), \\
&= 2\pi^2 e^2 \ln b \sum_{\sigma=\tau,1,2} \sum_j \int_{\partial\Gamma_j} ds_1 \int_{\partial\Gamma_j} ds_2 F_\sigma(|\mathbf{R}_j(s_1) - \mathbf{R}_j(s_2)|) \frac{\partial R_{j,\sigma}(s_1)}{ds_1} \frac{\partial R_{j,\sigma}(s_2)}{ds_2}, \\
&= 2\pi^2 e^2 \ln b \sum_{\sigma=\tau,1,2} \sum_j \int_{\partial\Gamma_j} ds \left(\frac{\partial R_{j,\sigma}(s)}{ds} \right)^2 \int d\Delta s F_\sigma\left(\frac{\partial R_{j,\sigma}(s)}{ds} \Delta s\right) + \dots.
\end{aligned} \tag{IV.7}$$

Here we used,

$$\begin{aligned}
J_\sigma(\mathbf{R}) &= 2\pi \sum_j \int_{\partial\Gamma_j} ds \frac{\partial R_{j,\sigma}(s)}{ds} \delta^3(\mathbf{R} - \mathbf{R}_j(s)), \\
\ln b F_\sigma(\mathbf{x}) &= \int_{b^{-1}\Lambda < |\mathbf{k}| < \Lambda} \frac{d^3\mathbf{k}}{(2\pi)^3} \frac{e^{i\mathbf{q}\mathbf{r} - i\omega\tau}}{k^4} \begin{cases} \mathbf{q}^2 + (2 - \gamma_\tau^{-1})\omega^2 & \text{for } \sigma = \tau, \\ \gamma_\tau^{-1}\mathbf{q}^2 + \omega^2 & \text{for } \sigma = 1, 2. \end{cases}
\end{aligned} \tag{IV.8}$$

The short-range part of the interaction $F_\sigma(\mathbf{x})$ ($\sigma = \tau, 1, 2$) may be calculated with a soft UV cutoff with the cylindrical symmetry,

$$F_\tau(\mathbf{x}) = -\Lambda^{-1} \frac{\partial}{\partial\Lambda^{-1}} \int \frac{d^3\mathbf{k}}{(2\pi)^3} e^{i\mathbf{q}\mathbf{r} - i\omega\tau} e^{-\Lambda^{-1}|\mathbf{q}|} \frac{|\mathbf{q}|^2 + (2 - \gamma_\tau^{-1})\omega^2}{k^4}, \tag{IV.9}$$

$$F_\mathbf{r}(\mathbf{x}) \equiv F_1(\mathbf{x}) = F_2(\mathbf{x}) = -\Lambda^{-1} \frac{\partial}{\partial\Lambda^{-1}} \int \frac{d^3\mathbf{k}}{(2\pi)^3} e^{i\mathbf{q}\mathbf{r} - i\omega\tau} e^{-\Lambda^{-1}|\mathbf{q}|} \frac{\gamma_\tau^{-1}|\mathbf{q}|^2 + \omega^2}{k^4}, \tag{IV.10}$$

with $\mathbf{x} = (\tau, \mathbf{r})$ and $\mathbf{k} = (\omega, \mathbf{q})$. As $F_\sigma(\frac{\partial\mathbf{R}}{\partial s}\Delta s)$ comes with $(\partial_s\mathbf{R}_\sigma)^2$ in Eq. (IV.7), it is natural to estimate the Δs -integral of $F_\tau(\frac{\partial\mathbf{R}}{\partial s}\Delta s)$ using a geometry of $\frac{\partial\mathbf{R}}{\partial s}\Delta s = \Delta s(1, 0, 0)$, and the Δs -integral of $F_\mathbf{r}(\frac{\partial\mathbf{R}}{\partial s}\Delta s)$ by the other geometry: $\frac{\partial\mathbf{R}}{\partial s}\Delta s = \Delta s(0, \cos\theta, \sin\theta)$. With this simplification, the one-dimensional Δs -integrals in Eqs. (II.55, II.56)

can be readily calculated, giving reasonable estimates of f_τ and f_r in the $D = 3$ case,

$$\begin{aligned} f_\tau &= \int d\Delta s F_\tau(\Delta s(1, 0, 0)) = -\Lambda^{-1} \frac{\partial}{\partial \Lambda^{-1}} \int \frac{d^2 \mathbf{q}}{(2\pi)^2} \frac{1}{|\mathbf{q}|^2} e^{-\Lambda^{-1}|\mathbf{q}|} \\ &= \Lambda^{-1} \frac{1}{2\pi} \int_0^\infty d|\mathbf{q}| e^{-\Lambda^{-1}|\mathbf{q}|} = \frac{1}{2\pi}, \end{aligned} \quad (\text{IV.11})$$

$$\begin{aligned} f_r &= \int d\Delta s F_r(\Delta s(0, 1, 0)) \\ &= -\Lambda^{-1} \frac{\partial}{\partial \Lambda^{-1}} \int d\Delta s \int_{-\infty}^{+\infty} \frac{d\omega}{2\pi} \int_0^\infty \frac{qdq}{(2\pi)^2} \int_0^{2\pi} d\theta \frac{1}{(\omega^2 + q^2)^2} e^{-\Lambda^{-1}q} e^{-iq|\Delta s| \cos \theta} (\gamma_\tau^{-1} q^2 + \omega^2) \\ &= -\Lambda^{-1} \frac{\partial}{\partial \Lambda^{-1}} \int d\Delta s \int_0^\infty \frac{qdq}{(2\pi)^2} \int_0^{2\pi} d\theta \frac{\gamma_\tau^{-1} + 1}{4q} e^{-\Lambda^{-1}q} e^{-iq|\Delta s| \cos \theta} \\ &= \Lambda^{-1} \int d\Delta s \int_0^{2\pi} d\theta \frac{1}{(\Lambda^{-1} + i\Delta s \cos \theta)^2} \frac{\gamma_\tau^{-1} + 1}{4} \frac{1}{(2\pi)^2} \\ &= \Lambda^{-1} \int_{-\infty}^{+\infty} d\Delta s \frac{\Lambda^{-1}}{(\Lambda^{-2} + |\Delta s|^2)^{\frac{3}{2}}} \frac{\gamma_\tau^{-1} + 1}{4} \frac{1}{2\pi} = \frac{\gamma_\tau^{-1} + 1}{4\pi}. \end{aligned} \quad (\text{IV.12})$$

Eqs. (IV.11, IV.12) give Eqs. (III.54, III.55).

C. fugacity renormalization with different gauge : its impact on physics

In the derivation of the fugacity renormalization, we expressed the vector potential $u_{\mu\nu}(\mathbf{k})$ in terms of the divergence-free auxiliary field $\varphi_\nu(\mathbf{k})$, Eq. (II.36), and integrated the auxiliary field $\varphi_\nu(\mathbf{k})$. This gauge choice facilitated the calculation for the general space-time dimension D , while for $D = 2$ and 3 , one may also integrate the vector potential $u_{\mu\nu}(\mathbf{k})$ directly. The direct integration of the vector potentials replaces the arithmetic mean between e^2/γ_τ and e^2 in Eqs. (III.25, III.36, III.55, III.65) by their geometric mean. For $D = 2$, Eqs. (III.25, III.36) are replaced by

$$\frac{dy}{d \ln b} = \left(4 - \frac{\gamma_\tau^{-1/2} e^2}{2\pi}\right) y. \quad (\text{IV.13})$$

For $D = 3$, Eqs. (III.55, III.65) are replaced by

$$\begin{cases} \frac{dt_\tau}{d \ln b} = t_\tau - \pi e^2, \\ \frac{dt_r}{d \ln b} = t_r - \pi e^2 \gamma_\tau^{-1/2}. \end{cases} \quad (\text{IV.14})$$

In the following, we will argue that these changes do *not* change the nature of the ordered-disordered phase transitions for $D = 2$ and 3 .

1. $D = 2$

As in Sec. III B, the modified RG equation has an anisotropic weak-coupling fixed line for the KT-like critical phase, as well as the isotropic strong coupling fixed point for the conventional 2D disordered phase. The phase transition between these two phases is also characterized by a saddle fixed point with an infinite space-time anisotropy as well. Differently from Sec. III B, the saddle fixed point of the modified RG equation is characterized by finite values of $y/\gamma_\tau^{1/2}$, ν and $e^2/\gamma_\tau^{1/2}$ rather than finite values of y , ν and e^2/γ_τ . To analyze the scaling properties of this saddle

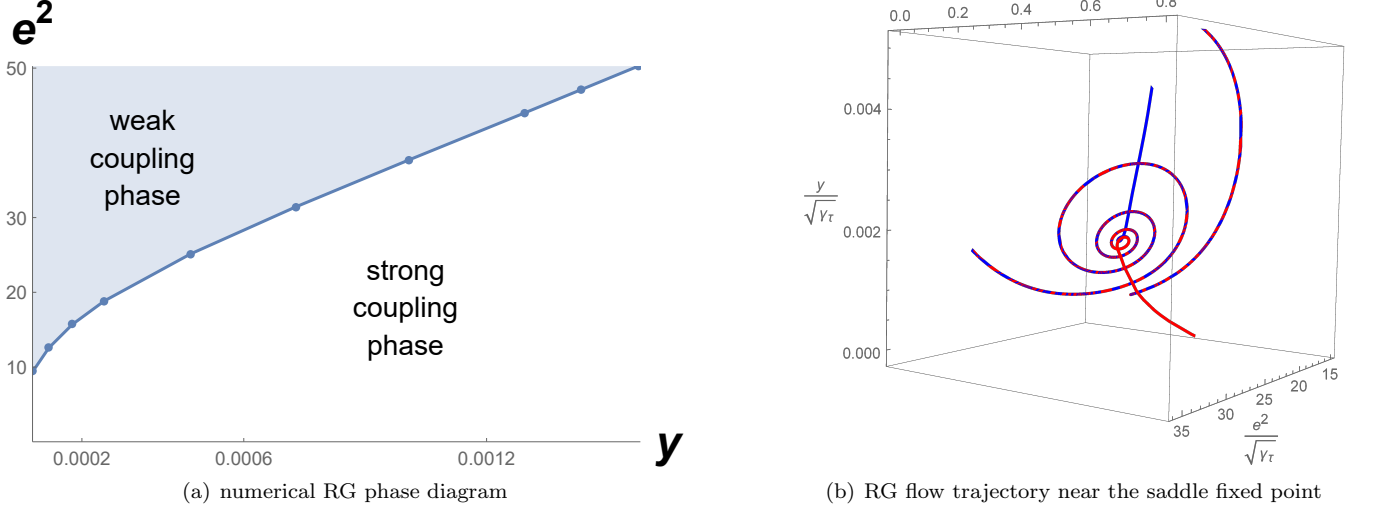


FIG. 14. (left) RG phase diagram with initial values of $\gamma_\tau = 1$ and $\nu = 0.2$. The horizontal and vertical axes are initial values of y , and e^2 , respectively. (right) Two RG flow trajectories near the saddle fixed point in the three-dimensional parameter space. The saddle fixed point is at $(e^2/\gamma_\tau^{1/2}, \nu, y/\gamma_\tau^{1/2}) = (8\pi, \nu_-, \rho_-) = (25.9\dots, 0.389\dots, 0.001798)$. The blue (red) curve denotes the RG flow trajectory when the initial parameters are chosen in the disordered (ordered) phase side of the phase boundary: $e^2/\gamma_\tau = e^2 = 10\pi$ and $\nu = 0.2$ and $y \lesssim y_c$ ($y \gtrsim y_c$) respectively [$y_c = 0.000728\dots$].

fixed point, let us rewrite the RG equations in terms of $e^2/\gamma_\tau^{1/2}$, $y/\gamma_\tau^{1/2}$, ν and e^2 :

$$\frac{d(e^2/\gamma_\tau^{1/2})}{d \ln b} = -\frac{\pi}{2} \left(\frac{y}{\gamma_\tau^{1/2}} \right) e^4 z_{2,r}(\nu) - \frac{\pi}{2} \left(\frac{y}{\gamma_\tau^{1/2}} \right) \left(\frac{e^2}{\gamma_\tau^{1/2}} \right)^2 z_{2,\tau}(\nu), \quad (\text{IV.15})$$

$$\frac{de^2}{d \ln b} = -\pi y e^4 z_{2,r}(\nu) = -\pi \left(\frac{y}{\gamma_\tau^{1/2}} \right) \left(\frac{e^2}{\gamma_\tau^{1/2}} \right) e^6 z_{2,r}(\nu), \quad (\text{IV.16})$$

$$\frac{d\nu}{d \ln b} = \nu \left(1 - \pi \frac{y}{\gamma_\tau^{1/2}} \frac{e^2}{\gamma_\tau^{1/2}} z_{2,r}(\nu) \right), \quad (\text{IV.17})$$

$$\frac{d(y/\gamma_\tau^{1/2})}{d \ln b} = \left(4 - \frac{1}{2\pi} \frac{e^2}{\gamma_\tau^{1/2}} - \frac{\pi}{2} \frac{y}{\gamma_\tau^{1/2}} \frac{e^2}{\gamma_\tau^{1/2}} z_{2,\tau}(\nu) + \frac{\pi}{2} y e^2 z_{2,r}(\nu) \right) \frac{y}{\gamma_\tau^{1/2}}, \quad (\text{IV.18})$$

As in Sec. III B, let us start from the zero of $z_{2,\tau}(\nu)$: $z = z_\pm$. The RG equations could have a fixed point at $e^2 = 0$, $\nu = \nu_\pm$, $e^2/\gamma_\tau^{1/2} = 8\pi$ and $y/\gamma_\tau^{1/2} = \rho_\pm$ with

$$\rho_\pm = \frac{\gamma_\tau^{1/2}}{\pi e^2 z_{2,r}(\nu_\pm)} = \frac{1}{8\pi^2} \frac{1}{z_{2,r}(\nu_\pm)}. \quad (\text{IV.19})$$

Since $z_{2,r}(\nu_+) < 0$, we only consider the $z = z_-$ case, with $\nu_- = 0.389$, and $\rho_- = 0.001798$. In fact, $(e^2, \nu, e^2/\gamma_\tau^{1/2}, y/\gamma_\tau^{1/2}) = (0, \nu_-, 8\pi, \rho_-)$ is a saddle fixed point: it has a relevant scaling variable, a marginally irrelevant scaling variable, and two irrelevant scaling variables. As in sec. III B, e^2 becomes the marginally irrelevant scaling variable,

$$\frac{de^2}{d \ln b} = -\frac{1}{64\pi^2} e^6 + \mathcal{O}(\delta(e^2/\gamma_\tau^{1/2})e^6, \delta(y/\gamma_\tau^{1/2})e^6, \delta(\nu)e^6). \quad (\text{IV.20})$$

where $\delta(e^2/\gamma_\tau^{1/2}) \equiv e^2/\gamma_\tau^{1/2} - 8\pi$, $\delta\nu \equiv \nu - \nu_-$ and $\delta(y/\gamma_\tau^{1/2}) \equiv y/\gamma_\tau^{1/2} - \rho_-$. The RG equations for these three quantities are linearized around the fixed point,

$$\frac{d}{d \ln b} \begin{pmatrix} \delta \left(\frac{\gamma_\tau^{1/2}}{e^2} \right) \\ \delta\nu \\ \delta \left(\frac{y}{\gamma_\tau^{1/2}} \right) \end{pmatrix} = \begin{pmatrix} 0 & \frac{\pi}{2} \rho_- \left(\frac{dz_{2,\tau}(\nu)}{d\nu} \right)_{|\nu=\nu_-} & 0 \\ 8\pi\nu_- & 1 & -\frac{\nu_-}{\rho_-} \\ 32\pi\rho_- & -4\pi^2\rho_-^2 \left(\frac{\partial z_{2,\tau}(\nu)}{\partial \nu} \right)_{|\nu=\nu_-} & 0 \end{pmatrix} \begin{pmatrix} \delta \left(\frac{\gamma_\tau^{1/2}}{e^2} \right) \\ \delta\nu \\ \delta \left(\frac{y}{\gamma_\tau^{1/2}} \right) \end{pmatrix}. \quad (\text{IV.21})$$

Thereby, the 3 by 3 matrix has eigenvalues of 1.455, $-0.227 \pm 1.541i$. The positive real eigenvalue is nothing but the scaling dimension of the relevant scaling variable, while a pair of two complex conjugate eigenvalues with a negative real part is for the two irrelevant scaling variables. The relevant scaling variable is given by a linear superposition of $\delta(e^2/\gamma_\tau^{1/2})$, $\delta\nu$, and $\delta(y/\gamma_\tau^{1/2})$ with the following coefficients,

$$\left(\delta\left(\frac{\gamma_\tau^{1/2}}{e^2}\right) \quad \delta\nu \quad \delta\left(\frac{y}{\gamma_\tau^{1/2}}\right) \right) = (-0.0618\dots \quad 0.998\dots \quad -0.00489\dots). \quad (\text{IV.22})$$

This indicates that the RG flow streams away from the saddle fixed point with increasing/decreasing $y/\gamma_\tau^{1/2}$, decreasing/increasing ν and increasing/decreasing $\gamma_\tau^{1/2}/e^2$. The complex conjugate eigenvalues suggest that the RG flow streams into the fixed point with a swirling trajectory [Fig. 14(b)].

The numerical RG phase diagrams are shown in a two-dimensional parameter space subtended by initial values of y and e^2 for given initial values of ν and $\gamma_\tau = 1$ [Fig. 14(a)]. As in Sec. III B, larger (smaller) initial values of y and smaller (larger) initial values of e^2 lead to the strong-coupling disordered phase (weak-coupling ordered phase). Numerical solutions of $e^2/\gamma_\tau^{1/2}$, e^2 , ν and $y/\gamma_\tau^{1/2}$ as functions of the RG scale $\ln b$ are shown in Figs. 15. When the initial parameters are on the weak-coupling side of the phase boundary, both $e^2/\gamma_\tau^{1/2}$ and e^2 approach finite non-universal values in the IR limit [$\ln b \rightarrow \infty$], while ν diverges [Figs. 15(a),15(b),15(c)]. When the initial parameters are on the strong-coupling side of the boundary, both $e^2/\gamma_\tau^{1/2}$ and e^2 approach zero, while γ_τ converges to 1, ν approaches zero, and y diverges [Figs. 15(d),15(e),15(f)]. In either case, the parameters make a detour around the saddle fixed point: they first flow into the saddle fixed point with the swirling trajectory, and then they are repelled from the saddle fixed point to strong/weak coupling regions [Figs. 14(b), 15]. As in Sec. III B, the saddle fixed point with infinite space-time anisotropy also endows the correlation time with the additional logarithmic divergence near the critical point. Namely, the correlation time ξ_τ and correlation length ξ_r near the critical point show the same space-time anisotropic divergence as in Sec. III B,

$$\xi_\tau = b\xi_{\tau,0} \sim |\mathbf{t}|^{-\frac{1}{y_\mathbf{t}}} \sqrt{|\ln \mathbf{t}|}, \quad (\text{IV.23})$$

$$\xi_r = b\xi_{r,0} \sim |\mathbf{t}|^{-\frac{1}{y_\mathbf{t}}}. \quad (\text{IV.24})$$

with $y_\mathbf{t} = 1/1.455\dots = 0.687\dots$. This is because the renormalized space-time anisotropy parameter shows the same logarithmic divergence as in Eq. (III.47):

$$e_0^4 \sim \frac{32\pi^2 y_\mathbf{t}}{|\ln \mathbf{t}|}, \quad \frac{e_0^2}{\gamma_{\tau,0}^{1/2}} \sim 8\pi.$$

2. $D = 3$

The modified RG equation in $D = 3$ gives the qualitatively same phase transition as in Sec. III C [see Figs. 16, 17]. The equation in the large b limit has the weak-coupling region with divergent e^2 and ν [Fig. 17(a)], negatively divergent t_τ and t_r [Fig. 17(b)], and convergent γ_τ [Fig. 17(c)], the intermediate coupling region with divergent γ_τ^{-1} at finite RG scale b [Fig. 17(f)], and the strong-coupling region with vanishing e^2 and ν [Fig. 17(g)], positively divergent $t_+ = t_\tau + t_r$ [Fig. 17(h)], and divergent γ_τ [Fig. 17(i)]. For larger initial values of e^2 and smaller $t \equiv t_\tau = t_r$ [light blue region in Fig. 16], the coupling constants in the large b limit flow into the weak-coupling region, describing the conventional 3D ordered phase. For smaller values of e^2 and larger $t = t_\tau = t_r$ [light gray and white regions in Fig. 16], they flow into the strong-coupling region for the conventional 3D disordered phase. When initial e^2 and t are in the intermediate coupling region [light red region in Fig. 16], the space-time anisotropy parameter γ_τ^{-1} always diverges at a finite RG scale $\ln b$ [Fig. 17(f)] with finite e^2 and positive t_τ [17(d),17(e)]. This indicates that the intermediate coupling region undergoes the Landau-pole instability to the quasi-disordered phase. In the quasi-disordered phase, the spatial proliferation of vortex lines polarized along τ renders the U(1) phase correlation along the spatial direction to be short-ranged, while leaving intact the U(1) phase correlation along the temporal direction.

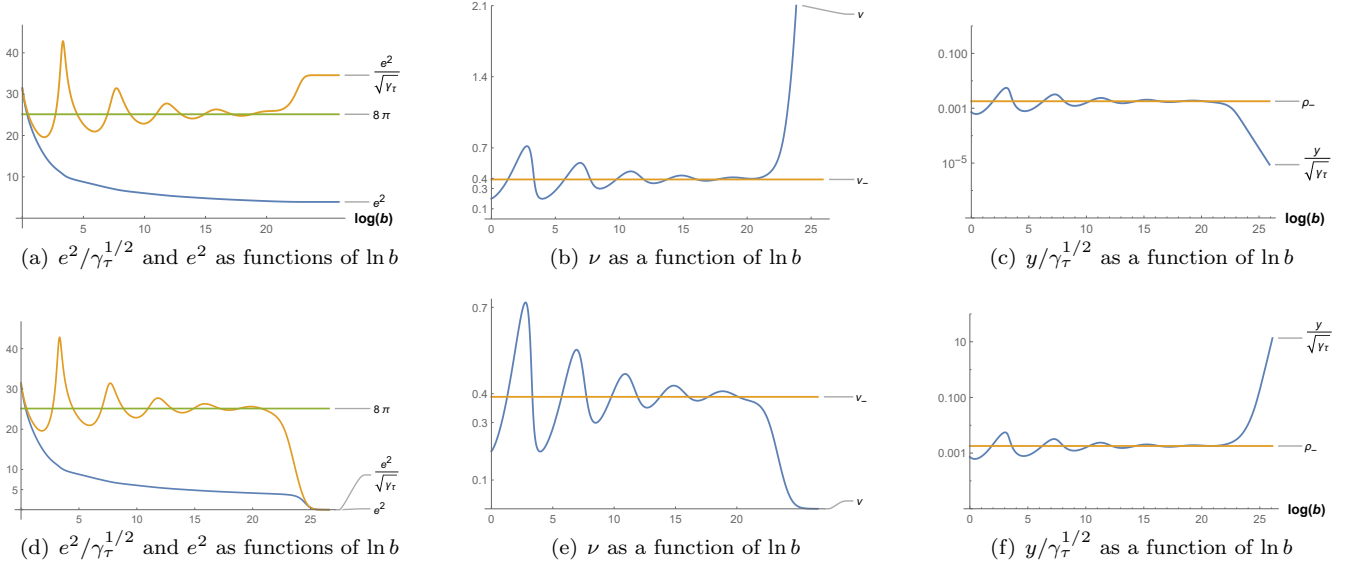


FIG. 15. Numerical solutions of $e^2/\gamma_\tau^{1/2}$, e^2 , ν and $y/\gamma_\tau^{1/2}$ as functions of the RG scale $\ln b$ for a set of initial parameters closed to the phase boundary between ordered and disordered phases. For Figs. 15(a), 15(b), 15(c), the initial parameters are chosen in the ordered phase side of the phase boundary: $e^2/\gamma_\tau = e^2 = 10\pi$ and $\nu = 0.2$ and $y \gtrsim y_c$ where $y_c = 0.000728\dots$. For Figs. 15(d), 15(e), 15(f), the initial parameters are chosen in the disordered phase side of the phase boundary.

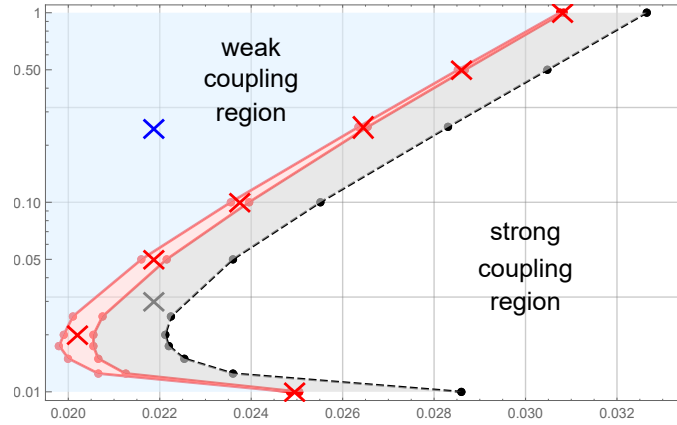


FIG. 16. Phase diagrams obtained from numerical solutions of the RG equations [Eqs. (III.61,III.62,III.63,IV.14) together with Eqs. (III.78,III.79)] with initial values of e^2 , $t_\tau = t_r \equiv t$, $\gamma_\tau = 1$ and $\nu = 1.2$. The vertical and horizontal axes axis are initial values of e^2 and t , respectively. The light blue, light red, and light gray (white) regions stand for ordered, quasi-disordered, and disordered phases, respectively. Namely, a set of initial parameters in the light blue region go to the weak-coupling region with divergent e^2 and ν , and negatively divergent t_τ and t_r , and constant γ_τ [see Figs. 17(a), 17(b), 17(c) for how the parameters evolve from the blue cross point “(i)”. Initial parameters in the light gray (white) region go to the strong-coupling region with vanishing e^2 and ν , positively divergent $t_+ = t_\tau + t_r$, and negatively (positively) divergent t_r , and divergent γ_τ^{-1} [see Figs. 17(g), 17(h), 17(i) for how the parameters evolve from the gray cross point “(ii)”. Initial parameters in the light red region go to the intermediate coupling region, where γ_τ^{-1} diverges at a finite value of the RG scale $\ln b$ [see Fig. 17(f) for how γ_τ^{-1} evolve from the red cross point “(ii)”].

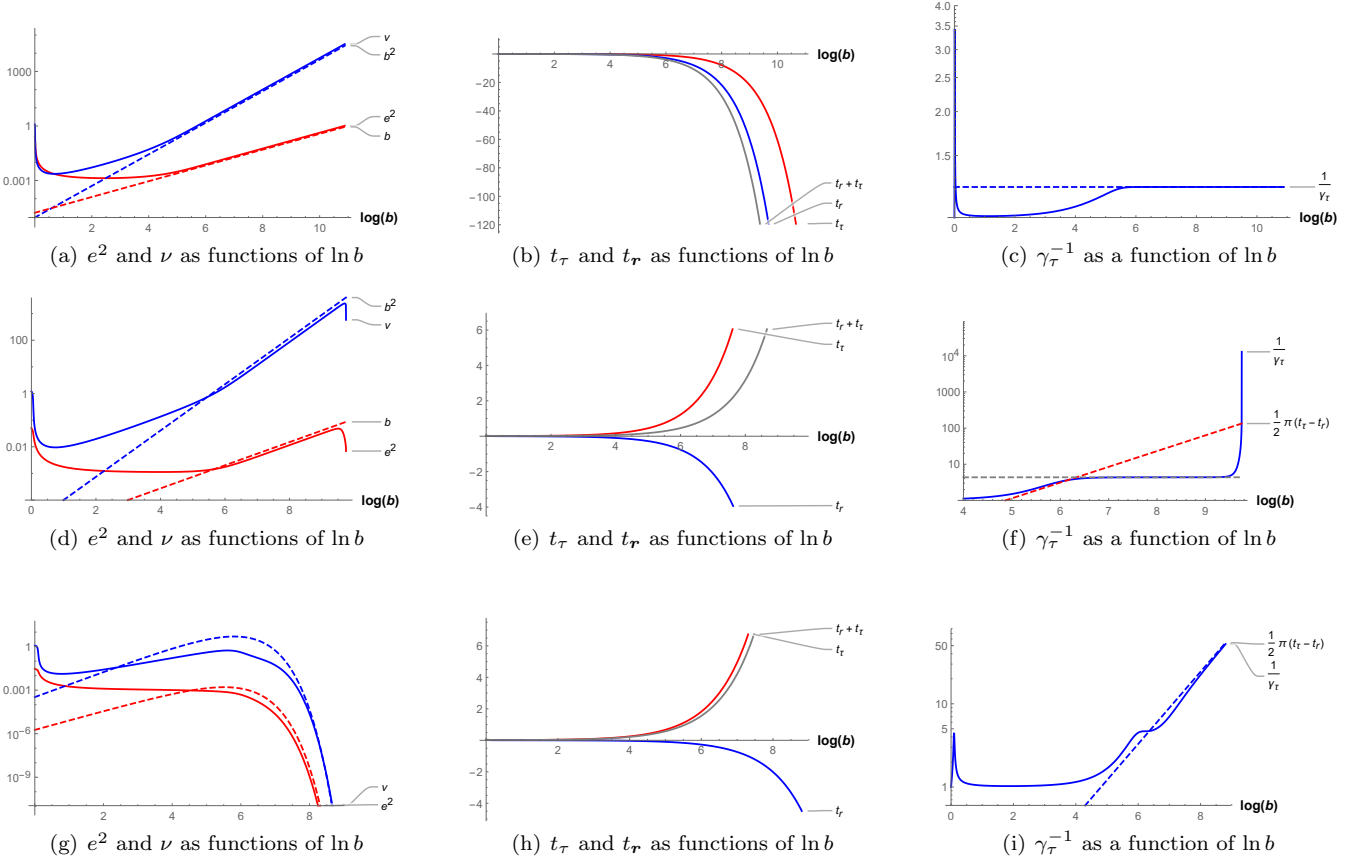


FIG. 17. Plots of e^2 , ν , t_τ , t_r and γ_τ^{-1} as functions of the RG scale $\ln b$. The plots are obtained from numerical solutions of the RG equations [Eqs. (III.61,III.62,III.63,IV.14) together with Eqs. (III.78,III.79)]. The initial value of ν and γ_τ^{-1} are 1.2 and 1, respectively. As for the initial values of e^2 and $t_\tau = t_r = t$, we chose $(e^2, t)|_{\ln b=0} = (0.25, 0.0219)$ [denoted by blue cross mark in Fig. 16] for Figs. 17(a),17(b),17(c), $(e^2, t)|_{\ln b=0} = (0.05, 0.0219)$ [denoted by red cross mark in Fig. 16] for Figs. 17(d),17(e),17(f), and $(e^2, t)|_{\ln b=0} = (0.03, 0.0219)$ [denoted by gray cross mark in Fig. 16] for Figs. 17(g),17(h),17(i). Dashed lines in Figs. 17(g), 17(i) are from Eq. (III.82).

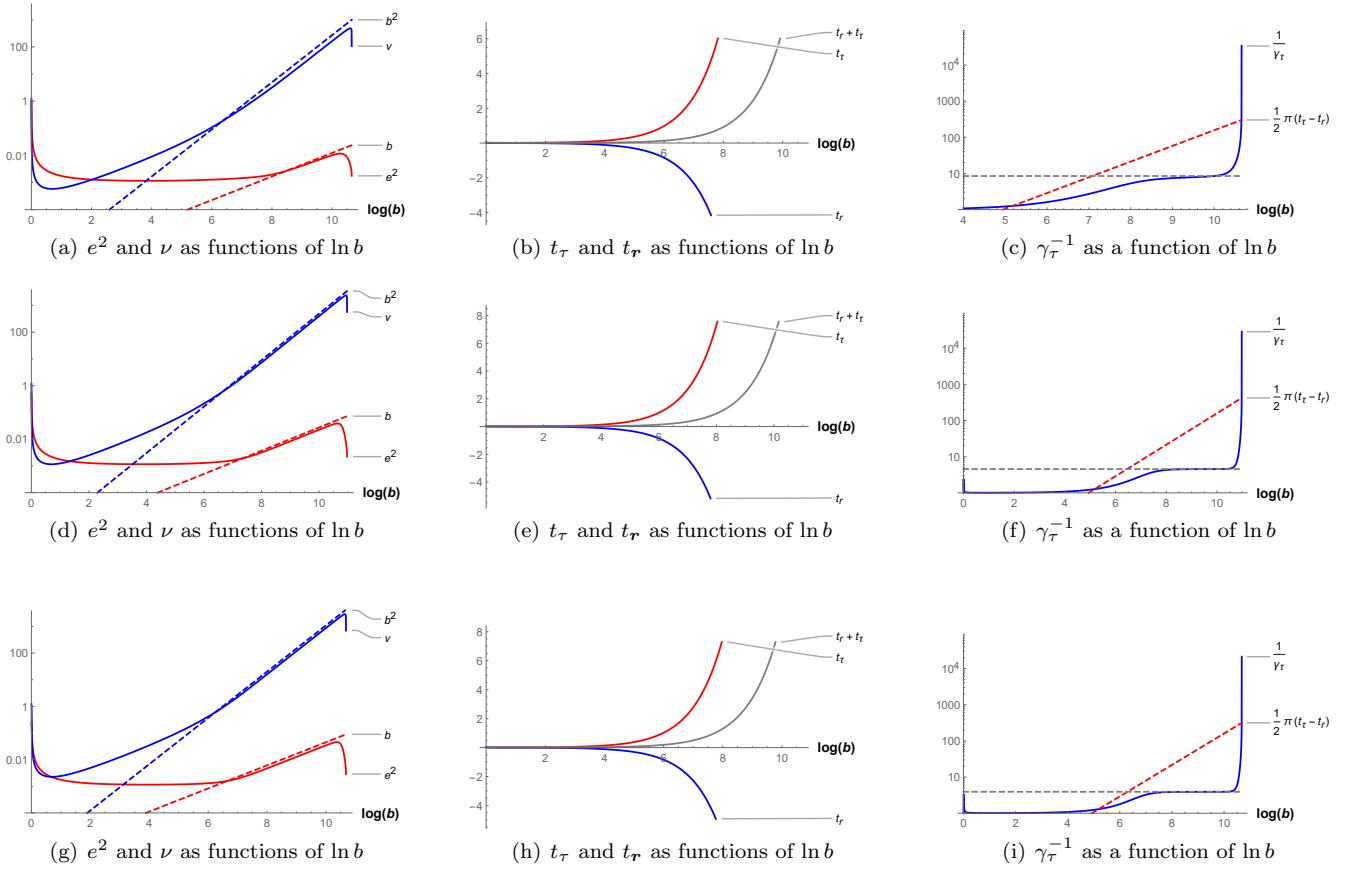


FIG. 18. Plots of e^2 , ν , t_τ , t_r and γ_τ^{-1} as functions of the RG scale $\ln b$ in the intermediate region [red color region in Fig. 16], where the initial value of ν and γ_τ^{-1} are 1.2 and 1, respectively. As for the initial values of e^2 and $t_\tau = t_r = t$, we chose $(e^2, t)|_{\ln b=0} = (1.0, 0.03081)$ [denoted by red cross mark in Fig. 16] for Figs. 18(a), 18(b), 18(c), $(e^2, t)|_{\ln b=0} = (0.50, 0.0286)$ [denoted by red cross mark in Fig. 16] for Figs. 18(d), 18(e), 18(f), and $(e^2, t)|_{\ln b=0} = (0.25, 0.02645)$ [denoted by red cross mark in Fig. 16] for Figs. 18(g), 18(h), 18(i).

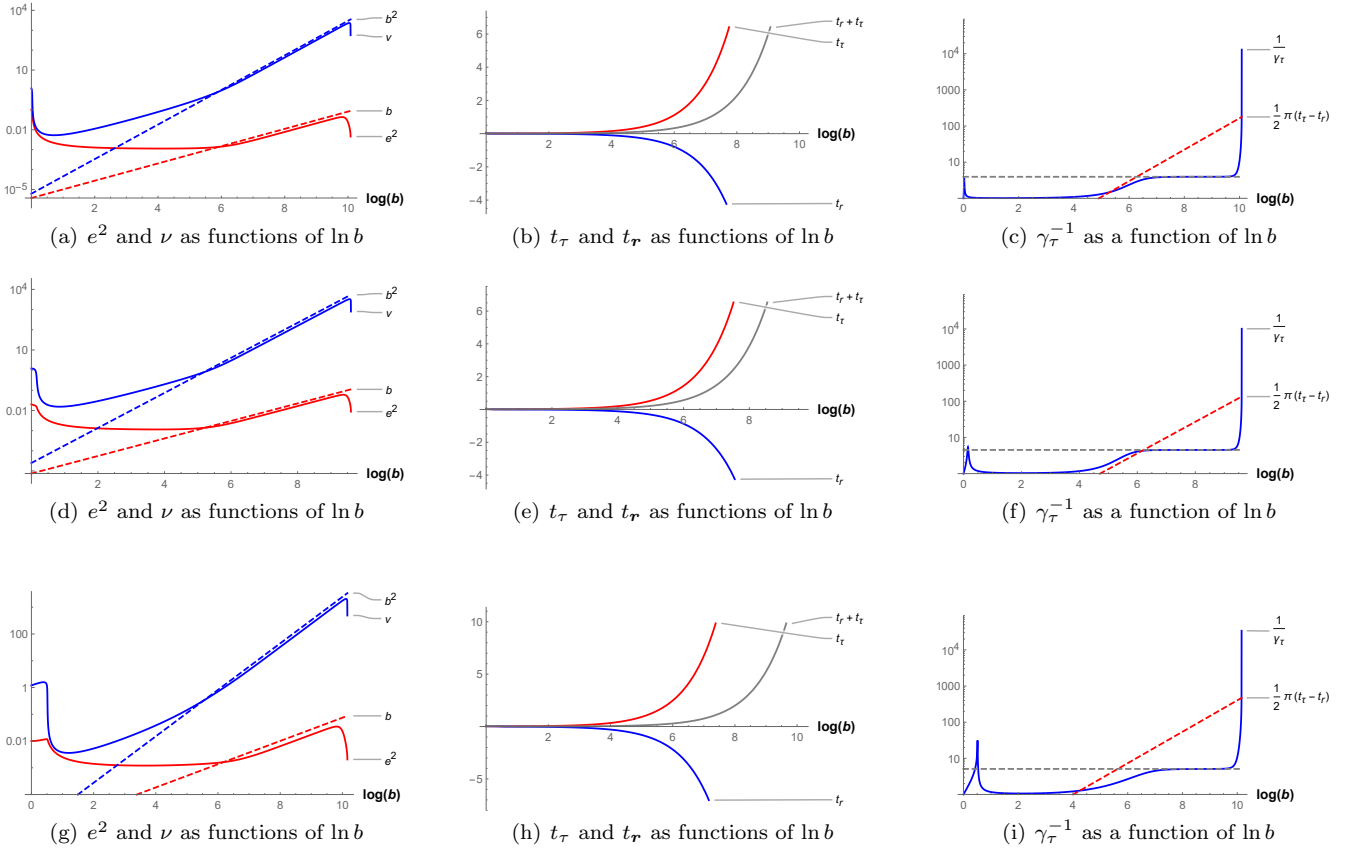


FIG. 19. Plots of e^2 , ν , t_τ , t_r and γ_τ^{-1} as functions of the RG scale $\ln b$ in the intermediate region [red color region in Fig. 16], where the initial value of ν and γ_τ^{-1} are 1.2 and 1, respectively. As for the initial values of e^2 and $t_\tau = t_r = t$, we chose $(e^2, t)|_{\ln b=0} = (0.1, 0.02375)$ [denoted by red cross mark in Fig. 16] for Figs. 19(a), 19(b), 19(c), $(e^2, t)|_{\ln b=0} = (0.02, 0.0202)$ [denoted by red cross mark in Fig. 16] for Figs. 19(d), 19(e), 19(f), and $(e^2, t)|_{\ln b=0} = (0.01, 0.02495)$ [denoted by red cross mark in Fig. 16] for Figs. 19(g), 19(h), 19(i).